ISLET COMPOSITION AND ARCHITECTURE IN STREPTOZOTOCIN-INDUCED DIABETIC RAT FOLLOWING PANCREATIC DUCT LIGATION

by

Patricia Clara Kotzé

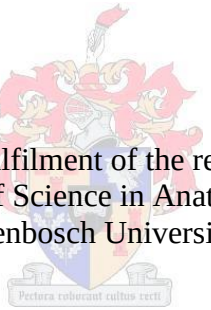

Thesis submitted in partial fulfilment of the requirements for the degree
Masters of Science in Anatomy at
Stellenbosch University

Supervisor: Dr V Tchokonte-Nana, PhD
Faculty of Medicine and Health Sciences

December 2015

DECLARATION

By submitting this thesis electronically, I declare that the entirety of the work contained therein is my own, original work, that I am the sole author thereof (save to the extent explicitly otherwise stated), that reproduction and publication thereof by Stellenbosch University will not infringe any third party rights and that I have not previously in its entirety or in part submitted it for obtaining any qualification.

December 2015

ABSTRACT

Diabetes Mellitus is a metabolic disease characterized by the loss of beta cells from the islets, thereby disrupting islet composition and architecture which are important components that influence islet function. The experimental technique of pancreatic duct ligation (PDL), which is thought to induce the regeneration of beta cells within the adult pancreas, was investigated as a novel treatment strategy for diabetes. This study aimed at investigating the possibility that the PDL model may have the capacity to restore normal islet composition and architecture in diabetic animals, which could make it an effective approach to reverse diabetes. Male Wistar rats (n=55) were divided into three study groups: the normal control (NC) group, the diabetic control (DC) group consisting of five subgroups (day 0, 3, 5, 10 and 30) and the experimental (EX) group consisting of four subgroups (day 3, 5, 10 and 30). The experimental group was exposed to PDL. All pancreata were divided into a P1 portion (proximal to the point of ligature) and P2 portion (distal to the point of ligature) for histological assessment. Animals' non-fasting blood glucose levels (BGLs) and body weights were monitored. The general morphology of the tissue was studied, while an immunohistochemical (IHC) study was performed to determine insulin, pancreatic polypeptide, glucagon and somatostatin protein expression in the P1 and P2 portions of the pancreas. From the IHC slides hormone fractions, staining intensity and distribution were determined as indication of islet composition and architecture. Despite apparent morphological recovery in the islet 30 days post-PDL, islet composition and architecture remained disrupted. Compared to diabetic animals, the proximal portion of the pancreas in experimental animals had a decreased beta cell fraction and increased delta cell fraction thirty days following PDL. These observed changes in islet composition in the part of the pancreas proximal to the ligature are novel findings. There was no change in the diabetic islet composition in the portion of the pancreas distal to the ligature thirty days following PDL. Furthermore, pancreatic duct ligation did not restore body weight or normoglycemia. We conclude that STZ disrupts islet composition and architecture and this could not be restored using PDL; we therefore suggest that a comparative study using a Type 2 diabetic model, where there is limited damage to pre-existing beta cells, may yield different results.

OPSOMMING

Diabetes Mellitus is ’n metaboliese siekte wat deur die verlies van beta selle uit die eilande van Langerhans gekarakteriseer word. Hierdie verlies van beta selle ontwrig eiland komposisie en argitektuur, twee belangrike komponente van eiland funksie. Die eksperimentele tegnieke van pankreatiese buisafbinding (in Engels PDL), wat moontlik beta sel regenerasie in die volwasse pankreas kan induseer, is ondersoek as behandelings-strategie vir diabetes. Hierdie studie het ten doel gehad om die moontlikheid te ondersoek dat die PDL model die kapasiteit het om normale eiland komposisie en argitektuur te herstel in diabetiese diere, wat dit ’n effektiewe benadering vir die omkeer van diabetes kan maak. Manlike Wistar rotte (n=55) was in 3 studie groepe verdeel: die normale kontrole (NC) groep, die diabetiese kontrole (DC) groep wat uit vyf subgroepe bestaan (dag 0, 3, 5, 10 en 30) en die eksperimentele (EX) groep wat uit vier subgroepe bestaan (dag 3, 5, 10 en 30). Die eksperimentele groep is aan PDL blootgestel. Alle pankreata is verdeel in ’n P1 porsie (proksimaal tot die afbinding) en ’n P2 porsie (distaal tot die afbinding) vir histologiese assessering. Die diere se nie-vastende bloed glukose vlakke en liggaamsgewig is gemonitor. Die algemene morfologie van die pankreas weefsel is bestudeer, terwyl ’n immunohistochemiese (IHC) studie gedoen is om insulien, pankreatiese polipeptied, glukagon en somatostatien proteïen uitdrukking in die P1 en P2 porsies van die pankreas te bepaal. Vanaf die IHC snitte is hormoon fraksie, kleur intensiteit en verspreiding bepaal as aanduidings van eiland komposisie en argitektuur. Ten spyte van ooglopende morfologiese herstel in die eilande op dag 30 na PDL, het eiland komposisie en argitektuur versteur gebly. In vergelyking met die diabetiese diere, het die proksimale deel van die pankreas van eksperimentele diere verlaagde beta sel fraksie en verhoogde delta sel fraksie getoon dertig dae na PDL. Die waarneming van veranderde komposisie in die deel van die pankreas proksimaal tot die afbinding is nuut. Daar was geen verandering in diabetiese eiland komposisie in die deel van die pankreas distaal tot die afbinding dertig dae na PDL nie. Verder het PDL nie liggaamsgewig of bloedsuiker genormaliseer nie. Ons gevolgtrekking is dat STZ eiland komposisie en argitektuur ontwrig en dat dit nie met PDL herstel kon word nie; daarom stel ons ’n vergelykende studie in ’n tipe 2 diabetes model voor, waar die skade aan reeds bestaande beta selle beperk is, wat ander resultate mag lewer.

PEER REVIEWED ABSTRACT

Kotze, P.C., Tchokonte-Nana, V., Williams, R.P. 2015. Streptozotocin-induced experimental diabetes is associated with disruption of total islet composition. 59th Annual Academic Day. Faculty of Medicine and Health Sciences. Stellenbosch University. Abstract p.124.

ACKNOWLEDGEMENTS

I would firstly like to thank Dr V Tchokonte-Nana and the Islet Research group for the guidance and support I received during the two years I worked on this project. I also appreciate the input and support received from Prof BJ Page and the staff and students of the Division of Anatomy and Histology.

I hereby acknowledge the financial assistance of the National Research Foundation (NRF) and the Harry Crossley foundation that made this project feasible.

Thank you to Mr M McCaul for taking the time to create and appropriate statistical model. Furthermore, thank you to Mr N Markgraaff, Mr D Jackson and the staff of the Central Animal Unit of the Faculty of Health Sciences for their assistance and support.

Lastly, thank you Mr RP Williams for the technical (and moral) support with every aspect of this project. Reggie, dankie.

CONTENTS

FIGURES

TABLES

APPENDICES

ACRONYMS & ABBREVIATIONS

Arx	Aristaless related homeobox
ATP	Adenosine triphosphate
BGL	Blood glucose level
BM-MSC	Bone morrow-derived mesenchymal stem cell
CAM	Cell adhesion molecule
cAMP	Cyclic adenosine monophosphate
CAU	Central animal unit
DC	Diabetic control
DM	Diabetes Mellitus
EX	Experimental
FMHS	Faculty of Medicine and Health Sciences
GLUT-2	Glucose transporter 2
GM	Geometric mean
H&E	Haematoxylin and eosin
HES1	Hairy/enhancer of split 1
IHC	Immunohistochemistry
Maf	Musculoaponeurotic Fibrosarcoma Oncogene
MSC	Mesenchymal stem cell
N-CAM	Neural cell adhesion molecule
NC	Normal control
NeuroD	Neuronal Diffirentiation
Ngn3	Neurogenin 3

Pax4	Paired box 4
Pax6	Paired box 6
PDL	Pancreatic duct ligation
Pdx1	Pancreatic and duodenal homeobox 1
PP	Pancreatic polypeptide
SSTR	Somatostatin receptor
STZ	Streptozotocin
T1DM	Type 1 diabetes mellitus
T2DM	Type 2 diabetes mellitus
TF	Transcription factor

1. INTRODUCTION

The islets of Langerhans are clusters of endocrine cells dispersed within the exocrine tissue of the pancreas. These clusters are composed of four cell types: beta cells, alpha cells, delta cells and PP cells. Islets are important micro-organs that primarily function to maintain blood glucose homeostasis through the actions of insulin (secreted by beta cells) and glucagon (secreted by alpha cells). The cellular composition and architecture of the islets are important components that influence their function.

A disruption in islet composition may result in metabolic disorders, like Diabetes Mellitus (DM), a disease in which beta cells are lost from the islets. This is accompanied by insufficient insulin production, consequently leading to chronically elevated blood glucose levels. Additionally, loss of insulin within the islet micro-environment allows increased glucagon production from the alpha cell type, which further contributes to hyperglycaemia.

Restoring normal islet composition may be an effective approach to reverse diabetes. The pancreatic duct ligation (PDL) model is said to induce the formation of new beta cells in non-diabetic animals. This same observation has been made in a diabetic animal model; however, the effects of PDL on islet composition (including non-beta cells) have not been established. Since there is a growing attempt to use PDL to reverse diabetes, knowledge of the effects of PDL on the islet as a whole may be crucial to the development of this technique as a therapeutic strategy for DM.

2. LITERATURE REVIEW

2.1 THE ISLETS OF LANGERHANS

2.1.1 Islet formation

The pancreas develops as two evaginations of the endodermal lining of the primitive foregut (Edlund 1998, Gittes 2009, Sadler, Langman 2012, Romer, Sussel 2015). These evaginations into the surrounding mesoderm give rise to a dorsal pancreatic bud and a ventral pancreatic bud (Figure 1.A) (Gittes 2009, Matveyenko, Vella 2015). As the duodenum (part of the primitive foregut) undergoes rotation to assume its final C-shaped position, the ventral bud moves dorsally to come to lie inferior to the dorsal pancreatic bud (Sadler, Langman 2012). Subsequently, the two pancreatic buds fuse, forming one gland posterior to the stomach, between the duodenum and spleen (Figure 1B) (Sadler, Langman 2012).

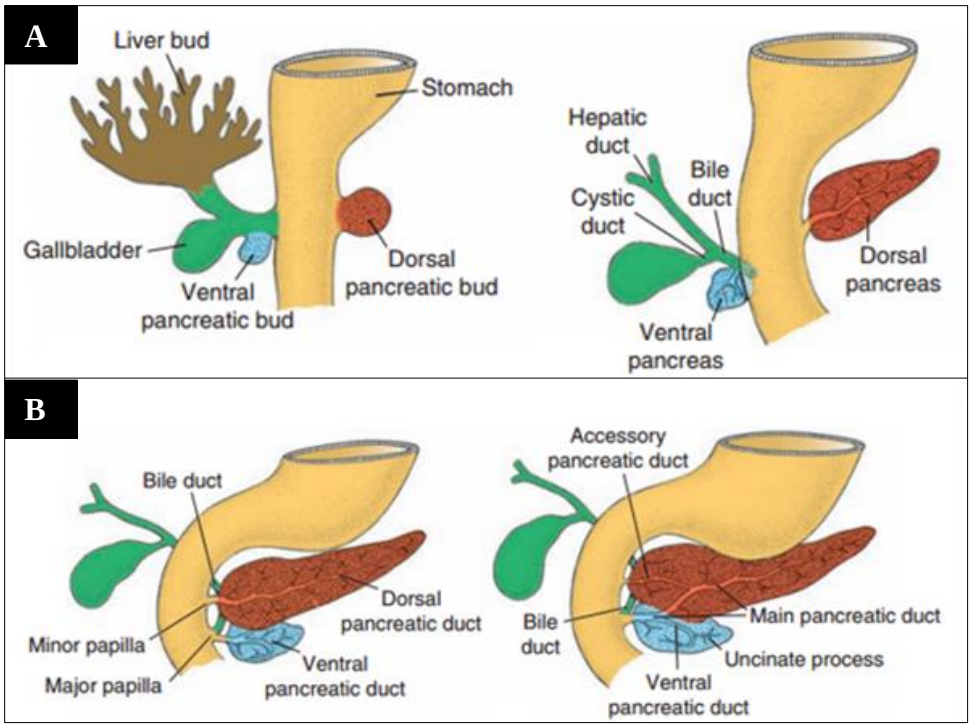

Figure 2.1. Development of the human pancreas. A: Development of the ventral and dorsal pancreatic buds. B: Final position of the ventral pancreatic bud and fusion of the dorsal and ventral pancreatic buds. (Sadler, Langman 2012).

During the early stages of development pro-pancreatic epithelium of the dorsal pancreatic bud is influenced by molecular signals from the notochord and endothelium of the dorsal aorta (Gittes 2009). The ventral pancreatic bud, however, is influenced by signals from the cardiogenic mesenchyme (Gittes 2009). Within the two buds the pro-pancreatic epithelial

cells proliferate, branch and differentiate to form both the exocrine (acinar and ductal) and the endocrine (islet) tissues of the adult pancreas (Edlund 1998).

In both the ventral and dorsal buds epithelial-mesenchymal interactions are important for normal pancreatic development (Gittes 2009, Marquez-Aguirre, Canales-Aguirre *et al.* 2015). Mesenchymal factors, including follistatin, promote development of the exocrine tissues of the pancreas (Miralles, Czernichow *et al*. 1998). Concomitantly, these mesenchymal factors repress pro-endocrine molecular signals, such as activin produced by the notochord (Miralles, Czernichow *et al*. 1998).

Apart from the external molecular signals, many developmental studies have focused on elucidating the dynamic sequential expression of various transcription factors (TFs) within pancreatic progenitors leading to differentiation into the various pancreatic cell types (Neubuser *et al.* 1997, Edlund 1998, Li *et al.* 1999, Apelqvist, Gradwohl, Dierich *et al.* 2000, Sander, Sussel *et al*. 2000, Gu, Dubauskaite *et al.* 2002a, Hald, Hjorth *et al*. 2003, Collombat, Mansouri *et al*. 2003, Sander, Nishimura, Kondo *et al*. 2006, Sugiyama, Gu, Stein *et al.* 2010, Benitez *et al.* 2013,). Pancreatic and duodenal homeobox 1 (Pdx1) is the first TF expressed in progenitor cells indicating their commitment to develop to pancreatic cell types (Edlund 1998, Romer, Sussel 2015); this includes all acinar, ductal and islet cells of the pancreas (Gu, Dubauskaite *et al*. 2002b, Romer, Sussel 2015, Marquez-Aguirre, Canales-Aguirre *et al.* 2015).

The differential expression of the TF neurogenin 3 (Ngn3) determines whether progenitor cells will commit to an endocrine or exocrine cell fate, Ngn3 positive cells being endocrine progenitors (Apelqvist, Li *et al.* 1999, Gradwohl, Dierich *et al*. 2000, Gu, Dubauskaite *et al*. 2002b, Marquez-Aguirre, Canales-Aguirre *et al.* 2015). In pancreata where all Pdx1 expressing cells are manipulated to express Ngn3, exocrine cell formation is inhibited and the pancreatic mass consists mainly of endocrine cells (Apelqvist, Li *et al*. 1999). The opposite is seen in pancreata where Ngn3 expression is blocked; in this instance, no differentiating endocrine progenitors are observed and none of the four endocrine cell types develop (Gradwohl, Dierich *et al*. 2000).

Ngn3 expression is said to be regulated by the Notch signalling pathway (Apelqvist, Li *et al.* 1999, Hald, Hjorth *et al*. 2003, Gittes 2009, Marquez-Aguirre, Canales-Aguirre *et al*. 2015). Activation of the notch signalling pathway prevents pro-pancreatic cells from terminally differentiating, blocking both exocrine and endocrine development (Hald, Hjorth *et al*. 2003).

Endocrine development is prevented as the Notch pathway upregulates expression of hairy/enhancer of split 1 (HES1), which in turn inhibits Ngn3 expression (Apelqvist, Li *et al*. 1999). When Ngn3 expression is inhibited in pro-pancreatic cells, these cells will differentiate to exocrine cell types, following the expression of pro-exocrine TFs (Gradwohl, Dierich *et al*. 2000). In endocrine progenitor cells, inhibition of Notch signalling allows for Ngn3 expression. Ngn3 expression will result in a cascade of endocrine TF expression and will determine whether the progenitor will develop into a beta cell, alpha cell, delta cell or pancreatic polypeptide (PP) cell in the islet of Langerhans. Since the pro-endocrine TFs lie downstream from Ngn3, Ngn3 expression is essential to initiate endocrine development (Gradwohl, Dierich *et al.* 2000, Sugiyama, Benitez *et al*. 2013).

One of the direct downstream targets of Ngn3 is the Neuronal Differentiation (NeuroD) TF (Gittes 2009, Sugiyama, Benitez *et al*. 2013). While expressed in all endocrine progenitors (Gradwohl, Dierich *et al.* 2000), NeuroD is specifically important in beta cells for beta cell function, expression of the insulin 1 gene and for maintaining beta cell maturity (Gu, Stein *et al.* 2010). Similarly, the pro-endocrine TF paired box 6 (Pax6) is expressed in all endocrine progenitors and plays a role in endocrine cell formation, hormone expression and development of islet architecture (Sander, Neubuser *et al.* 1997, Gittes 2009,).

Initially endocrine progenitors also express both Aristaless related homeobox (Arx) and paired homeobox 4 (Pax4), before one TF subsequently becomes predominant (Collombat, Mansouri *et al*. 2003). Arx and Pax4 form a pair of pro-endocrine TFs important for proper development of endocrine progenitors into the four different islet cell types (Gittes 2009, Collombat, Mansouri *et al*. 2003). If Arx expression becomes predominant, the formation of alpha cells is promoted, while beta and delta cell formation is promoted when Pax4 expression becomes predominant (Collombat, Mansouri *et al.* 2003).

Other important endocrine TFs include the homeobox proteins Nkx2.2 and Nkx6.1, as well as the Musculoaponeurotic Fibrosarcoma Oncogene homologs A and B (MafA and MafB). In mice with a deleted Nkx2.2 gene, none of the islet cells express any hormones; indicating the importance of Nkx2.2 in the formation of mature and functional islet cells (Sander, Sussel *et al.* 2000). Nkx6.1, another TF that regulates hormone expression, lies downstream from Nkx2.2 and is important in beta cell development (Sander, Sussel *et al.* 2000). As the beta cells develop, Pdx1 is again expressed and is seen to be co-expressed with Nkx6.1 (Sander, Sussel *et al*. 2000). Upregulation of Pdx1 expression in developing beta cells is associated

with switching expression of the TF MafB to the TF MafA; MafA being expressed in mature beta cells while MafB is expressed in mature alpha cells (Nishimura, Kondo *et al.* 2006). As recently reviewed, the interactions between TFs and how exactly they induce specification of islet cell types has not been elucidated (Romer, Sussel 2015). It is, however, clear that a normal sequence of TF expression during islet development is crucial for the formation of functional islets with the proper composition and architecture.

2.1.2 Islet composition and architecture

As stated earlier, the islets of Langerhans consist of four endocrine cell types, the beta cells (secreting insulin), alpha cells (secreting glucagon), delta cells (secreting somatostatin) and PP cells (secreting pancreatic polypeptide) (Steiner, Kim *et al*. 2010). The relative amount of each cell type per islet is described as islet composition, while islet architecture describes the location of each cell type within the islet (Steiner, Kim *et al*. 2010). Islet composition and architecture may vary between the different parts of the pancreas and between islets of different species (Kim, Miller *et al*. 2009, Steiner, Kim *et al*. 2010).

2.1.2.1 Human islets

Human islets of Langerhans have been described as consisting of approximately 53.9% beta cells, 34.4% alpha cells, 10.4% delta cells and few (1.3%) PP cells (Figure 2.2) (Brissova, Fowler *et al*. 2005, Steiner, Kim *et al.* 2010). The exact composition of the islets may, however, vary between different regions in the human pancreas – for example the uncinate process and head of the pancreas have been indicated as PP cell rich areas (Gersell, Gingerich *et al.* 1979). Gersell *et al*. (1979) reports that beta and alpha cells are more abundant within islets of the tail of the pancreas compared to the islets of the head of the pancreas. Contradictory findings indicate that islet composition may be similar in the different areas of the pancreas, except for alpha cells being more numerous in islets of the neck of the pancreas (Cabrera, Berman *et al*. 2006). Islet composition may also vary between islets within the same area of the pancreas (Cabrera, Berman *et al*. 2006). When comparing human islet composition to that of other species (monkey, pig, rabbit, mouse and bird), human islets generally have a smaller fraction of beta cells (Kim, Miller *et al*. 2009).

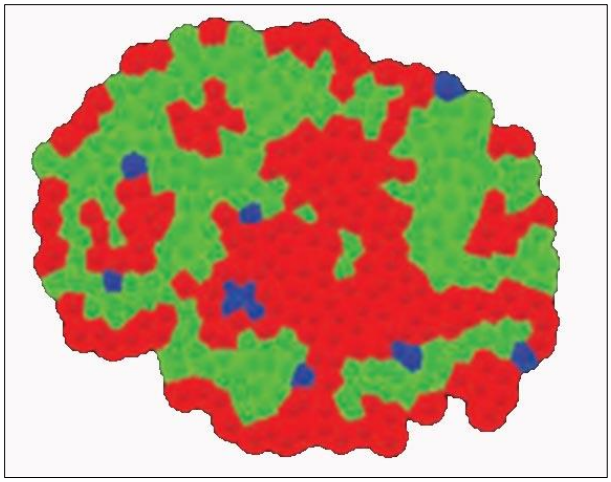

Figure 2.2. Schematic representation of the human islet of Langerhans. beta cells (green); alpha cells (red); delta cells (blue). PP cells are not shown. (Adapted from Steiner, Kim *et al*. 2010).

Human islets also differ from those of other species in terms of islet architecture (Kim, Miller *et al.* 2009, Steiner, Kim *et al.* 2010). A study conducted by Erlandsen *et al.* (1976) described human islets as being lobulated and noted that the observed lobules contained central beta cell clusters surrounded by alpha, delta and PP cells. However, other studies describe the islets as being randomly arranged (Figure 2.2), with no cluster of beta cells and all endocrine cell types dispersed throughout the islet (Brissova, Fowler *et al*. 2005, Cabrera, Berman *et al.* 2006). Moreover, different architectures for small and large islets have been reported (Bosco, Armanet *et al.* 2010, Farhat, Almelkar *et al.* 2013). In these models, small human islets have a central core of beta cells surrounded by a mantle of non-beta cells (Bosco, Armanet *et al*. 2010, Farhat, Almelkar *et al*. 2013), while in larger islets, non-beta cells are more frequently observed within the core of islets (Bosco, Armanet *et al.* 2010) and the endocrine cell types are evenly dispersed (Farhat, Almelkar *et al.* 2013). Furthermore, Bosco *et al*. (2010) proposed that the endocrine cells of the islets are arranged into a folded trilaminar epithelial plate, where a central layer of beta cells is bordered on each side by non-beta cells.

2.1.2.2 Rodent islets

The composition and architecture of rodent islets of Langerhans have also been extensively described in the literature (Erlandsen, Hegre *et al.* 1976, Weiczoreck, Pospischil *et al.* 1998, Esni, Taljedal *et al.* 1999, Zafar, Mughal 2002, Brissova, Fowler *et al.* 2005, Cabrera, Berman *et al.* 2006, Steiner, Kim *et al.* 2010). Rat and mice islets are composed 60-85% beta cells, 15-25% alpha cells, 6-10% delta cells and less than 1% PP cells (Figure 2.3) (Erlandsen, Hegre *et al*. 1976, Weiczoreck, Pospischil *et al.* 1998, Brissova, Fowler *et al*. 2005, Steiner, Kim *et al.* 2010) . As in humans, the composition of rodent islets may also vary in different parts of the

pancreas. In albino rats, it was found that alpha cells are more abundant in the head area of the pancreas than in the tail, while beta cells and delta cells are more abundant in the tail area than in the head of the pancreas (Zafar, Mughal 2002). PP cells are reported to be relatively more abundant in what some authors describe as the lower duodenal (head) area of the pancreas (Elayat, El-Naggar *et al*. 1995). When comparing the islet composition of mice and human islets, mice islets generally have a higher fraction of beta cells than human islets, while alpha cells are more abundant in human islets (Cabrera, Berman *et al*. 2006).

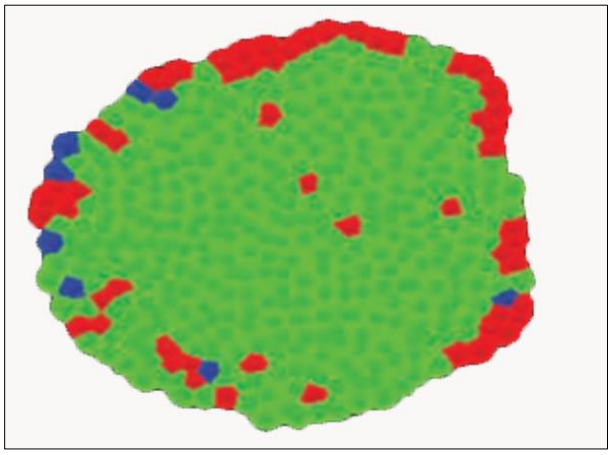

Figure 2.3. Schematic representation of the rodent islet of Langerhans. beta cells (green); alpha cells (red); delta cells (blue). PP cells are not shown. (Adapted from Steiner, Kim *et al*. 2010).

With regards to the architecture, rodent islets are consistently described in the literature as having a central core of beta cells surrounded by non-beta cells (Figure 2.3) (Erlandsen, Hegre *et al*. 1976, Elayat, El-Naggar *et al*. 1995, Weiczoreck, Pospischil *et al*. 1998, Weiczoreck, Pospischil *et al*. 1998, Esni, Taljedal *et al*. 1999, Zafar, Mughal 2002, Brissova, Fowler *et al*. 2005, Cabrera, Berman *et al*. 2006, Kim, Miller *et al*. 2009). The mantle consists mainly of alpha cells, with some delta cells that are located either in the periphery of the islets, between alpha cells or intermediately between alpha and beta cells (Erlandsen, Hegre *et al*. 1976, Zafar, Mughal 2002). PP cells are located at the periphery of rodent islets and are observed as isolated cells or small clusters (Erlandsen, Hegre *et al*. 1976, Elayat, El-Naggar *et al*. 1995). Research suggests that the segregation of the different cell types within the islets of Langherhans may be governed by cell adhesion molecules (CAM's), especially neural cell adhesion molecules (N-CAM) (Esni, Taljedal *et al*. 1999). Since the different islet cell types may be segregated within the islet, the pattern of islet perfusion may play an important role in intercellular communication within the islets (Brunicardi, Stagner *et al*. 1996).

2.1.3 Microvasculature within the islets

Three different models of islet perfusion (Figure 2.4) were summarized in a review of islet microcirculation published in 1996 (Brunicardi, Stagner *et al*. 1996). These models include: 1) a model where non-beta cells are perfused before beta cells, 2) a model where beta cells are perfused before non-beta cells and 3) a model where islets are perfused from one pole to another (Brunicardi, Stagner *et al*. 1996, Ballian, Brunicardi 2007). When these models were again reviewed in 2007 more debate was created (Ballian, Brunicardi 2007).

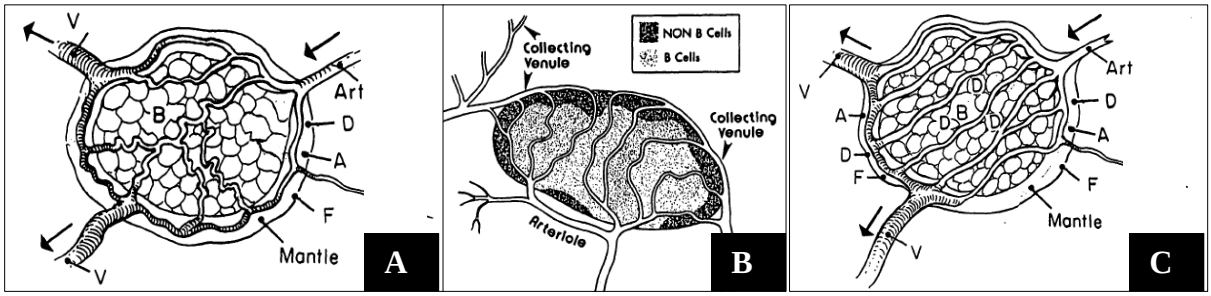

Figure 2.4. The three models of islet microcirculation A: Model 1, non-beta cells perfused before beta cells; B: Model 2, beta cells perfused before non-beta cells; C: Model 3, Islet perfusion from one pole to the other. Key: (A) alpha cells; (Art) arteriole; (B) beta cells; (D) delta cells; (F) PP cells; (V) venule. (Adapted from Brunicardi, Stagner *et al*. 1996).

In model 1 (Figure 2.4A), the technique of corrosion casting in combination with scanning electron microscopy was largely used to allow visualization of the islet vasculature. Studies in support of this model describe an insular arteriole that supplies arterial blood to the islets (Murakami, Miyake *et al*. 1997, Ohtani, Wang 1997). In rats, rabbits and mice this afferent vessel ends in the mantle region of the islet (where non-beta cells are located); here it branches to form a primary capillary network in the mantle layer that will again branch to form a secondary capillary plexus in the core of the islet (Fujita *et al*. 1993, Murakami, Miyake *et al*. 1997, Ohtani, Wang 1997, Murakami). Experiments in rats, where the vasculature was incompletely injected with the casting medium, indicated that the capillary plexus of the mantle layer of the islet was filled prior to the core capillary plexus (Murakami, Miyake *et al*. 1997).

In the islets of Formosan monkeys, where alpha and delta cells form the core of the islet with beta cells in the periphery, perfusion was found to occur from the core to the mantle of the islet (Murakami, Fujita *et al*. 1993). These results indicate that even when islet architecture differs between species, islet perfusion may follow the same pattern where non-beta cells are perfused before beta cells. The implication of this model of islet microcirculation would be that beta cell function is regulated by the hormones secreted by the non-beta cells (Murakami,

Fujita *et al*. 1993, Murakami, Miyake *et al*. 1997). It is, however, generally accepted by authors that there is a plausible flow of blood within the islet from the mantle to the core and back to the mantle (Fujita *et al*. 1993, Ohtani, Wang 1997, Murakami), indicating that intra-islet communication via the microcirculation may be more intricate than what is proposed by model 1.

In model 2 (Figure 2.4B) retrograde and anterograde islet perfusion techniques were mostly used. Anterograde perfusion is perfusion in the normal direction and retrograde perfusion is when the direction of perfusion is reversed. Experiments performed on rat, dog and human islets indicate that, during anterograde perfusion, the subsequent addition of an anti-insulin antibody into circulation causes the levels of glucagon and somatostatin to rise (Stagner, Samols 1986, Samols, Stagner *et al*. 1988, Stagner, Samols 1992), while in retrograde perfusion, the subsequent addition of an anti-insulin antibody does not change glucagon and somatostatin levels (Stagner, Samols 1986, Samols, Stagner *et al*. 1988, Stagner, Samols 1992). The addition of the anti-insulin antibody would only change glucagon and somatostatin levels when the direction of perfusion was such that alpha cells and delta cells were exposed to insulin prior to addition of the antibody. Consequently, during anterograde perfusion, alpha and delta cells are exposed to insulin. It was therefore concluded that in rats, dogs and humans, beta cells are perfused before non-beta cells (Stagner, Samols 1986, Samols, Stagner *et al*. 1988, Stagner, Samols 1992).

Experiments with retrograde and anterograde infusion of glucose, insulin, glucagon and somatostatin confirmed these results (Stagner, Samols 1986, Stagner, Samols *et al*. 1988). Interestingly, an early corrosion cast experiment performed on rat islets also supports this model of islet perfusion. This study found that afferent arterioles enter the islet in areas where the non-beta cell mantle is discontinuous and then branch to form a capillary network within the beta cell core (Bonner-Weir, Orci 1982). An immunohistochemical analysis of islet microcirculation also describes this perfusion pattern in the rat (Weiczoreck, Pospischil *et al*. 1998).

The third model (Figure 2.4C), proposing that blood flow through the islet may be polar, describes a more complex microcirculation pattern within the islet. Liu *et al*. (1993) used fluorescence video-microscopy to dynamically evaluate islet perfusion. It was observed that the arteriole supplying the islet branches into a capillary network within the mantle layer of one hemisphere of the islet, blood then fills the mantle layer, followed by the core of that

hemisphere of the islet (Liu, Guth *et al*. 1993). Thereafter, blood would first fill the core and then the mantle of the opposite hemisphere of the islet (Liu, Guth *et al*. 1993). Furthermore, microsphere injection into the islet microvasculature indicated that the route of a single red blood cell is torturous though the capillary network and that blood may also flow from the mantle to the core and back to the mantle within the same hemisphere; therefore, perfusion in the islet may not follow a strictly polar route (Liu, Guth *et al*. 1993).

A more recent study, conducted on mice pancreatic islets, revealed that within the same pancreas different perfusion patterns may be found. The majority of the islets displayed perfusion from the core to the mantle (model 2), but 35% of islets had a polar perfusion pattern (Nyman, Wells *et al*. 2008). Authors supporting a model of a more complex or dynamic perfusion pattern in the islets of Langerhans also argue that, since there is variation in islet architecture within the same animal, the relationship between islet architecture and perfusion may not be as simple as proposed by model 1 and model 2 (Kim, Miller *et al*. 2009). For example, in human islets different architectures are reported for small and large islets. In large islets beta cells less frequently have direct contact to blood vessels than in smaller islets (Farhat, Almelkar *et al*. 2013). In another study on human islets different endocrine cell types are seen randomly arranged along the blood vessels (Cabrera, Berman *et al*. 2006). For example, a beta cell may be bordered by an alpha cell or delta cell on either side along the blood vessel or found to face non-beta cells located on the opposite side of the blood vessel (Cabrera, Berman *et al*. 2006). This random arrangement of cells along the capillaries indicates that there may be no specific order in cellular perfusion within the human islets of Langerhans.

Venous drainage is not described in detail in model 2 and model 3. However, studies supporting model 1 propose that islets are drained by three different efferent vessels: 1) insulo-portal vessels that drain blood from the islet capillary plexus to the acinar capillary plexus, 2) emissary venules that drain blood from the islet directly to the systemic circulation and 3) insulo-ductal portal vessels that drain blood from the islets to the periductal plexuses (Ohtani, Wang 1997). The venous drainage of the islet depends on the islet's position within the pancreas; islets may be intralobular (within an acinar lobule), interlobular (between acinar lobules) or periductal (close to pancreatic ducts) (Ohtani, Wang 1997).

In the rat and guinea pig, small intralobular islets have insulo-acinar portal vessels, while larger intralobular islets would, in addition to insulo-acinar portal vessels, also have emissary

veins (Ohtani, Wang 1997). Interlobular islets are reported to have both emissary and insulo-acinar portal vessels, whereas periductal islets would (in addition to these two vessels) also have insulo-ductal portal vessels (Ohtani, Wang 1997). Incomplete injection of casting medium into the islet vasculature has shown that islets are drained via their insulo-acinar portal vessels first, before being drained by additional emissary vessels (Murakami, Miyake *et al*. 1997).

Of the three distinct models of islet perfusion described in the literature, to date, no model has been proven to be superior to the other, neither has a model been proven to be invalid. On the contrary, more than one model of perfusion has been observed within the same animal (Nyman, Wells *et al*. 2008). Regardless of the model of perfusion supported by different studies, it is generally agreed that islets are highly vascularized and that islet perfusion has important implications for islet function.

2.1.4 Islet function and mechanism of action of cell component

The islets of Langerhans mainly function to maintain blood glucose homeostasis via the hormones insulin and glucagon. Insulin is responsible for decreasing blood glucose levels after a meal when blood glucose levels rise. The increased concentration of circulating glucose is the primary stimulus initiating insulin release from beta cells by means of an excitation-secretion process (Matschinsky, Ellerman 1967, Pralong, Bartley *et al*. 1990, Aspinwall, Lakey *et al*. 1999, Rorsman, Eliasson *et al*. 2000, Sherwood 2010). Rising glucose levels cause more glucose to enter the beta cell (via the GLUT-2 transporter) and glucose is subsequently metabolised to ATP; ATP in turn triggers depolarization of the beta cell causing calcium to enter the cell and promote insulin exocytosis (Matschinsky, Ellerman 1967, Pralong, Bartley *et al*. 1990, Rorsman, Eliasson *et al*. 2000, Sherwood 2010). Insulin action triggers the uptake of glucose, fatty acids and amino acids from the blood by targeting the liver, skeletal muscles and adipocytes. Concomitantly insulin stimulates metabolic pathways for the utilization of glucose, storage of carbohydrates and fat, and for protein synthesis (Sherwood 2010).

The effects of insulin are opposed by glucagon, secreted from the pancreatic alpha cells between meals when blood glucose levels are low (Jiang, Zhang 2003, Sherwood 2010). Glucagon mainly targets the liver where it acts via the cAMP second messenger pathway to increase hepatic glucose production by stimulating glycogenolysis and gluconeogenesis (Jiang, Zhang 2003, Sherwood 2010). Concomitantly, glucagon prevents the storage of

glucose by inhibiting glycogen synthase, ultimately resulting in an increase in blood glucose levels (Ezrin, Salter *et al*. 1958, Jiang, Zhang 2003, Sherwood 2010). Other catabolic effects of glucagon include increasing breakdown of fat, thereby increasing serum free fatty acid levels, and hepatic protein degradation (Pontiroli, Perfetti *et al*. 1993, Sherwood 2010,).

Contrary to the actions of insulin and glucagon, islet somatostatin does not influence glucose homeostasis by acting on peripheral body tissues (Cherrington, Caldwell *et al*. 1977). Somatostatin does, however, influence glucose homeostasis by its inhibitory paracrine effects on both insulin and glucagon secretion (Hauge-Evans, King *et al*. 2009). Insulin and glucagon secretagogues concomitantly stimulate delta cells to release somatostatin that will limit the beta and alpha cell's response to the stimulus (Hauge-Evans, King *et al*. 2009). There are several different subtypes of somatostatin receptors (SSTRs) that are expressed by beta and alpha cells for somatostatin, where SSTR2 is regarded as the main mediator of somatostatin induced inhibition of insulin and glucagon secretion in humans (Reubi, Kappeler *et al*. 1998, Ludvigsen, Olsson *et al*. 2004, Singh, Brendel *et al*. 2007, Kailey, van de Bunt *et al*. 2012). Somatostatin specifically inhibits insulin secretion by hyperpolarizing and preventing calcium influx into the beta cell and by directly preventing insulin exocytosis (Kailey, van de Bunt *et al*. 2012).

The fourth islet hormone, pancreatic polypeptide (PP), also influences energy balance via its effects on peripheral tissues. This peptide hormone is secreted by the PP cells in response to food intake, specifically the digestion of lipids in the duodenum (Feinle-Bisset, Patterson *et al*. 2005). It is interesting to note that PP cells are not stimulated by nutrients in the blood stream (Adrian, Bloom *et al*. 1977) as is the case with stimulation of the other three islet cell types. PP functions to decrease food intake (Ueno, Inui *et al*. 1999, Asakawa, Inui *et al*. 2003, Batterham, Le Roux *et al*. 2003, Jesudason, Monteiro *et al*. 2007) and slows the rate of gastric emptying (Ueno, Inui *et al*. 1999, Asakawa, Inui *et al*. 2003, Schmidt, Naslund *et al*. 2005). This is achieved by PP's inhibitory effects on vagus nerve activity, hypothalamic feeding-stimulating protein expression and ghrelin release in the stomach (Asakawa, Inui *et al*. 2003, Kojima, Ueno *et al*. 2007).

The release and function of each islet hormone should, however, not be viewed in isolation; islet composition and architecture form critical components of whole islet function. This is evident when considering islet somatostatin that mainly has a paracrine influence within the islet, allowing the fine-tuning of beta and alpha cell responses to fluctuating blood glucose

levels (Hauge-Evans, King *et al*. 2009). Furthermore, a two-way interaction between beta and alpha cells is reported to influence both insulin and glucagon secretion (Ishihara, Maechler *et al*. 2003, Franklin, Gromada *et al*. 2005, Wang, Zhang *et al*. 2011). Glucagon secreted by alpha cells allows for increased glucose stimulated insulin release by beta cells (Wang, Zhang *et al*. 2011), while insulin and zinc secreted from beta cells inhibit glucagon secretion (Ishihara, Maechler *et al*. 2003, Franklin, Gromada *et al*. 2005).

A study on the paracrine relationships between the cells of the islets proposed the following regulatory relationships within the islet: 1) beta cell secretion inhibits glucagon release from alpha cells, 2) alpha cell secretion stimulates beta cell and delta cell secretion and 3) somatostatin release inhibits secretion from beta, alpha and PP cells (Weir, Samols *et al*. 1979). It is, therefore, important for islet function that the islets are composed of the correct amounts of each cell type. Apart from paracrine interactions within the islet, morphological studies indicate the presence of gap junctions and direct communicating pathways between homologous and heterologous groups of endocrine cells within the islet (Orci, Malaisse-Lagae *et al*. 1975, Meda, Kohen *et al*. 1982).

In rodent islets, gap junctions allow for synchronous intracellular calcium oscillations (electrical coupling) throughout the beta cell population of the islet (Benninger, Head *et al*. 2011). Electrical coupling may be important for beta cell function as the beta cells within an islet are heterogeneous in terms of their excitability. At sub-threshold glucose levels, gap junctions appear to allow the less-excitable beta cells to supress increased intracellular calcium levels in the more-excitable beta cells, and the islet beta cell population then responds with uniform electrical activity (Benninger, Head *et al*. 2011). While gap junctions do not function to directly stimulate or supress insulin release, dissociated beta cells are observed to display increased insulin release at sub-threshold glucose levels and, therefore, it can be argued that other cellular adhesion molecules are important in regulating insulin secretion (Benninger, Head *et al*. 2011).

A more recent study contradicts these findings stating that, while beta cells are electrically coupled, gap junctions do not mediate the flow of calcium between beta cells when one beta cell is stimulated (Stozer, Gosak *et al*. 2013). However, the authors do agree that beta cell functional activity is synchronized and that the structure of the islet may play an important role in this synchronization (Stozer, Gosak *et al*. 2013). Apart from physical connections between cells, insulin itself has also been indicated to regulate (stimulate) insulin release

independent of intracellular calcium levels; this autocrine effect was proposed to explain why clusters of beta cells are able to secrete more insulin than isolated beta cells when stimulated by glucose (Aspinwall, Lakey *et al*. 1999).

In both human and rodent islets, it was found that small islets (less than 150 µm or 125 µm in diameter) secrete more insulin than large islets (MacGregor, Williams *et al*. 2006, Lehmann, Zuellig *et al*. 2007, Fujita, Takita *et al*. 2011, Huang, Novikova *et al*. 2011, Farhat, Almelkar *et al*. 2013), indicating that the size of the islet also has implications for beta cell function. This phenomenon may be due to beta cells within the small islets having a higher insulin content than those found in large islets (Huang, Novikova *et al*. 2011, Farhat, Almelkar *et al*. 2013). Another explanation could be a difference in the composition of small and large islets. Studies on human islets reported a larger beta cell fraction in small islets as compared to large islets (Lehmann, Zuellig *et al*. 2007, Farhat, Almelkar *et al*. 2013), but no compositional difference was observed in rodent islets (Huang, Novikova *et al*. 2011). A study on rodents did, however, indicate increased endocrine cell density in small islets that could account for increased insulin release from small islets (Huang, Novikova *et al*. 2011).

Farhat *et al*. (2013) also proposed that, in human islets, the different architectures of small and large islets may influence beta cell function. Therefore, the clustering of beta cells in the core of small islets may favour beta cell insulin secretion. The superior functioning of small islets is also emphasised in clinical and experimental islet transplantation studies. In this context, cells within small islets are found to be more viable after isolation from a donor and small islets also have better transplantation outcomes than larger islets (MacGregor, Williams *et al*. 2006, Lehmann, Zuellig *et al*. 2007). In general, better transplantation outcomes are obtained when transplanting morphologically intact islets compared to pelleted islets (Rackham, Jones *et al*. 2013).

Similarly, Cabrera *et al*. (2006) also noted the effect of islet architecture on beta cell function. The authors compared human and rodent islet responses to glucose stimulation and found that human islets (where beta cells are dispersed) did not respond to glucose with synchronous intracellular calcium oscillations (Cabrera, Berman *et al*. 2006). This is in contrast to findings in rodent islets where all islet beta cells responded to glucose with synchronous intracellular calcium oscillations, as beta cells were clustered within the core of the islet (Cabrera, Berman *et al*. 2006).

Furthermore, Shiota *et al*. (2013) found that alpha cell deficient rodent islets can have normal beta cell function, while Wang *et al*. (2011) reported that alpha cell deficient human islets had impaired beta cell function. Together, these findings support the view that compositional differences between human and rodent islets may also have an impact on islet function. Based on the above, alpha cells may therefore have a stronger regulatory role in human islets, possibly because alpha cells are more numerous in human islets; this view was previously proposed by Cabrera *et al*. (Cabrera, Berman *et al*. 2006).

From the discussion above, it is clear that the islets of Langerhans are important endocrine micro-organs. Islet composition and architecture are integral to islet function as demonstrated by pathological conditions such as DM that result from a disruption in islet composition.

2.2 CHANGES IN ISLET COMPOSITION AND ARCHITECTURE

2.2.1 Pathological changes in the islet

The malfunction of insulin secretion by beta cells results in hyperglycaemia which is a characteristic of both type 1 and type 2 DM (Sherwood 2010). In Type 1 DM (T1DM), a lack of insulin secretion is due to the autoimmune destruction of the pancreatic beta cells (Sherwood 2010, Atkinson 2000). In this instance, beta cells, which are the most abundant cell type within the islet, are damaged and lost from the islets, thereby disrupting the islet composition. Patients with T1DM have increased postprandial blood glucose levels (BGL) and decreased insulin response resulting from the pathological change in islet composition (Greenbaum, Prigeon *et al*. 2002, Heptulla, Rodriguez *et al*. 2005). In addition to the lack of insulin, beta cell deficiency also results in the unregulated secretion of glucagon from the alpha cells. In T1DM patients, there is no suppression of glucagon secretion following a meal (Greenbaum, Prigeon *et al*. 2002, Heptulla, Rodriguez *et al*. 2005), therefore worsening postprandial hyperglycaemia as hepatic glucose output is continuously stimulated. While T1DM is managed by exogenous insulin administration, research indicates that insulin pump therapy is not sufficient to control postprandial hyperglycaemia (Heptulla, Rodriguez *et al*. 2005), highlighting the importance of intra-islet insulin and beta cell function.

In type 2 DM (T2DM) beta cells still produce insulin, but peripheral body tissues become resistant to the insulin (Sherwood 2010). Moreover, loss of beta cells from the islet has been reported in patients with T2DM (Kilimnik, Zhao *et al*. 2011), implicating a change in islet composition in the pathophysiology of T2DM. An excessive appetite overworks the beta

cells, which leads to their death. This loss of beta cells from pancreatic islets is widely reported (Janson *et al*. 2003, Kilimnik, Zhao *et al*. 2011, Butler, Henquin, Rahier 2011, Jurgens, Toukatly *et al*. 2011). The destruction of beta cells may occur via apoptosis associated with the deposition of amyloid, which is characteristic of the islets of T2DM patients (Butler, Janson *et al*. 2003, Jurgens, Toukatly *et al*. 2011). As with T1DM, the loss of beta cells from the islets results in hyperglucagonemia; this unregulated glucagon secretion has been directly linked to decreased insulin pulse mass in T2DM (Menge, Gruber *et al*. 2011). The importance of islet composition is repeatedly emphasised by studies on both T1DM and T2DM and even more so by studies on experimentally induced diabetes in animal models.

In experimental studies, diabetes can be chemically induced using the beta-cytotoxic agents streptozotocin (STZ) or alloxan (Kjems, Kirby *et al*. 2001, Mythili, Vyas *et al*. 2004, Meier, Kjems *et al*. 2006). These beta-cytotoxic agents primarily cause destruction of the pancreatic beta cells, while other islet cells remain unaffected (except at higher doses where damage may occur to the alpha cells) (Kjems, Kirby *et al*. 2001, Mythili, Vyas *et al*. 2004, Meier, Kjems *et al*. 2006). Selective chemical destruction of islet beta cells results in a hyperglycaemic phenotype (Mythili, Vyas *et al*. 2004), as is characteristic of human diabetes. Chemically induced diabetic animals display postprandial hyperglycaemia, decreased insulin response and hyperglucagonemia (Kjems, Kirby *et al*. 2001, Meier, Kjems *et al*. 2006, Meier, Ueberberg *et al*. 2011).

From the experimental models, it could be determined that even when 25% of the islet beta cells survive, glucose-induced insulin secretion is non-existent (Meier, Ueberberg *et al*. 2011). This indicates disproportionate changes in islet composition as integral to the pathophysiology of diabetes. Furthermore, administration of exogenous insulin in a diabetic model could not reverse the diabetic phenotype (Meier, Ueberberg *et al*. 2011). This provides evidence that endogenous beta cell function, whether it is locally released insulin or another beta cell secretory product, such as zinc (Ishihara, Maechler *et al*. 2003, Franklin, Gromada *et al*. 2005), is critical for the normal functioning of islets as a whole (Meier, Ueberberg *et al*. 2011).

Normoglycemia could, however, be obtained in diabetic animals without insulin administration, when reversing hyperglucagonemia (Yu, Park *et al*. 2008). Moreover, glucagon receptor knockout mice treated with STZ remained normoglycemic despite beta cell

destruction (Lee, Wang *et al*. 2011b). These findings indicate that unregulated alpha cell secretion in islets with beta cell deficiency may be a key contributor to the pathological hyperglycaemic phenotype characteristic of DM.

Since normal islet composition is essential for blood glucose homeostasis, therapeutic strategies that aim to reverse diabetes would either have to replace diabetic islets by the transplantation of morphologically intact islets, or these strategies should find ways of manipulating islet plasticity to allow restoration of normal islet morphology. Islet plasticity refers to the ability of the islet to adapt morphologically to meet the physiological needs of the organism or in response to injury (Hanley, Austin *et al*. 2010, Jacovetti, Abderrahmani *et al*. 2012, Saisho, Butler *et al*. 2013, Nollevaux, Rahier *et al*. 2013, Bramswig, Everett *et al*. 2013). Experimental models of pancreatic injury, such as pancreatic duct ligation, have been investigated as a means of manipulating adult islet plasticity.

2.2.2 Adult islet plasticity

Human beta cell mass remains relatively constant under normal physiological conditions, between the ages 20 and 100 (Saisho, Butler *et al*. 2013), however, beta cell mass is not static. Conditions such as obesity, that result in an increase in insulin demand, are associated with increased beta cell mass (Hanley, Austin *et al*. 2010, Saisho, Butler *et al*. 2013). This increase is the result of an increase in the number of pancreatic beta cells and not the size of beta cells (Saisho, Butler *et al*. 2013). Increased beta cell mass is also associated with pregnancy and it is thought that micro-RNAs that influence beta cell replication and survival are responsible for the adaptive beta cell expansion during pregnancy and obesity (Jacovetti, Abderrahmani *et al*. 2012). If the mechanisms responsible for this adaptive increase in beta cell mass fail, T2DM may develop (Hanley, Austin *et al*. 2010). Therefore, the understanding of pancreatic plasticity is an important step in finding new treatment strategies for DM, where the first step could be to identify cellular sources from which new beta cells can be formed (Marquez-Aguirre, Canales-Aguirre *et al*. 2015).

2.2.2.1 Cellular sources of new beta cells in the adult pancreas

Sources of new beta cells in the adult human pancreas are still largely unknown (Saisho, Butler *et al*. 2013). Experimental *in vivo* and *in vitro* studies investigating beta cell mass plasticity propose that new beta cells in the adult pancreas may originate from various sources including pre-existing beta cells (Dor, Brown *et al*. 2004, Georgia, Bhushan 2004, Nir,

Melton *et al*. 2007, Teta, Rankin *et al*. 2007, Meier, Butler *et al*. 2008, Nollevaux, Rahier *et al*. 2013), alpha cells (Collombat, Mansouri *et al*. 2003, Thorel, Nepote *et al*. 2010, Chung, Levine 2010, Bramswig, Everett *et al*. 2013), pancreatic duct cells (Zhou, Brown *et al*. 2008, Rukstalis *et al*. 2010, Miyashita, Criscimanna, Speicher *et al*. 2011, Swales, Martens *et al*. 2012, Li, Miyatsuka *et al*. 2014), centroacinar duct cells (Nagasao, Yoshioka *et al*. 2003, Rovira, Scott *et al*. 2010, Tchokonte-Nana 2011), acinar cells (Collombat, Mansouri *et al*. 2003, Thorel, Nepote *et al*. 2010, Chung, Hao *et al*. 2010, Bramswig, Everett *et al*. 2013) and mesenchymal stem cells (MSCs) (Sordi, Malosio *et al*. 2005, Moriscot, de Fraipont *et al*. 2005, Shin *et al*. 2005, Timper, Seboek *et al*. 2006, Gao, Song *et al*. 2014, Choi). Knowledge of pancreatic islet plasticity is crucial for the development of a method that allows for the *in vivo* generation of beta cells as a novel treatment strategy for DM (Juhl, Bonner-Weir *et al*. 2010).

During normal beta cell mass expansion between birth and adulthood, beta cell replication is the most important source of new beta cells (Meier, Butler *et al*. 2008). Similarly, beta cell self-renewal appears to be the predominant mechanism of beta cell mass expansion during normal growth of mice pancreata (Dor, Brown *et al*. 2004, Georgia, Bhushan 2004, Teta, Rankin *et al*. 2007). Subsequently, the islets found in adult mice are all derived from islets already present during early adulthood (Dor, Brown *et al*. 2004). During normal growth, beta cell replication was identified as the mechanism by which new beta cells formed in mice following the ablation of a large amount of pre-existing beta cells, as well as after partial pancreatectomy (Dor, Brown *et al*. 2004, Nir, Melton *et al*. 2007, Nollevaux, Rahier *et al*. 2013). Similarly, the formation of new beta cells during pregnancy occurs via replication of pre-existing beta cells (Teta, Rankin *et al*. 2007).

Teta *et al*. (Teta, Rankin *et al*. 2007) proposed that beta cells have the ability to replicate more than once; however, serial replications are slowed during normal growth due to a replication refractory period. This refractory period may be overcome during conditions such as pregnancy (Teta, Rankin *et al*. 2007). Although these authors did not observe other cell types contributing significantly to beta cell formation, the possibility of alternative sources from which beta cells can be formed have not been ruled out.

Islet alpha cells have been proposed as one such alternative source from which beta cells can be formed (Thorel, Nepote *et al*. 2010, Chung, Hao *et al*. 2010). In order to study the transdifferentiation of alpha cells *in vivo*, animal models were created where almost all pre-

existing beta cells were destroyed; this was done by either using the β-cytotoxic chemical alloxan (Chung, Hao *et al*. 2010) or by selectively inducing expression of the diphtheria toxin receptor on beta cells (Thorel, Nepote *et al*. 2010). Following near total beta cell destruction, Chung *et al*. (2010) used pancreatic duct ligation (PDL) to induce beta cell regeneration, while Thorel *et al*. (2010) allowed for natural regeneration. In both sets of experiments it was concluded that the replication rate of the few remaining beta cells could not account for the total beta cell formation that was observed (Thorel, Nepote *et al*. 2010, Chung, Hao *et al*. 2010). Upon further investigation, intermediate cells expressing both alpha and beta cell markers (for example glucagon and insulin, glucagon and Pdx1, and glucagon and Nkx6.1), indicated transdifferentiation of pancreatic alpha cells to beta cells (Thorel, Nepote *et al*. 2010, Chung, Hao *et al*. 2010). This genetic reprogramming of alpha cells involves expression of the transcription factor Ngn3 (Collombat, Mansouri *et al*. 2003). An alpha-to-beta cell conversion has also been induced in transgenic mice by ectopic expression of the transcription factor Pax4 (Collombat, Mansouri *et al*. 2003).

Human pancreatic alpha cells display a pattern of histone modification (an epigenetic modification) similar to that of human embryonic stem cells, indicating that there is a high degree of epigenetic plasticity in human alpha cells (Bramswig, Everett *et al*. 2013). When this pattern is disrupted, alpha cells may be partially converted to beta cells (Bramswig, Everett *et al*. 2013). These *in vitro* findings suggest that human alpha cells, similar to rodent alpha cells, may have the ability to transdifferentiate to beta cells in conditions of beta cell destruction (Chung, Hao *et al*. 2010, Bramswig, Everett *et al*. 2013).

Another *in vitro* study on human islet plasticity, focused on duct cells as a source of new beta cells; these authors induced ectopic Ngn3 expression in duct cells and found that this could initiate transdifferentiation to a neuro-endocrine state (Swales, Martens *et al*. 2012). Therefore, human pancreatic duct cells also display some degree of plasticity. More recently, experiments inducing the expression of Pdx1 prior to Ngn3 and MafA promoted insulin expression in a ductal cell line (Miyashita, Miyatsuka *et al*. 2014). *In vivo,* transdifferentiation of duct cells to beta cells was observed in mice (Criscimanna, Speicher *et al*. 2011).

Criscimanna *et al*. (2011) created a transgenic mouse model where selective expression of the diphtheria toxin receptor was used to destroy beta, alpha, acinar and some of the pancreatic duct cells. Both the endocrine and exocrine compartments of the pancreas regenerated within three to four weeks. In this model of severe injury, newly formed cells originated from duct

cells induced to express Pdx1 (Criscimanna, Speicher *et al*. 2011). Interestingly, these authors reported the possibility of duct cells first dedifferentiating (since there was a loss of expression of ductal markers) and then redifferentiating; alternatively duct cells may directly transdifferentiate into the various other pancreatic cell types (Criscimanna, Speicher *et al*. 2011). This concept of dedifferentiation and redifferentiation of duct cells was implicated in the regeneration of the pancreas following partial pancreatectomy in rats (Li, Rukstalis *et al*. 2010). It appears that severe pancreatic injury induces an embryological pattern of development in the adult pancreas, where pancreatic cells originate from ducts and TFs such as Pdx1 and Ngn3 are re-expressed (Li, Rukstalis *et al*. 2010, Criscimanna, Speicher *et al*. 2011).

In contrast to the results discussed above, others argue against duct cells as facultative islet progenitor cells (Cardalda *et al*. 2009a, Kopinke, Murtaugh 2010 Kopp, Dubois *et al*. 2011a, Solar). Lineage tracing experiments indicate that during embryological development both the endocrine and exocrine tissues of the pancreas arise from duct-like precursors (Solar, Cardalda *et al*. 2009b, Kopinke, Murtaugh 2010, Kopp, Dubois *et al*. 2011b). However, during normal physiological growth and following PDL, duct cells were not found to contribute to beta cell formation (Solar, Cardalda *et al*. 2009b, Kopinke, Murtaugh 2010, Kopp, Dubois *et al*. 2011b). These contradicting reports may be a result of the use of different models of pancreatic injury, which possibly indicates that duct cells only act as progenitor cells in cases of severe damage to the endocrine and exocrine compartments of the pancreas (Criscimanna, Speicher *et al*. 2011). Alternatively, the contradiction may be due to the use of different species and strains (Solar, Cardalda *et al*. 2009a).

Furthermore, it is suggested that endocrine progenitor activity may be limited to a certain subgroup of ductal cells, the centroacinar or terminal duct cells (Tchokonte-Nana 2011). *In vitro*, centroacinar cells form pancreatospheres that express insulin, C-peptide or amylase (Rovira, Scott *et al*. 2010). Expression of the pro-endocrine TF Ngn3 was found to precede insulin expression, indicating that the centroacinar cells have endocrine progenitor activity (Rovira, Scott *et al*. 2010). In agreement with these findings, *in vivo* experiments where rat pancreatic islets were damaged by STZ report that the centroacinar cells respond by proliferating and subsequently start expressing insulin (Nagasao, Yoshioka *et al*. 2003).

Similar to centroacinar cells, pancreatic acinar cells isolated from rats aggregate to form spheres in culture; acinar cells in these spheres shift towards an endocrine fate by

upregulating the expression of insulin, glucagon and important endocrine TFs (Song, Ko *et al*. 2004). Since there was no co-expression of insulin and amylase, the authors propose that the acinar cells may first convert to duct-like cells before transdifferentiating to beta cells (Song, Ko *et al*. 2004). Baeyens *et al*. (2009) reported that Notch signalling must be overcome to allow Ngn3 expression before acinar cells can be converted to beta cells. Additionally, these authors revealed that the newly formed beta cells are immature; however, when transplanted into diabetic animals, the beta cells matured and were capable of regulating glycaemia (Baeyens, Bonne *et al*. 2009). *In vivo*, acinar cells have been converted to functional beta cells by the transient administration of epidermal growth factor and ciliary neurotrophic factor (two cytokines), and Ngn3 expression was a prerequisite for beta cell regeneration (Baeyens, Lemper *et al*. 2014).

As previously discussed, induced expression of Pdx1, Ngn3 and MafA in a ductal cell line could convert duct cells to beta cells (Miyashita, Miyatsuka *et al*. 2014); however, in normal and STZ-induced diabetic mice expression of these three TFs resulted in the conversion of acinar cells to beta cells (Zhou, Brown *et al*. 2008). Moreover, different combinations of these TFs result in the conversion of acinar cells to other endocrine cell types (Li, Nakanishi *et al*. 2014). For example, ectopic Ngn3 expression alone converted acinar cells to delta cells, while Ngn3 in combination with MafA converted acinar cells to alpha cells (Li, Nakanishi *et al*. 2014). While these studies point out acinar cells as a source of endocrine cells, *in vivo* models of pancreatic injury (partial pancreatectomy and PDL) indicate that acinar cells only contributed to acinar regeneration and not to islet regeneration (Desai, Oliver-Krasinski *et al*. 2007).

The literature reviewed above gives examples of beta cell formation by means of regeneration from previously differentiated cellular sources; *in vitro* beta cells may, however, also be formed by means of neogenesis from mesenchymal stem cells (MSCs). Growth factors and hormones, obtained from pancreatic extracts of pancreatectomized rats, stimulate rat bone morrow-derived MSCs (BM-MSCs) to form islet like structures with beta cells in culture (Choi, Shin *et al*. 2005). Likewise, human BM-MSCs and adipose tissue-derived MSCs have been converted to insulin producing cells by manipulating TF expression and the culture microenvironment (Moriscot, de Fraipont *et al*. 2005, Timper, Seboek *et al*. 2006).

In vivo studies have suggested that MSCs may interact with pre-existing beta cells to induce new beta cell formation (Tchokonte-Nana 2011). Sordi *et al*. (2005) found that human BM-

MSCs express chemokines and chemokine receptors that allow their migration to the islets of Langerhans, a process that was confirmed to occur when these cells were transplanted into a mouse model. Following transplantation, BM-MSCs are located within and around islets (Sordi, Malosio *et al*. 2005, Gao, Song *et al*. 2014). Gao *et al*. (2014) subsequently proved that BM-MSCs influence beta cell formation in a paracrine manner, as diabetic mice treated with BM-MSC conditioned medium obtained even lower blood glucose levels than diabetic mice treated with BM-MSC transplantation.

While various studies discussed in this section propose different cellular sources from which beta cells may be generated, it is generally agreed upon that the adult pancreas does possess some degree of plasticity. Furthermore, it becomes apparent that the mechanism of beta cell formation and the source from which newly formed beta cells arise may vary depending on the stimulus. One possible stimulus for beta cell formation is PDL, a procedure still much debated in the literature.

2.2.2.2 Pancreatic duct ligation (PDL)

During the surgical procedure of PDL the main pancreatic duct is occluded, modelling pancreatic injury and reportedly inducing beta cell formation (Edstrom, Falkmer 1968, Page 2000, Tchokonte-Nana 2011, Van de Casteele, Leuckx *et al*. 2013). PDL has been described as a good model for human pancreatitis (Meyerholz, Samuel 2007). It is important to note that these authors ligated the pancreatic duct close to its entrance into the duodenum, effectively occluding the entire duct, and causing damage to the entire pancreas (complete PDL) (Meyerholz, Samuel 2007). However, in models investigating beta cell formation, partial PDL is commonly used, in this instance the duct may be occluded at a point one third proximal to the tail of the pancreas, leaving a proximal segment of unligated pancreatic tissue (Tchokonte-Nana 2011, Cavelti-Weder, Shtessel *et al*. 2013). Partial PDL will be further discussed and was used in the current study.

Within five days following partial PDL, drastic morphological changes occur in the part of the pancreas distal to the ligature; these changes have been grouped into four landmarks of morphological similarity (Tchokonte-Nana 2011). Within one day of PDL (first landmark) oedema and ductal dilation can be observed, accompanied by macrophage infiltration and the start of acinar cell deletion (Hamamoto, Ashizawa *et al*. 2002, Tchokonte-Nana 2011). Tchokonte-Nana (2011) further reported mesenchymal proliferation during this period. Acinar cell death and ductal dilation continued during the second landmark (36-60 hours post-PDL)

(Hamamoto, Ashizawa *et al*. 2002, Tchokonte-Nana 2011). The third landmark (three days post-PDL) is characterized by complete acinar cell deletion. Acinar tissue was found to be remodelled by the fourth landmark (84-120 hours) (Tchokonte-Nana 2011). The four landmarks described above are based on a PDL model in Sprague-Dawley rats (Tchokonte-Nana 2011) and the PDL induced morphological changes previously observed in a Wistar rat model correlates with these landmarks (Hamamoto, Ashizawa *et al*. 2002).

In terms of morphology, the islets of Langerhans are seemingly unaffected by the surrounding damage to the exocrine pancreas (Tchokonte-Nana 2011). However, Catala *et al*. (2001) reported disruption of islet architecture following complete PDL in a rabbit model. In their model fibrotic tissue caused islets to dissociate, concomitantly inducing beta cell death (Catala, Daumas *et al*. 2001). These contradictory results may be due to the respective use of partial and complete PDL or the use of different species.

In mice, PDL-induced acinar cell death is reported to occur up to 1 week post-PDL (Hakonen, Ustinov *et al*. 2011). An early PDL study did not report any acinar regeneration (Edstrom, Falkmer 1968), although this observation has been reported in more recent studies (Tchokonte-Nana 2011, Cavelti-Weder, Shtessel *et al*. 2013). In another study on Sprague-Dawley rats, acinar formation was only observed 10 days post-PDL and only in one third of the animals studied (Page 2000). Regardless of the time frame, it is consistently reported, in different species and strains, that PDL induces initial apoptosis of acinar cells and proliferation of ductal cells (Page 2000, Hamamoto, Ashizawa *et al*. 2002, Xu, D'Hoker *et al*. 2008, Hakonen, Ustinov *et al*. 2011, Chintinne, Stange *et al*. 2012, Rankin, Wilbur *et al*. 2013). Furthermore, these morphological changes only occur in the part of the pancreas distal to the ligature, while the part preceding the ligature remains unaffected (Ustinov *et al*. 2011, Cavelti-Weder, Shtessel *et al*. 2013, Hakonen, Rankin, Wilbur *et al*. 2013, Hao, Lee *et al*. 2013).

In mice, beta cell volume, beta cell mass, absolute beta cell number and total islet number are increased in the PDL tail (part of the pancreas distal to the ligature) (D'Hoker *et al*. 2008, Hakonen, Ustinov *et al*. 2011, Xu, Van de Casteele, Leuckx *et al*. 2013). Beta cell formation was predominantly the result of increased replication of pre-existing beta cells; additionally, beta cell formation from Ngn3 positive progenitors was observed (Van de Casteele, Leuckx *et al*. 2013). Moreover, these authors report that Ngn3 expression is essential for beta cell formation following PDL (including for beta cell replication) (Xu, D'Hoker *et al*. 2008, Van

de Casteele, Leuckx *et al*. 2013). In Ngn3 deficient mice, beta cell formation was decreased by 66% and the authors proposed that Ngn3 positive progenitors may be the source of replicating beta cells (Xu, D'Hoker *et al*. 2008). While epidermal growth factor signalling is essential for increased beta cell formation during pregnancy and obesity, PDL induced regeneration was found to occur effectively without epidermal growth factor signalling (Hakonen, Ustinov *et al*. 2011).

When interpreting the results of PDL studies, it is important to consider the method by which beta cell formation was assessed. The beta cell mass is often quantified as the insulin positive area per area of pancreas (Hakonen, Ustinov *et al*. 2011, Hao, Lee *et al*. 2013). These results may overestimate beta cell formation since acinar deletion causes total pancreatic area to decrease and islet density to increase (Chintinne, Stange *et al*. 2012). Chintinne *et al*. (2012) proposes that beta cell count may provide more accurate results. These authors do not report an increase in total beta cell number two weeks following PDL; however, PDL resulted in an increase in the number of small beta cell clusters which is indicative of neogenesis (Chintinne, Stange *et al*. 2012). The formation of insulin rich endocrine areas following PDL is also reported in rats; these endocrine formations became indistinguishable from pre-existing islets by day 10 post-PDL (Page 2000). Furthermore, beta cells within these small clusters are reported to have increased proliferative capacity and it was hypothesised that total beta cell number may increase at later time points post-PDL (Chintinne, Stange *et al*. 2012).

Apart from the fact that PDL has an effect on beta cells, it may also influence the other endocrine cell types and whole islet architecture. An increase in alpha cell number two weeks post-PDL has previously been reported in mice (Chintinne, Stange *et al*. 2012). In rats, alpha cells are reportedly deleted from the mantle zone of islets, while PP and delta cells appear within the islet core two and a half days post-PDL (Page 2000). PDL induced endocrine formations had a beta cell core surrounded by a thin alpha cell layer with no delta or PP cells (Page 2000).

Despite mounting evidence for PDL as an effective method for inducing beta cell formation, recent studies present evidence to the contrary, reporting that beta cells are not generated following PDL (Rankin, Wilbur *et al*. 2013). Rankin *et al*. (2013) obtained similar changes in the exocrine pancreas as previously reported, however, in their model PDL failed to increase beta cell mass, beta cell proliferation or to induce conversion of non-beta cells to beta cells.

The PDL procedure has also been applied in combination with beta cell ablation and again results are contradicting. In a study where beta cells were ablated using STZ, PDL could not trigger beta cell formation even after 10 months (Cavelti-Weder, Shtessel *et al*. 2013). These findings are challenged by the results of a study using alloxan to destroy pre-existing beta cells. In this study PDL resulted in the conversion of alpha cells to beta cells (Chung, Hao *et al*. 2010). Newly formed islets in this model were disorganized and beta cell area, as well as blood glucose levels, did not normalize; therefore, in an attempt to rectify these abnormalities, the model was further elaborated by reversing the ligation one week after alloxan and PDL treatment (Hao, Lee *et al*. 2013). Reversal of the ligature resulted in a wave of beta cell replication (with no additional neogenesis) that normalized beta cell area and blood glucose levels (Hao, Lee *et al*. 2013).

3. PROBLEM STATEMENT

Diabetes mellitus is a metabolic disease characterized by the loss of beta cells from the islets (Atkinson 2000, Sherwood 2010, Kilimnik, Zhao *et al*. 2011), thereby disrupting islet composition and architecture which are important components that influence islet function (Weir, Samols *et al*. 1979, Meda, Kohen *et al*. 1982, Cabrera, Berman *et al*. 2006, Wang, Zhang *et al*. 2011, Farhat, Almelkar *et al*. 2013). Islet replacement therapy remains the hope in the treatment for diabetes, but the lack of donor organs is a clinical challenge. Novel techniques for the *in vivo* regeneration of beta cells within the adult pancreas may, however, be a better alternative. The use of PDL as a trigger for beta cell regeneration in the adult pancreas has previously been established (Wang, Kloppel *et al*. 1995, Page, du Toit *et al*. 2000, Tchokonte-Nana 2011, Hakonen, Ustinov *et al*. 2011, Van de Casteele, Leuckx *et al*. 2013) and the possibility that this model may have the capacity to restore normal islet composition and architecture could make it an effective approach to reverse diabetes. Many studies have attempted to study islet composition and architecture following PDL in diabetic animal models, but have focussed on only one or two cell types (Chung, Hao *et al*. 2010). The present study is the first that has made a comprehensive investigation of islet composition and architecture, including the four islet cell types, and compared the effects of PDL treatment on both portions of the pancreas, proximal and distal to the ligature, in a diabetic PDL model. We hypothesise that PDL may restore islet composition and architecture in diabetic animals.

4. AIM AND OBJECTIVES

4.1 AIM

This study aims to determine the relative cellular composition and architecture of islets in STZ-induced diabetic rats and to establish the effect of PDL treatment on this composition and architecture.

4.2 OBJECTIVES

In order to achieve this aim, the following objectives were set:

1. To assess the histomorphology of the pancreas of
    a. normal control animals
    b. STZ-induced diabetic control animals at day 0, 3, 5, 10 and 30
    c. experimental PDL treated STZ-induced diabetic animals at day 3, 5, 10 and 30;
2. To determine islet cell type composition using protein expression of insulin, glucagon, somatostatin and pancreatic polypeptide in the pancreas of
    a. normal control animals
    b. STZ-induced diabetic control animals at day 0, 3, 5, 10 and 30
    c. experimental PDL treated STZ-induced diabetic animals at day 3, 5, 10 and 30;
3. To establish the architecture of islets by identifying the distribution and location of the islet cell types within the islets using protein expression of insulin, glucagon, somatostatin and pancreatic polypeptide in the pancreas of
    a. normal control animals
    b. STZ-induced diabetic control animals at day 0, 3, 5, 10 and 30
    c. experimental PDL treated STZ-induced diabetic animals at day 3, 5, 10 and 30;
4. To measure blood glucose and insulin levels of normal control, diabetic control and experimental animals

5. MATERIALS AND METHODS

5.1 ETHICAL APPROVAL

Ethical clearance was obtained from the Stellenbosch University's Research Ethics Committee (ethics number SU-ACUM14-00018). The study protocol complies with the guiding principles laid down by Animal Welfare Organization as well as the Society for the Prevention of Cruelty to Animals (SPCA) and is in agreement with the ethical guidelines as proposed by the South African National Standard (SANS) on the care and use of animals for scientific purposes.

5.2 THE ANIMALS

Healthy male Wistar rats (n=55) weighing between 180-260g were randomly selected from the Central Animal Unit (CAU) of the Faculty of Medicine and Health Sciences (FMHS) of Stellenbosch University. The rats were housed at the Animal Unit at room temperature on a 12 hour light/dark cycle, and were fed standard rat pellets (Appendix A) with free access to water. Rats were weighed using an electric scale and their non-fasting blood glucose levels (BGL) were recorded (Appendix B) as baseline measurements. Rats were then fasted overnight (with water available *ad libitum*) prior to the induction of diabetes.

5.2.1 Diabetes induction

Following the fast, animals received an intraperitoneal injection of 45mg/kg streptozotocin (STZ) dissolved in a cold sodium citrate buffer (Appendix C). Subsequently, non-fasting BGL and body weight (BW) of the animals were measured every second morning (between 08:00 and 10:00), for ten days. Animals were not fasted to avoid further stress and excessive weight loss. Diabetes induction was accompanied by an increase in water intake and urination. For this reason there was a need to add an additional bottle of water to each cage on day nine post-STZ injection. On day 10 post-STZ injection, animals with BGL exceeding 14.0mmol/L were considered diabetic and were included in the study groups. Day 10 post-STZ injection was considered as experimental day 0.

5.2.2 Study groups

Animals were divided into control animals and experimental animals (Appendix D). The control animals were divided into two (2) groups, the normal control (NC) group (n=6) and the diabetic control (DC) group (n=27). The NC group consisted of non-diabetic untreated rats having BGLs of less than 9.10 mmol/L and euthanized prior to the overnight fast and STZ

injection. The DC group consisted of diabetic rats (n=27) that did not receive further surgical procedure. The DC group was further divided into subgroups of 0-, 3-, 5-, 10- and 30 days corresponding to the day at which they were euthanized, and were named the DC0 group, DC3 group, DC5 group, DC10 group and DC30 group, respectively.

The experimental animals (n=22) formed the experimental (EX) group and consisted of diabetic animals that received surgical procedure with a pancreatic duct ligation (PDL). The EX group was divided into subgroups of 3-, 5-, 10- and 30 days corresponding to the day at which they were euthanized, and were named the EX3 group, EX5 group, EX10 group and EX30 group, respectively.

Non-fasting BGL and the BW of all animals were measured at the time points corresponding to the study groups.

5.3 PANCREATIC DUCT LIGATION

Animals in the experimental groups underwent PDL. The surgery was carried out in a surgical theatre of the CAU of the FMHS of Stellenbosch University. Prior to surgery, animals were housed in clean cages at the CAU and water and food were made available *ad libitum*. On the day of PDL, the animals were anaesthetised via the inhalation of Isofor (Appendix E) vaporized in oxygen. When foot or tail pinching no longer elicited a withdrawal response and rats had no spontaneous movement, abdominal hair (approximately 1cm) on both sides of the linea alba was removed with an electric shaver and the exposed skin was cleaned with alcohol.

The animals were subsequently placed in dorsal recumbence on the surgical table and an incision was made along the midline through the linea alba, starting approximately 1cm inferior to the xiphoid process and extending for approximately 1.5 cm towards the pubic symphysis. The duodenum, stomach and spleen were identified by placing pressure on the lateral side of the left upper quadrant of the abdomen. The stomach and duodenum were drawn out and reflected cranially to expose the pancreas lying posterior to it. The pancreas appeared as a diffuse tissue mass and sterile cotton buds were used to carefully expose the pancreatic duct, which appeared as a thin translucent structure within the diffuse tissue mass of the pancreas. An operating microscope (Appendix E) was used to ensure correct identification of the pancreatic duct. A single tight suture was made with non-resorbable suture material to occlude the pancreatic duct at a point 1/3 proximal to the tail (splenic part)

of the pancreas (Figure 5.1). Warm saline solution was introduced into the abdomen to prevent dehydration of the organs and the abdominal cavity was closed by two layers of stitching: first the muscle layer, followed by the skin layer. The PDL procedure lasted for about ten minutes. An antiseptic rub was applied to the wound to prevent infection and scratching. Intraperitoneal injections of 100 µl of Baytril, an antibiotic for the prevention of infection, and 100 µl Temgesic, for pain relief, were given to the animals post-operation. The animals were returned to their cages in a thermally controlled environment for recovery and were housed with free access to food and water until they were euthanized.

To minimize the number of animal used in the study (as per the ethics requirements), no animals were sham operated. This exclusion follows observations made from research studies in the Islet Research Group at Stellenbosch University (Page, du Toit *et al*. 2000, du Toit, Longo-Mbenza *et al*. 2011, Tchokonte-Nana 2011) and by many other authors (Hamamoto, Ashizawa *et al*. 2002, Chintinne, Stange *et al*. 2012, Rankin, Van de Casteele, Leuckx *et al*. 2013, Cavelti-Weder, Shtessel *et al*. 2013, Wilbur *et al*. 2013), that there is no difference between sham operated and control animals and that the sham operation does not induce changes in the pancreas as is observed following PDL.

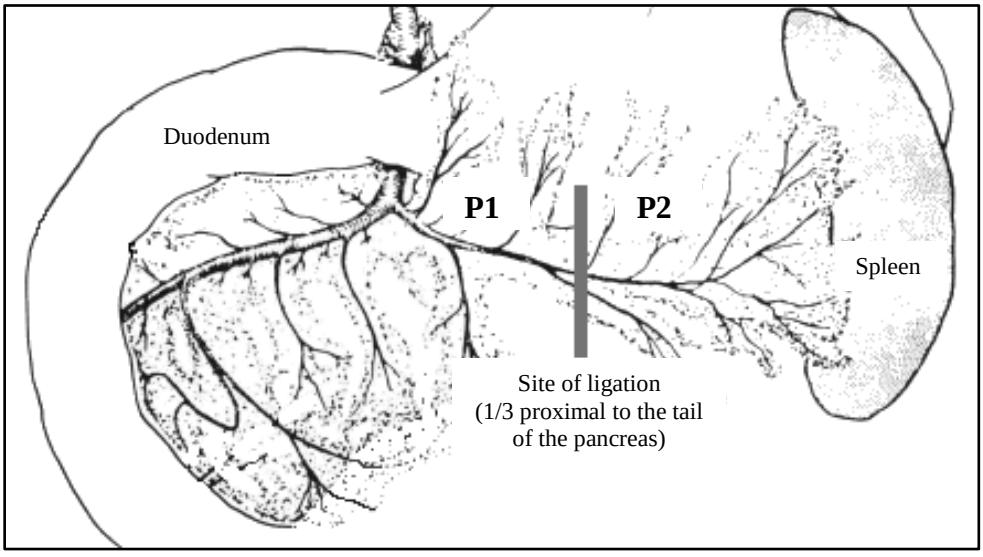

Figure 5.1. The pancreas of the rat in-situ. Adapted image (Page 2000).

5.4 TISSUE AND BLOOD SAMPLE COLLECTION

5.4.1 Tissue collection

Pancreata were collected for histological evaluation at the time points corresponding to the animal's designated study group. Animals were prepared for surgery and the abdominal cavity was opened according to the procedures described in Section 5.3. The pancreas was exposed by drawing out the duodenum and stomach, and was removed along with the spleen.

All pancreata were divided into two portions at a point 1/3 proximal to the tail of the pancreas (Figure 5.1). Proximal portions of the pancreata were designated as P1 tissue portions, while the distal portions of the pancreata were designated as P2 tissue portions. Tissue portions were individually placed in formalin for 48 hours prior to processing.

5.4.2 Blood collection

Blood samples (5 ml) were collected from the animals by cardiac puncture while they were under terminal anaesthesia. The samples were kept in anti-coagulation blood collection tubes with gel for serum separation. Animals were then euthanized by exsanguination and the carcases incinerated. Within two hours of collection, blood samples were centrifuged at 1000 rmp for 10 minutes; blood serum (2 ml) was collected from each tube and stored at -80 ˚C until the serum insulin levels were determined using an insulin ELISA kit (Appendix F).

5.5 HISTOLOGICAL STUDY

5.5.1 Processing and Sectioning

The fixed pancreatic portions were transferred to labelled cassettes and exposed to standard histological tissue processing procedures (Appendix G). The resulting processed tissues were embedded using a mould filled with melted paraffin wax (60 ˚C). Tissue blocks obtained were placed in a freezer to cool for approximately two hours before sectioning.

Tissue sections were cut at 3µm thickness using a Leica RM 2125 RT microtome (Appendix H). Five sections were made per tissue block in the following manner: sections 1, 2 and 3 were cut, then the tissue blocks were trimmed for a least 24 µm to ensure that different islets would be obtained before cutting sections 4 and 5. The first section was placed on a labelled frosted slide (a) and was used for the H&E staining (Figure 5.2). Sections 2 and 4 were mounted together on a labelled positively charged slide (b), while sections 3 and 5 were

mounted together on a labelled positively charged slide (c); slides b and c were used for immunohistochemical (IHC) staining (Figure 5.2).

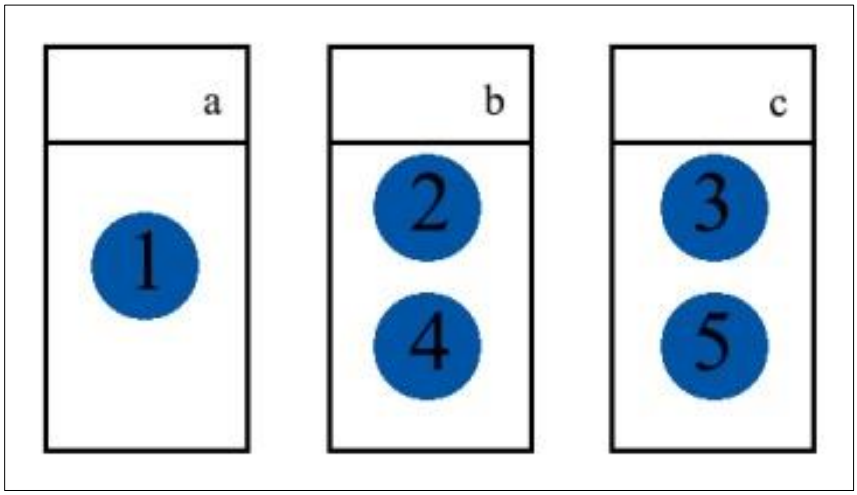

Figure 5.2. Tissue sections on a frosted slide (a) and positively charged slides (b & c).

The tissue slides were labelled as follows: the animals' subgroups were used as prefixes, individual animals were represented by the radicals A to F, the tissue portions were indicated by the suffixes P1 and P2, and lastly "a", "b", and "c" representing the sections were used as indices. For example, a slide labelled as $DC30AP1_b$ would indicate a slide with the 2^{nd} and 4^{th} section made from a P1 portion of pancreas harvested from animal A in the DC30 subgroup.

5.5.2 Haematoxylin and eosin (H&E) staining

Haematoxylin and eosin staining was performed on all slides with index "a", using a Leica Auto Stainer XL (Appendix H) with a pre-programmed protocol (Appendix I). These slides were used to evaluate the general morphological appearance of the pancreas of the P1 and P2 portions of the pancreas of the different study groups.

5.5.3 Immunohistochemical staining

A sequential double-staining approach was used to stain pancreatic tissue sections on all slides with indices "b" and "c", using a Leica Bond Max imuno-autostainer (Appendix H) with a pre-programmed protocol (Appendix J). All slides with index "b" were stained for insulin and pancreatic polypeptide using anti-insulin (MU029-UC, BIOCOMbiotech, Centurion, South Africa) and anti-pancreatic polypeptide (AB113694, BIOCOMbiotech, Centurion, South Africa) antibodies, respectively. All slides with index "c" were stained for glucagon and somatostatin using anti-glucagon (AB10988, BIOCOMbiotech, Centurion, South Africa) and anti-somatostatin (AB22682, BIOCOMbiotech, Centurion, South Africa)

antibodies, respectively (Appendix K). Tissues slides from NC groups were used as positive controls for the immunohistochemical stains. The Bond Polymer Refine Detection Kit (Appendix H) stained the target proteins BROWN for the antibody that was applied first (Insulin or glucagon), while the antibody that was applied second (pancreatic polypeptides or somatostatin) had the target proteins stained RED with the Bond Polymer Refine Red Detection Kit (Appendix H). All tissue slides were taken for manual rehydration (Appendix J) following the staining procedures; the slides were then mounted in DPX and cover slipped for viewing under the light microscope.

5.6 MORPHOMETRIC ANALYSIS

Immunohistochemically stained tissue sections were morphometrically analysed to determine islet composition and architecture. The slides were mounted under the Zeiss Aksioskop2 microscope (serial number 801452, Carl Zeiss, AG, Oberkochen, Germany), the tissue area was manually scanned for islets and the image acquisition was done using AxioVision software (version 4.7.2.0, Carl Zeiss Microscopy, AG, Oberkochen, Germany). In each study group, a total number of 100 islets were used per P1 and P2 portion of the pancreas. Morphometric analysis of individual islets were done using the ZEN Lite 2012 software (blue edition, version 1.1.2.0,Carl Zeiss Microscopy GmbH, Germany) for the following measurements:

1. Total islet surface area (Λ+R) [where Λ represents the hormone positive cells and R represents hormone negative cells];
2. Islet surface area positive for insulin, glucagon, somatostatin or PP, respectively (Λ);

The hormone fraction (Fr) was calculated for each islet as the ratio of the surface area positive for a specific hormone (Λ) to the total islet surface area (Λ+R) and was expressed as a percentage.

$$Fr = \frac{\Lambda}{\Lambda + R}$$

The fractions from 100 islets per portion of the pancreas were used to determine the mean hormone fractions and this represented the islet composition in each portion of the pancreas.

Furthermore, to consider the relative amount of each hormone present within the hormone positive fraction, the staining intensity of each hormone was studied and classified as none, low, moderate or high.

The final islet architecture was determined using the distribution of each cell type within the islet and was classified as core (C-classification), mantle (M-classification) or both (B-classification).

5.7 STATISTICAL ANALYSIS

Hormone fraction data were transported into STATA 13 (StataCorp, 2013, Stata: Release 13, Statistical Software, College Station, Texas, USA) for statistical analyses. Simple descriptive statistics was used to describe the variables. No missing data was present. Data was checked for outliers and data errors; from the insulin fraction data one entry was excluded due to data entry error. Variables were tested for normality qualitatively (histograms and qq plots) and quantitatively. For hypothesis testing, where outcome data was not normally distributed, log transformations were done to obtain normality. Multilevel mixed-effects linear regression was used to determine differences between interventions/groups taking into account the repeated measurements within rats. Predictors were considered as fixed effect parameters and the unique rat id as the random effects. An alpha (p-value) of 0.05 was considered statistically significant. No post-hoc analysis was performed. The BGL, BW, hormone staining intensity and cell type distribution data was used for descriptive purposes only and was not statistically analysed.

6. RESULTS

6.1 BLOOD GLUCOSE LEVELS AND BODY WEIGHT

6.1.1 Diabetes induction period

The DC and EX animals (n=49) were treated with STZ to induce diabetes over a period of 10 days. During the diabetes induction period non-fasting BGL and BW measurements were taken on various days, as indicated in Figure 6.1 (Appendix L and Appendix M).

Prior to STZ injection (at baseline) these animals had an average BGL of 6.81mmol/L. Following the overnight fast the BGL (fasted) decreased to 4.37 mmol/L and on the same day, animals were injected with STZ. A sharp increase in BGL was evident as early as day one post-STZ injection (STZ 1d), with an average BGL of 25.68 mmol/L. By day 10 post-STZ injection (STZ 10d) all animals were diabetic (BGL > 14.00 mmol/L) with an average BGL of 29.39 mmol/L.

In addition to the BGL measurements, the effects of STZ injection were also reflected in the rat's BW measurements (Figure 6.1B). Animals had an average BW of 227.2 g at baseline, which decreased to 216.2 g following the overnight fast. There was a fluctuation in the BW throughout the 10 days following STZ treatment. However, the BW still remained lower by day 10 (STZ 10d) than at baseline.

STZ d10 was considered as day 0 of the experimental period and was referred to as day 0 (d0). On this day (d0) diabetic animals were divided into a DC groups and an EX groups.

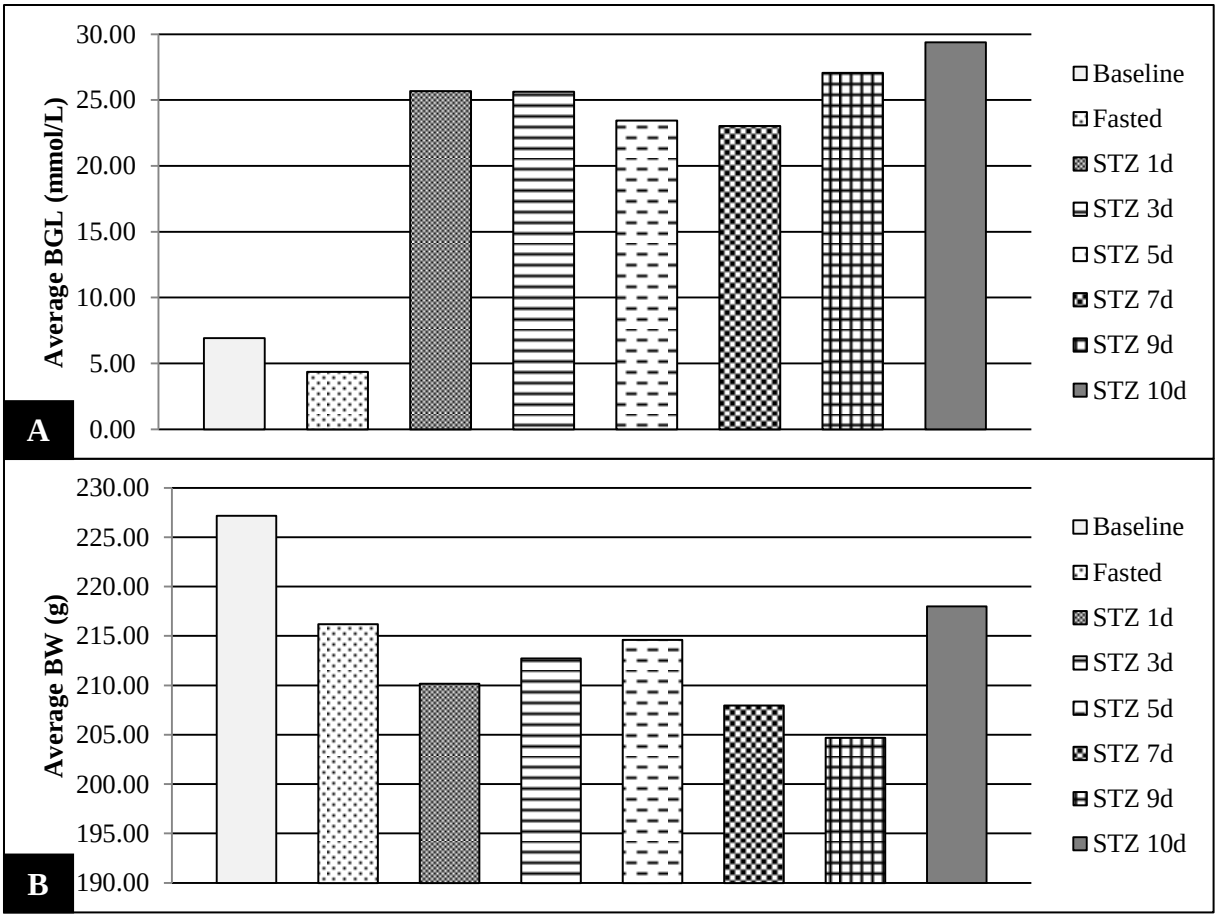

Figure 6.1. Column charts showing non-fasting BGL (A) and BW (B) of 49 rats for baseline, fasted and 10 days post-STZ injection. (STZ) streptozotocin; (d) day.

6.1.2 Experimental period

Non-fasting BGL and BW measurements taken during the experimental period are indicated in Figure 6.2 (Appendix L and Appendix M).On day 0, the BGL of all the DC and EX groups was >20.00 mmol/L. The EX30 group had the highest BGL (32.32 mmol/L), while the DC5 group had the lowest BGL (24.38 mmol/L) (Figure 6.2A). On day 3, BGL was increased compared to day 0 in the DC3, DC5 and DC10 groups, while BGL decreased in the remaining DC and EX groups. On this day the DC10 groups had the highest BGL (33.30 mmol/L) and the DC30 group had the lowest BGL (19.46 mmol/L). On day 5, BGL increased in the EX10, DC30 and EX30 groups and was the highest in the EX30 group (29.04 mmol/L), while BGL decreased in the DC5, EX5 and DC10 groups and was the lowest in the EX5 group (23.37 mmol/L). BGL on day 10 increased in the DC10 group to the highest value observed at this time point (33.30 mmol/L), while a decrease was observed in the EX10, DC30 and EX30 group with the lowest BGL observed in the DC30 group (19.46 mmol/L). On day 30, BGL was increased in both the DC30 and EX30 groups. BGL was higher in the EX30 group (29.04

mmol/L) compared to the DC30 group (24.10 mmol/L). While the BGL fluctuated in the DC and EX groups over the experimental period, there was no tendency for BGL to decrease over time.

Fluctuations were also observed in the animals' BW (Figure 6.2B). On day 0, the EX5 group had the highest BW. By day 3, BW increase was observed in the DC3, DC5, DC30 and EX30 groups with the DC5 group having the highest BW (227.2 g), while BW decrease was observed in the remaining DC and EX groups. On day 5, BW increase was observed in the DC5, EX5, DC10 and EX10 groups with the DC5 group having the highest BW (228.4 g); at the same time BW decrease was observed in the DC30 and EX30 groups. BW on day 10 was again decreased in the DC30 and EX30 groups, while further increase was observed in the DC10 and EX10 groups, with EX10 group having the highest BW (224.6 g). On day 30, BW increase was observed in the DC group (217.4 g), while a decrease was observed in the EX30 group (182.6 g). Throughout the experimental period, the EX30 group recorded the lowest BW, ranging between 211.6 g (day 3) and 182.6 g (day 30).

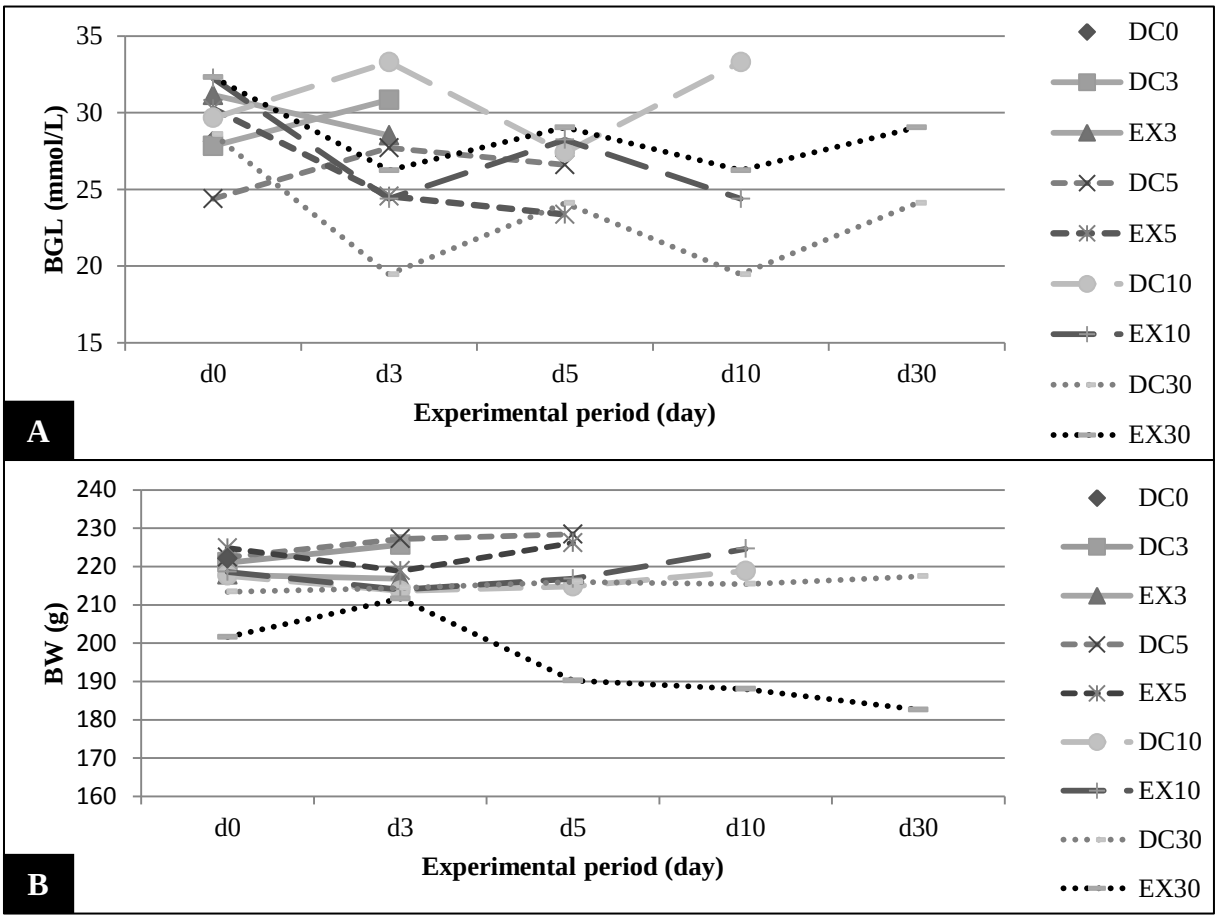

Figure 6.2. Line charts showing non-fasting BGL (A) and BW (B) in DC and EX groups during the experimental period. (DC) diabetic control; (EX) experimental.

6.2 SERUM INSULIN

Serum insulin of non-fasted animals in the NC, DC and EX groups was evaluated as an indication of beta cell function (Appendix N). A standard curve was generated using the human insulin ELISA kit which is known to react with rat samples. In our samples (non-diluted serum), few measured values were within the range of the standard curve (Figure 6.3), this included one animal in the NC group and 10 animals in the EX group. All other measurement fell below the range of the standard curve. Out of the 10 animals in the EX group, one measurement in the EX30 group was similar to the measurement from the NC group that was within the range of the standard curve. No animals in the DC groups had measurements within the range of the standard curve. This variation may indicate poor specificity of the human ELISA kit for our diabetic rat serum samples; and the fact that the animals were not fasted prior to blood collection could also have contributed to the variation.

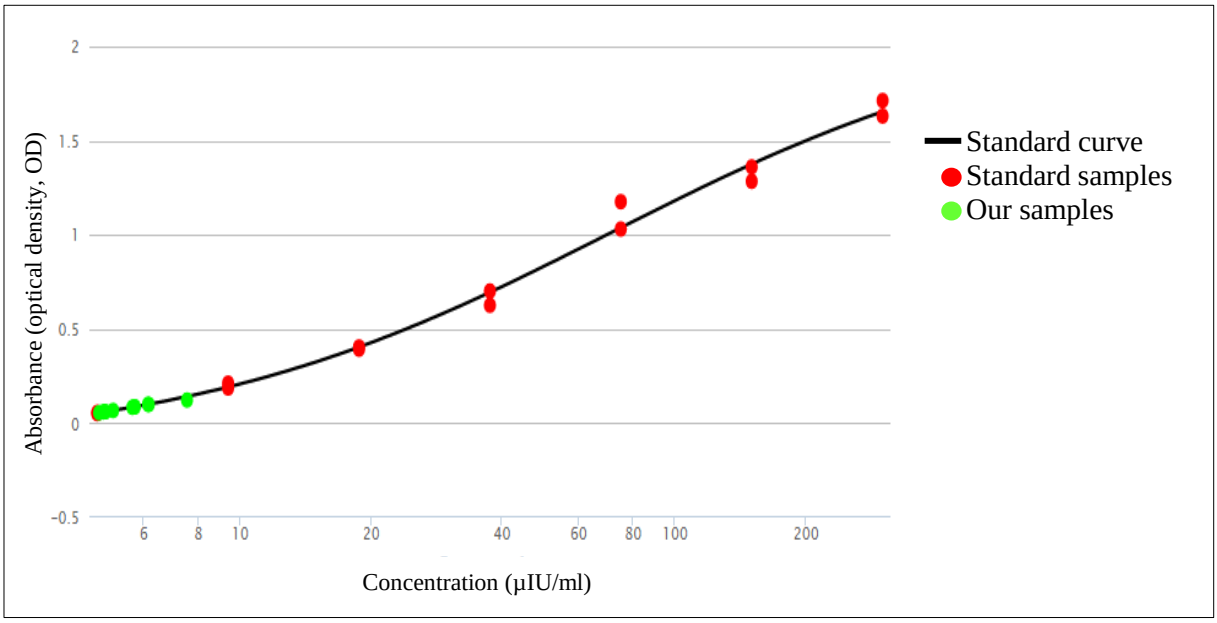

Figure 6.3. Graph showing non-fasting serum insulin samples within the range of the standard curve and standard measurements of the human insulin ELISA kit.

6.3 HISTOMORPHOLOGICAL EVALUATION OF THE PANCREAS

The microscopic slides from the NC, DC and EX groups were used to assess the morphological changes in the P1 and P2 portions of the pancreas (Figure 6.4 and Figure 6.5).

6.3.1 Control groups

In the NC group the exocrine compartment in both P1 and P2 tissue portions appeared healthy. Pyramidal acinar cells were arranged into acini and both intercalated and interlobular

ducts appeared normal. Islets of various shapes and sizes appeared pale in colour compared to acinar cells. These endocrine cells were densely packed and clearly delineated from surrounding exocrine tissue (Figure 6.4; NCP1 and NCP2).

In all the DC groups the exocrine compartment appeared healthy in both the P1 and P2 tissue portions, while progressive morpho-pathological changes were observed in their islets. In the DC0P1 and P2 slides the islets presented with acellular areas and with an indistinct separation between the endocrine and exocrine compartment. Furthermore, islet cells presented with necrotic changes, including degranulation, hydropic changes and pyknotic nuclei (Figure 6.4; DC0P1 and DC0P2).

In DC3P1 and P2 slides the pathological (necrotic) changes observed in the islets were similar to those of the DC0 group. In this group, however, the damage in the islets appeared more progressive with the presence of numerous acellular areas. Additionally, islets presented with an irregular shape with some islet cells having enlarged nuclei (Figure 6.4; DC3P1 and DCP2). This observation was common in the DC5P1 and P2 slides (Figure 6.4; DC5P1 and DCP2). The islet pathology observed in DC3 and DC5 groups persisted in DC10 and DC30 groups, with a slight increase in cellular density within the islets of DC10P1, DC10P2, DC30P1 and DC30P2 slides (Figure 6.4; DC10P1, DC10P2, DC30P1 and DC30P2).

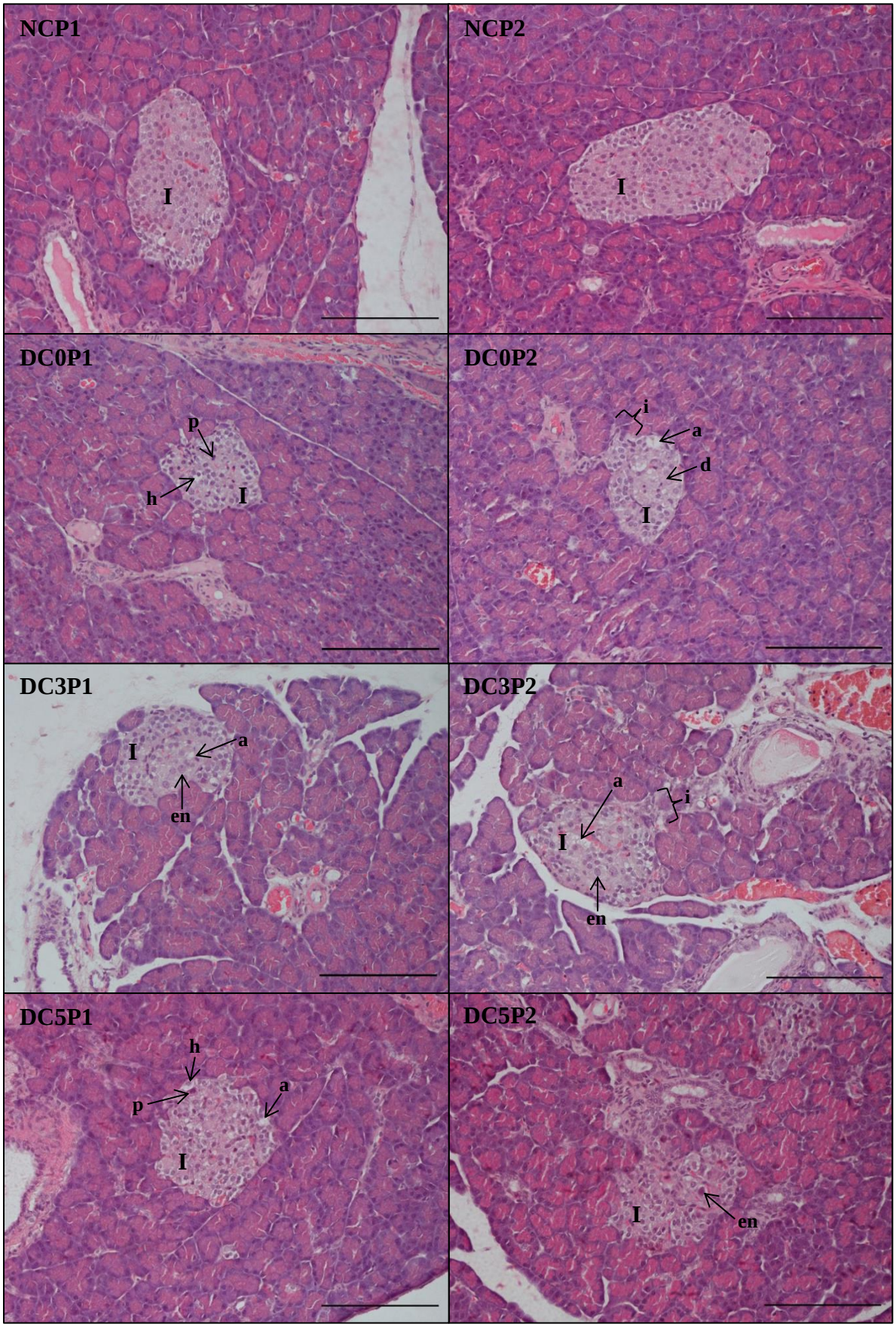

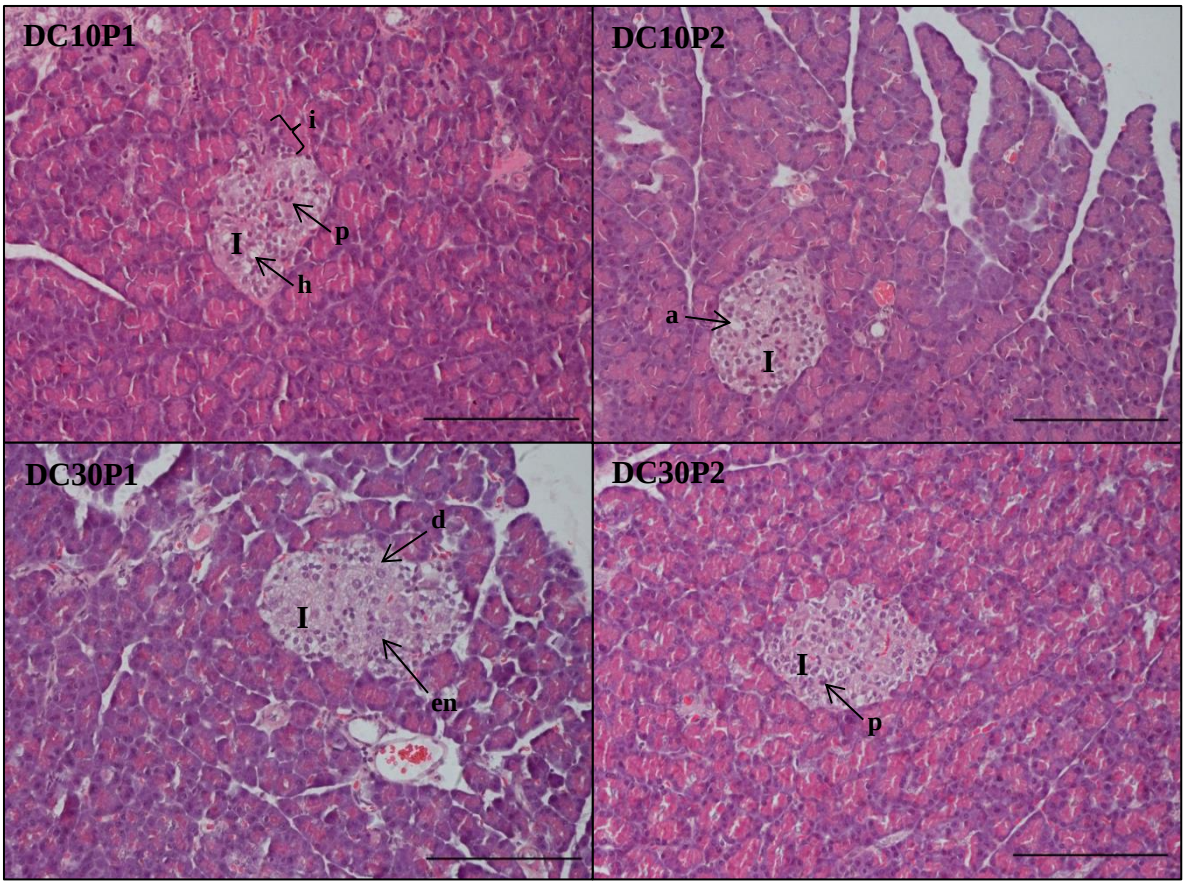

Figure 6.4. Representative H&E photomicrographs of P1 and P2 portions of the pancreas in NC and DC groups. Scale bar represents 100 µm. (NC) normal control; (DC) diabetic control; (P1) proximal portion of the pancreas; (P2) distal portion of the pancreas; (I) islet; (p) pyknotic nucleus; (h) hydropic changes; (a) acellular areas; (d) degranulation; (en) enlarged nucleus; (i) indistinct border.

6.3.2 Experimental groups

The EX animals presented with morphological changes in both the exocrine and endocrine compartments of the pancreas. Changes in the exocrine compartment differed between the P1 portion (proximal to the ligature) and P2 portion (distal to the ligature) within the same pancreas.

In the EX3P1 slides, exocrine tissues appeared unaffected by the PDL procedure (Figure 6.5; EX3P1). The exocrine compartment of the EX3P2 slides was severely affected by the PDL procedure, presenting with wide spread oedema, acinar deletion, ductal dilation and ductal proliferation. The islets in the P1 and P2 portions of the EX3 group presented with similar pathology as observed in the DC3 group; this includes degranulation, hydropic changes and pyknotic nuclei (Figure 6.5; EX3P1 and EX3P2). The deterioration of the morphology of the pancreas in the P2 portion does not allow clear delineation of islets in this portion.

The morphology of the exocrine tissue in the P1 portion of the EX5 group was not affected by the PDL procedure (Figure 6.5; EX5P1). The P2 portion presented with remodelling of the exocrine compartment showing healthy exocrine tissue; although some areas had oedema and mesenchymal proliferation (Figure 6.5; EX5P2). There was no change in the islet morphology in both P1 and P2 portions of the EX5 group compared to the EX3 group and islet morphology was similar to that observed in the DC5 group. (Hamamoto, Ashizawa *et al*. 2002)

The morphology of the exocrine tissue in the P1 and P2 portion of the EX10 group appeared healthy, with slight oedema and mesenchymal proliferation in the P2 portion (Figure 6.5; EX10P1 and EX10P2). Degenerative islets were similar in both portions (P1 and P2) of the EX10 group with the same morpho-pathology as observed in the DC10 group; with an increased cellular density within the islets of the P2 portion (Figure 6.5; EX10P2).

The exocrine tissue in the P1 and P2 portions of the EX30 group presented with a healthy morphology (Figure 6.5; EX30P1 and EX30P2). The damage in the islets of this group appeared less pronounced in the P1 and P2 portions than in any other treated group, although the shape of the islets remain irregular. There was an increase in the cellular density with normal appearance of the nuclei. Some islet cells did, however, present with degranulation and hydropic changes.

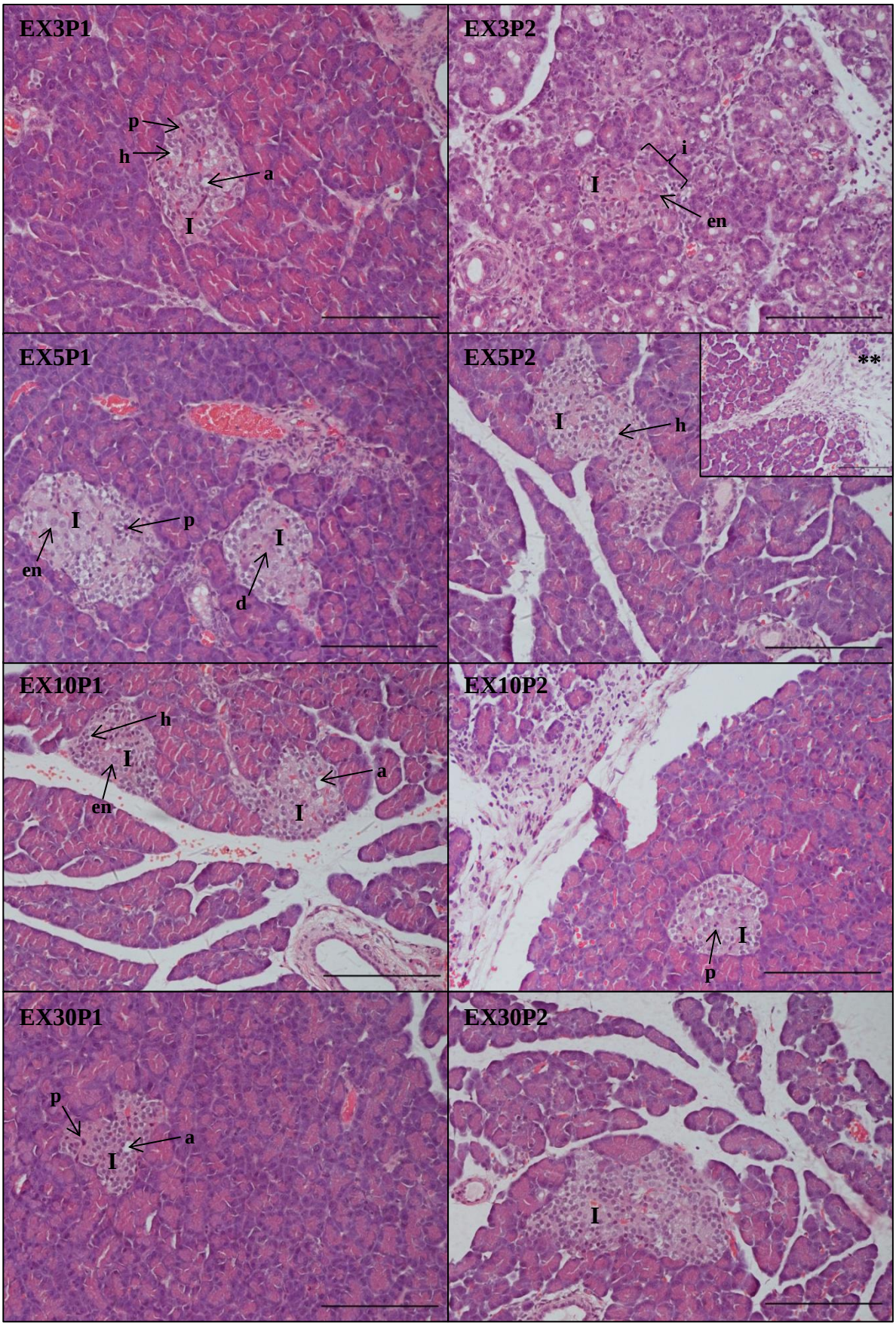

Figure 6.5. Representative H&E photomicrographs of P1 and P2 portions of the pancreas in EX group. Scale bar represents 100 µm. (EX) Experimental; (P1) proximal portion of the pancreas; (P2)

distal portion of the pancreas(I) islet; (p) pyknotic nucleus; (h) hydropic changes; (a) acellular areas; (d) degranulation; (en) enlarged nucleus; (i) indistinct border (**) insert showing changes in the exocrine compartment.

6.4 IMMUNOHISTOCHEMICAL EVALUATION OF ISLET COMPOSITION AND ARCHITECTURE IN THE PANCREAS

6.4.1 Insulin and Pancreatic Polypeptide protein expression

An IHC study was done to assess the protein expression of insulin and pancreatic polypeptide in the pancreas. The figures that follow demonstrate representative islets from the NC group (Figure 6.6), DC groups (Figure 6.7) and EX Groups (Figure 6.8) stained for insulin (red) and pancreatic polypeptide (brown). The IHC slides were used for the sole purpose of determining hormone fractions and to describe hormone staining intensity and distribution within the islet of the P1 and P2 tissue portions in the NC, DC and EX groups.

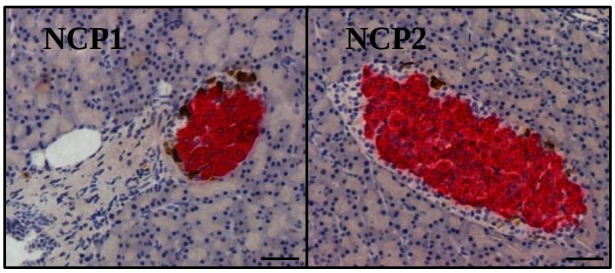

Figure 6.6. Representative IHC photomicrographs of islets in the P1 and P2 portions of the NC group with insulin (red) and pancreatic polypeptide (brown). Scale bar represents 50 µm. (NC) normal control; (P1) proximal portion of the pancreas; (P2) distal portion of the pancreas.

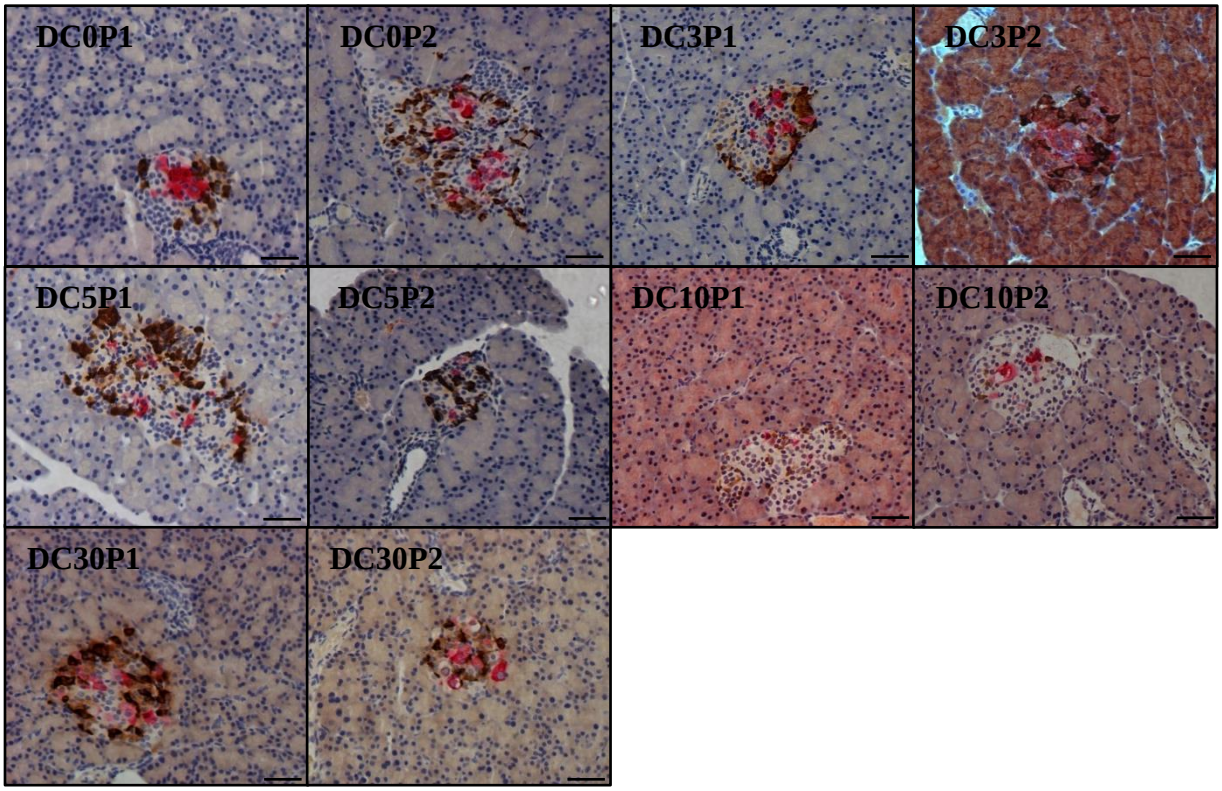

Figure 6.7. Representative IHC photomicrographs of islets in the P1 and P2 portions of the DC groups with insulin (red) and pancreatic polypeptide (brown). Scale bar represents 50µm. (DC) diabetic control; (P1) proximal portion of the pancreas; (P2) distal portion of the pancreas.

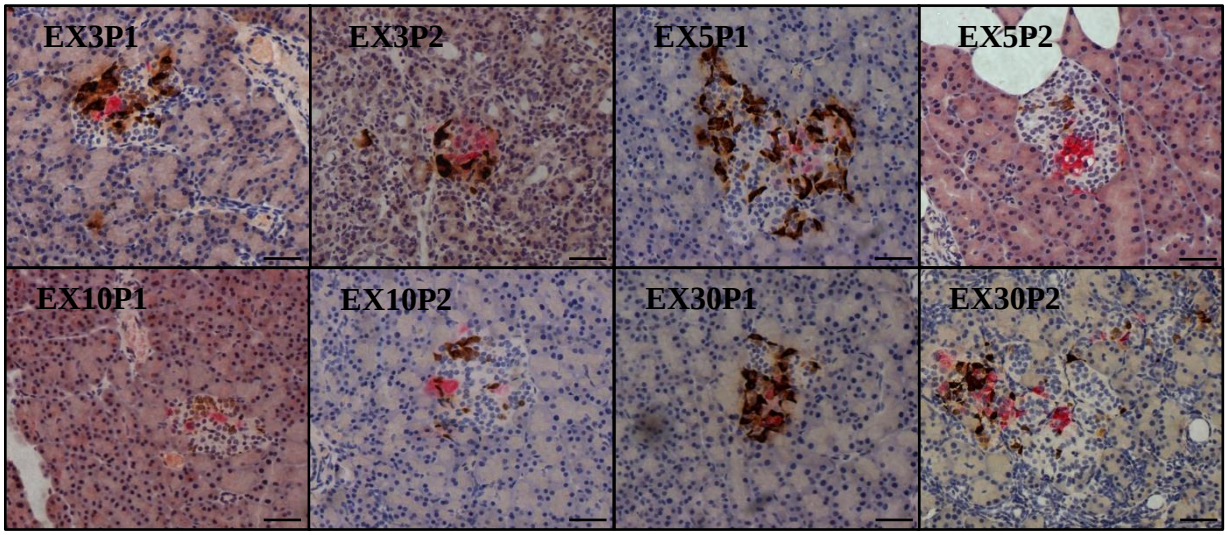

Figure 6.8. Representative immunohistochemical photomicrographs of islets in the P1 and P2 portions of the EX groups with insulin (red) and pancreatic polypeptide (brown). Scale bar represents 50µm. (DC) diabetic control; (P1) proximal portion of the pancreas; (P2) distal portion of the pancreas.

6.4.1.1 Insulin Fraction

Islet insulin fraction was morphometrically determined to establish the islet composition. This data was log transformed and the coefficients were interpreted as a percentage change in the geometric mean (GM) (Table 1).

Insulin fractions in the P1 and P2 portions were compared within each group. In the normal pancreata (NC group) insulin fraction was significantly higher in the P2 portion compared to the P1 portion (p=0.048). On average the insulin fraction GM was 16.37% higher in the P2 portion. A significant difference in insulin fraction between P1 and P2 tissue portions was also observed in the DC0 group. In this group, insulin fraction GM was 54.96% higher in the P2 portion compared to the P1 portion (p=0.000). Conversely, insulin fraction was significantly lower in the P2 portion (insulin fraction GM 72.65% lower on average) compared to the P1 portion in the DC3 group (p=0.000). However, P1 and P2 portions did not differ significantly in terms of insulin fraction in the DC5 and DC10 groups (p=0.406 and p=0.294, respectively). There was a significant difference in the insulin fraction in the P1 and P2 portion of DC30 group, with the fraction in the P2 portion being higher compared to the P1 portion (insulin fraction GM was increased with an average of 27.75%, p=0.035). No significant difference was found between insulin fractions in the P1 and P2 portions of the EX3 and EX10 groups, respectively (p=0.110 and p=0.522, respectively). However, insulin fraction was significantly higher in the EX5 P2 portion compared to the EX5 P1 portion; on average insulin fraction GM was 54.79% higher in the P2 portion (p=0.003). Insulin fraction tended to be higher in the P2 portion of the EX30 group compared to the respective P1 portions, but this was not considered significant (p=0.055).

Insulin fractions were compared between the P1 portion of the NC group and the P1 portions of all DC and EX groups; similarly insulin fractions were compared between the P2 portion of the NC group and the P2 portions of all DC and EX groups. Both P1 and P2 portions of the DC and EX groups had a significant decrease in insulin fraction compared to the NC group (p=0.000). On average the GM of the insulin fraction in the DC and EX groups was more than 100% lower throughout the experimental period when compared to the NC group. Moreover, the greatest difference was obtained in the EX30 versus the NC group, where the GM of the P1 and P2 portions were on average more than 200% lower.

To further analyse the data, insulin fractions were compared between the P1 portion of the DC0 group and the P1 portions of the DC3, DC5, DC10, DC30 and all EX groups. In a similar manner the insulin fractions of the P2 portion of the DC0 group and the P2 portions of the DC3, DC5, DC10, DC30 and all EX groups were also compared. Only the P1 portion in the EX30 group (EX30P1) has a significantly lower insulin fraction compared to the insulin fraction of the P1 portion of the DC0 group (p=0.001), while insulin fraction in the P1 portions in the other groups did not differ significantly from the insulin fraction of the P1

portions of the DC0 group (p>0.050). In the P1 portion of the EX30 group insulin fraction GM was on average 109.53% lower compared to the P1 portion of the DC0 group. When comparing P2 portions, the P2 portions of the DC3 and DC5 pancreata had significantly lower insulin fractions compared to the P2 portion of the DC0 group (p=0.001 and p=0.018, respectively). Insulin fraction GM was on average 111.47% and 85.44% lower in the P2 portions of the DC3 and DC5 groups when respectively compared to the P2 portion of the DC0 group. The insulin fraction of the P2 portions of the DC10 and DC30 groups did not significantly differ from the P2 portions of the DC0 group (p=0.245 and 0.280, respectively). In the EX3 group, the insulin fraction of the P2 portion was significantly decreased compared to the insulin fraction of the P2 portion of the DC0 group (p=0.025); insulin fraction GM being on average 76.67% lower in the P2 portion of the EX3 group. There was no significant difference in insulin fraction between P2 portions of the EX5 and DC0 groups (p=0.549). P2 portions of the EX10 and EX30 groups had significantly lower insulin fractions (GM on average 82.08% and 127.03% lower, respectively) compared to the P2 portion of the DC0 group (p=0.021 and p=0.000, respectively).

Insulin fractions of the corresponding portions (P1 or P2) were compared between DC and EX groups of the same experimental day. On day 3, 5 and 10 insulin fraction did not significantly differ between DC and EX groups when comparing both the P1 and P2 portions, respectively (p>0.050). On day 30 insulin fraction in the P1 portions differed significantly between DC and EX groups (p=0.001); the insulin fraction GM in the P1 portion of the EX30 groups was on average 101.20% lower compared to insulin fraction of the P1 portion of the DC30 group. Insulin fraction did not differ significantly in the P2 portions between the DC30 and EX30 groups (p=0.065).

Table 1. Insulin fraction data summary for 100 islets per portion of the pancreas

Group		25th percentile	50th percentile (median)	75th percentile	Arithmetic mean [95%CI]	Geometric mean (GM) [95%CI]
NC	P1	63.30	74.82	82.06	67.42 [62.79-72.54]	58.72 [51.14-67.42]
	P2	71.61	78.24	85.82	73.91 [70.23-77.79]	68.72 [62.48-75.56]
DC0	P1	0.68	11.62	23.12	14.90 [11.91-17.89]	13.58 [10.70-17.23]
	P2	8.87	22.91	36.33	24.15 [20.43-27.88]	22.68 [19.31-26.65]
DC3	P1	5.01	11.72	25.95	17.57 [14.08-21.06]	15.57 [12.94-18.73]
	P2	1.92	5.97	12.59	9.37 [6.94-11.81]	7.57 [6.14-9.33]
DC5	P1	2.09	7.96	18.00	17.34 [12.55-22.13]	11.49 [8.86-14.90]
	P2	0.59	4.87	23.15	17.83 [12.79-22.86]	11.39 [8.46-15.35]
DC10	P1	0.00	8.11	24.41	14.10 [10.74-17.45]	16.58 [13.23-20.78]
	P2	0.00	0.00	13.81	9.85 [6.67-13.02]	14.14 [11.02-18.12]
DC30	P1	2.73	9.24	21.75	16.81 [12.59-21.03]	13.00 [10.30-16.41]
	P2	0.00	10.06	34.12	20.88 [16.13-25.63]	18.21 [13.96-23.74]
EX3	P1	3.64	9.80	22.29	22.70 [7.41-37.98]	13.90 [11.17-17.30]
	P2	3.16	9.32	21.53	14.85 [11.64-18.06]	11.36 [8.91-14.49]
EX5	P1	0.00	0.00	11.06	7.82 [5.24-10.41]	10.34 [7.45-14.35]
	P2	0.00	10.43	27.17	16.51 [12.74-20.27]	18.48 [15.01-22.76]
EX10	P1	0.00	3.72	13.19	8.59 [5.97-11.21]	11.06 [8.75-13.99]
	P2	1.27	7.61	15.52	11.00 [8.54-13.46]	10.01 [8.15-12.29]
EX30	P1	0.00	0.00	3.53	11.66 [-5.11-28.43]	4.94 [3.44-7.10]
	P2	0.00	1.99	7.65	6.76 [4.22-9.31]	6.54 [4.89-8.74]

(NC) normal control; (DC) diabetic control; (EX) experimental; (P1) proximal portion of the pancreas; (P2) distal portion of the pancreas.

6.4.1.2 Insulin Staining Intensity

Insulin staining intensity was observed and classified as none, low, moderate or high. Figure 6.9 represents insulin staining intensity obtained from 100 islets per tissue portion (P1 and P2) in each one of the study groups.

All islets in the NC group stained positive for insulin, with predominantly high insulin staining intensity in the islets in the P1 and P2 portions. Insulin staining intensity in the P1 and P2 portions of the DC0, DC3 and DC5 groups were predominantly classified as moderate and low. This was also the case in the P1 portion of the DC10 group. In the DC30 and EX3 groups insulin staining intensity was predominantly classified as low and none (for both P1 and P2 portions). This was also the case for the P2 portions of the EX5, EX10 and EX30 groups. In DC and EX groups some islets were devoid of insulin expression; in the P1 portions of the EX5 and EX30 groups and in the P2 portion of the DC10 group more than 50% of the islets were devoid of insulin (staining intensity classified as “none”).

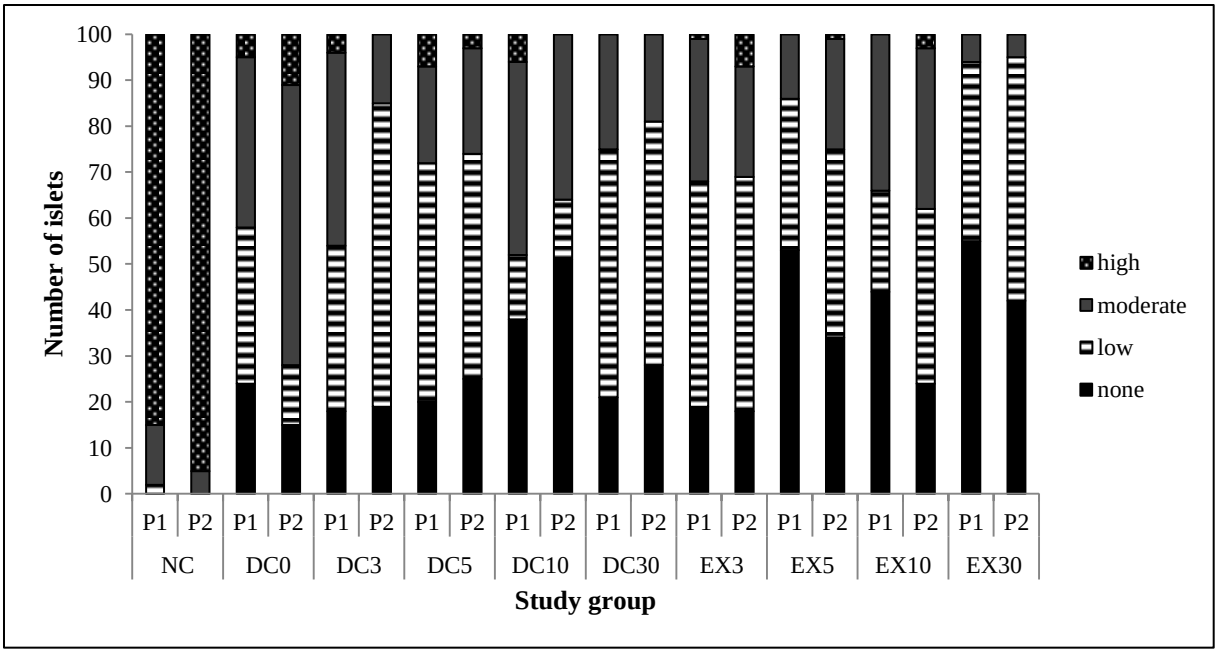

Figure 6.9. Chart showing the insulin staining intensity obtained from 100 islets per tissue portion (P1 and P2) in NC, DC and EX groups. (NC) normal control; (DC) diabetic control; (EX) experimental; (P1) proximal portion of the pancreas; (P2) distal portion of the pancreas.

6.4.1.3 Insulin Distribution

Insulin positive cells in NC, DC and EX groups were classified according to their locations within the islet as core (C-classification), mantle (M-classification) or both (B-classification). The distribution of insulin positive cells in the P1 and P2 portions of the pancreas of each study group is represented in Figure 6.10.

In the NC group insulin positive cells were mostly seen as a single cluster of beta cells extending from the core to the mantle (B-classification) of the islet predominantly. A few islets had insulin positive cells exclusively within the islet core (C-classification) in the P1 portion of the NC group.

In DC and EX groups insulin positive cells were seen in both the core and the mantle (B-classification), but did not form a single cluster as was seen in the NC group; this reflects the decrease in insulin positive area. Most insulin positive islets were predominantly B-classification in DC and EX groups, except in the P2 portion of the DC3 group and in the P1 portion of the EX30 group, where C-classification was most frequently observed. M-classification was observed in only one islet in the P1 portion of the NC group. However, M-classification appeared in DC end EX groups, but was not predominant in any portions of the pancreas.

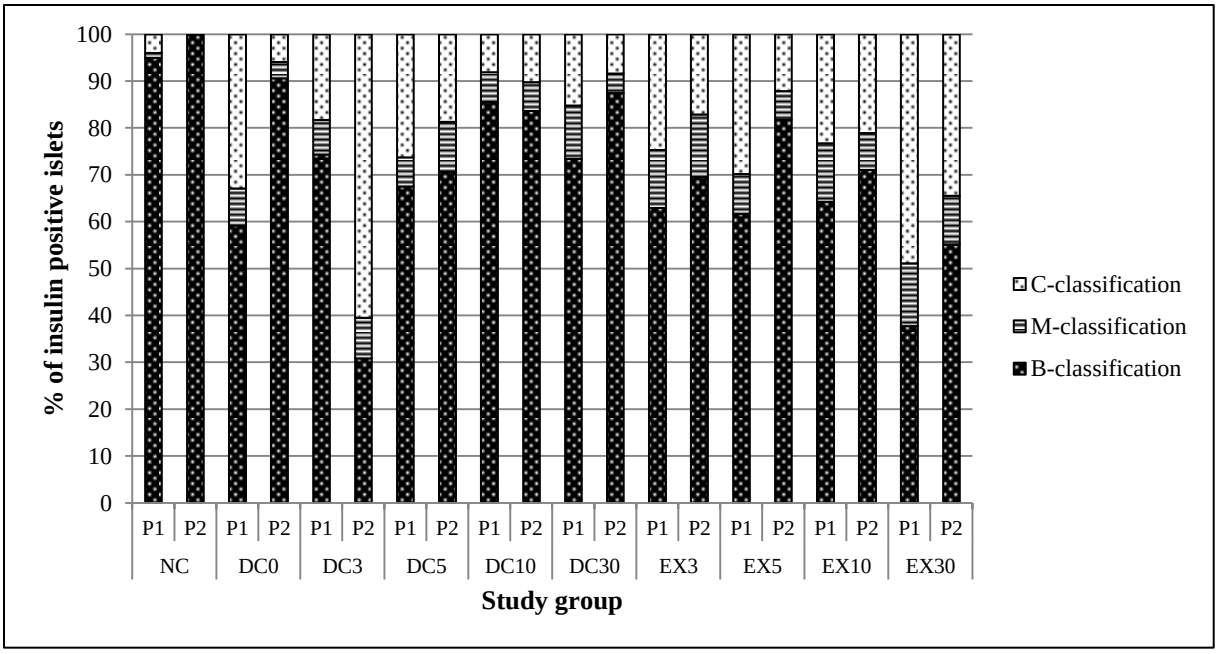

Figure 6.10. Chart showing the distribution of insulin positive cells within the islets of NC, DC and EX groups. (C-classification) core; (M-classification) mantle; (B-classification) both; (NC) normal control; (DC) diabetic control; (EX) experimental; (P1) proximal portion of the pancreas; (P2) distal portion of the pancreas.

6.4.1.4 Pancreatic Polypeptide Fraction

Islet pancreatic polypeptide fraction was morphometrically determined to establish the islet composition. This data was log transformed and the coefficients were interpreted as a percentage change in the geometric mean (GM) (Table 2).

PP fractions in the P1 and P2 portions were compared within each group. The PP fraction did not significantly differ between the P1 and P2 portions of the NC group (p=0.635). In the DC0 group, however, PP fraction was significantly lower in the P2 portion compared to the P1 portion (p=0.000). The PP fraction GM was on average 88.58% lower in the P2 portion of the DC0 group compared to the P1 portion of the DC0 group. P1 and P2 portions did not significantly differ in terms of PP fraction in the DC3 group (p=0.255). PP fraction GM was on average 35.28% lower in the P2 portion of the DC5 group compared to the P1 portion of the DC5 group (p=0.006). DC10 and DC30 groups also had significantly lower PP fractions in their P2 portions compared to their respective P1 portions (p=0.005 and p=0.000, respectively). In the P2 portions of the DC10 and DC30 groups PP fraction GM was on average 38.05% and 74.65% lower when respectively compared to their P1 portions. The EX3, EX5 and EX30 groups all had significantly lower PP fractions in their P2 portions compared to their P1 portions (p=0.000, p=0.001 and p=0.000, respectively). In these three

groups PP fraction GM was on average 53.61%, 44.93% and 46.34% lower in the respective P2 portions compared to their P1 portions. No significant difference in PP fraction was found between P1 and P2 portions in the EX10 group (p=0.090).

PP fractions were compared between the P1 portion of the NC group and the P1 portions of all DC and EX groups; similarly PP fractions were compared between the P2 portion of the NC group and the P2 portions of all DC and EX groups. All P1 and P2 portions of the DC and EX groups had a significant decrease in PP fraction compared to the NC group (p=0.000), except the P2 portion of the DC10 group which did not differ from the P2 portion of the NC group (p=0.963). In the P1 portions of the DC0, DC3, DC5, DC10 and DC30 groups PP fraction GM was 146.93%, 92.94%, 104.62%, 47.96% and 169.72% higher when respectively compared to the P1 portion of the NC group. PP fraction GM in the P1 portions of the EX3, EX5, EX10 and EX30 groups was on average 183.46%, 118.56%, 80.58% and 144.84% higher when respectively compared to the P1 portion of the NC group. When comparing P2 portions, the PP fraction GM was on average 50.45%, 100.16%, 66.30% and 85.67% higher in the DC0, DC3, DC5 and DC30 groups, respectively, compared to the P2 portion of the NC group. PP fraction was also higher in the P2 portions of the EX3, EX5, EX10 and EX30 groups compared to P2 portions of the NC group; PP fraction GM being an average of 120.53%, 66.03%, 53.31% and 91.64% higher in these groups, respectively.

PP fractions were compared between the P1 portion of the DC0 group and the P1 portions of the DC3, DC5, DC10, DC30 and all EX groups; similarly PP fractions were compared between the P2 portion of the DC0 group and the P2 portions of the DC3, DC5, DC10, DC30 and all EX groups. P1 portions of the DC3, DC5 and DC10 groups had significantly lower PP fractions compared to the P1 portion of the DC0 group (p=0.007, p=0.034 and p=0.000); the PP fraction GM was on average 53.89%, 42.26% and 98.81% lower in in the P1 portions of these groups. PP fraction in the P1 portion of the DC30 group did not differ significantly from the PP fraction in the P1 portion of the DC0 group (p=0.561). The P1 portions of the EX3, EX5 and EX30 groups did not significantly differ from the P1 portion of the DC0 group in terms of PP fraction (p=0.062, p=0.147 and p=0.920, respectively). PP fraction GM was, however, on average 66.31% lower in the P1 portion of the EX10 group compared to the P1 portion of the DC0 group (p=0.001). When comparing the P2 portions, the DC3 group tended to have a PP fraction GM that was 49.75% higher on average than the PP fraction GM in the P2 portion of the DC0 group; this difference was, however, not significant (p=0.052). No significant difference was found between the P2 portions of the DC5, DC10 and DC30 groups

compared to the P2 portion of the DC0 group (p=0.550, p=0.069 and p=0.190, respectively). The P2 portions of the EX3 group had a PP fraction GM that was on average 70.06% higher than that of the P2 portion of the DC0 group (p=0.006). PP fraction in the P2 portions of the EX5, EX10 and EX30 groups did not significantly differ from the P2 portion of the DC0 group (p=0.548, p=0.917 and P=0.125, respectively).

PP fractions of corresponding portions (P1 or P2) were compared between the DC and EX groups of the same experimental day. PP fraction GM was on average 90.82% higher in the P1 portion of the EX3 group compared to the P1 portion of the DC3 group (p=0.000), while PP fraction did not differ significantly between the P2 portions of the DC3 and EX3 groups (p=0.413). No significant difference was found between PP fractions of the DC5 and EX5 groups when comparing both P1 and P2 portions (p=0.543 and p=0.976, respectively). Likewise, the PP fraction in the P1 portion of the EX10 group did not significantly differ from the PP fraction in the P1 portion of the DC10 group. In the P2 portion, however, EX10 pancreata had a significantly higher PP fraction compared to the DC10 group (p=0.034); in the P2 portion of the EX10 group PP fraction GM was on average 52.22% higher. DC30 and EX30 groups did not differ significantly when comparing PP fractions in both the P1 and P2 portions (p=0.142 and p=0.789, respectively).

Table 2. Pancreatic polypeptide fraction data summary for 100 islets per portion of the pancreas

Group		25th percentile	50th percentile (median)	75th percentile	Arithmetic mean [95%CI]	Geometric mean (GM) [95%CI]
NC	P1	0.79	3.97	7.24	6.01 [4.36-7.67]	4.93 [3.95-6.14]
	P2	0.98	4.10	8.48	6.72 [5.10-8.33]	5.30 [4.24-6.63]
DC0	P1	8.13	20.45	37.52	26.89 [22.08-31.71]	21.28 [17.51-25.85]
	P2	2.54	7.84	15.50	11.63 [8.85-14.40]	8.67 [7.02-10.72]
DC3	P1	0.00	7.88	19.37	12.27 [9.63-14.91]	12.12 [9.84-14.92]
	P2	7.76	14.20	24.32	18.09 [15.02-21.15]	14.04 [11.92-16.53]
DC5	P1	8.27	13.15	22.33	17.15 [14.23-20.07]	13.80 [11.66-16.33]
	P2	3.67	7.97	19.24	13.00 [10.28-15.71]	9.82 [7.95-12.12]
DC10	P1	2.31	5.84	9.72	8.61 [6.53-10.69]	7.63 [6.32-9.21]
	P2	0.00	3.93	7.68	5.57 [4.16-6.99]	5.30 [4.36-6.43]
DC30	P1	11.00	25.50	43.83	28.74 [24.29-33.19]	26.41 [22.14-31.50]
	P2	4.56	9.41	21.26	14.68 [11.68-17.68]	12.65 [10.60-15.10]
EX3	P1	11.56	30.50	56.23	33.88 [28.63-39.12]	31.01 [26.09-36.86]
	P2	8.02	18.81	36.96	23.09 [19.68-26.50]	17.63 [14.63-21.24]
EX5	P1	5.61	13.95	27.18	20.14 [16.25-24.03]	15.65 [12.81-19.12]
	P2	2.95	6.53	18.96	13.54 [10.47-16.60]	10.25 [8.20-12.81]
EX10	P1	4.97	10.18	15.70	12.52 [9.90-15.15]	10.89 [9.22-12.86]
	P2	1.61	7.73	14.43	11.12 [8.67-13.56]	9.12 [7.33-11.35]
EX30	P1	13.15	20.60	40.27	26.94 [22.65-31.22]	20.44 [17.16-24.35]
	P2	4.25	12.14	22.96	16.83 [13.25-20.12]	13.53 [11.17-16.40]

(NC) normal control; (DC) diabetic control; (EX) experimental; (P1) proximal portion of the pancreas; (P2) distal portion of the pancreas.

6.4.1.5 Pancreatic Polypeptide Intensity

Pancreatic polypeptide staining intensity was observed and classified as none, low, moderate or high. Figure 6.11 represents pancreatic polypeptide staining intensity obtained from 100 islets per tissue portion (P1 and P2) in each one of the study groups.

In all groups PP staining intensity was predominantly classified as high, except in the P1 portion of the DC10 group and the P2 portions of the DC10 and EX10 groups, where PP staining intensity was predominantly classified as moderate. In these three groups only a small number of islets were classified as staining with high intensity (11, 6 and 5 islets, respectively). Islets devoid of PP staining were observed in all groups; however, in the P1 portions of the DC5 and EX30 groups and in the P2 portions of the DC3 and EX3 groups less than 10 islets were observed to have no PP staining.

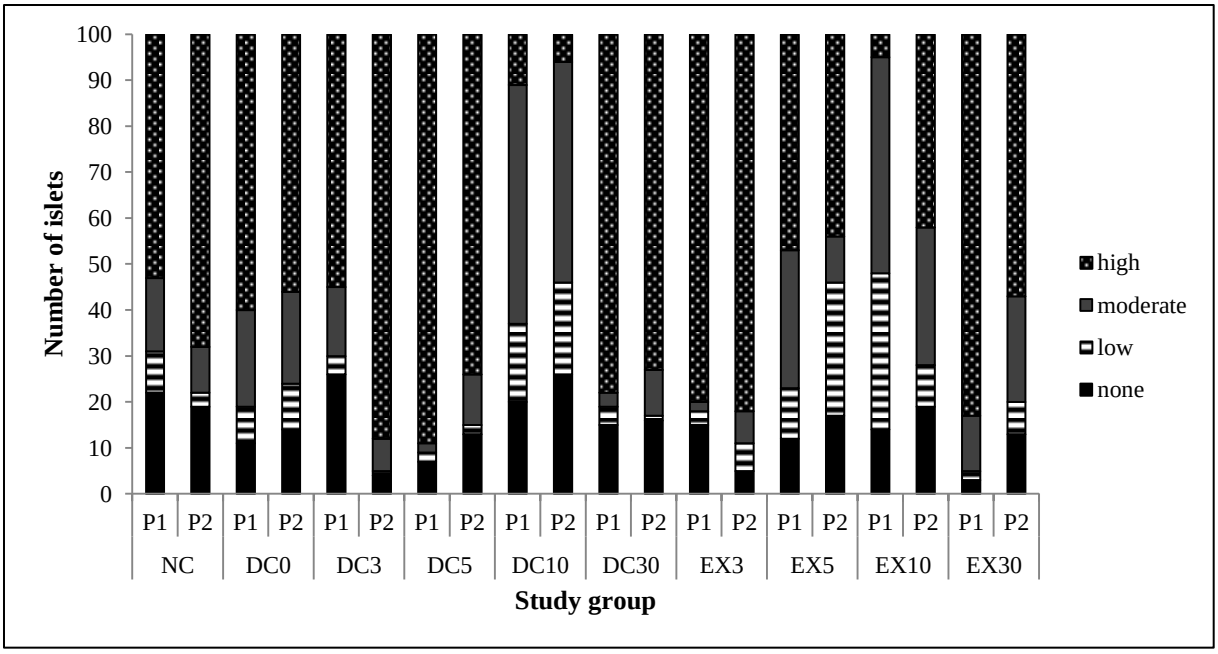

Figure 6.11. Chart showing pancreatic polypeptide staining intensity obtained from 100 islets per tissue portion (P1 and P2) in NC, DC and EX groups. (NC) normal control; (DC) diabetic control; (EX) experimental; (P1) proximal portion of the pancreas; (P2) distal portion of the pancreas.

6.4.1.6 Pancreatic Polypeptide Distribution

Pancreatic polypeptide positive cells in NC, DC and EX groups were classified according to their locations within the islet as core (C-classification), mantle (M-classification) or both (B-classification). The distribution of PP positive cells in the P1 and P2 portions of the pancreas of each study group is represented in Figure 6.12.

PP positive cells were predominantly located within the mantle of islets in the NC groups (M-classification). These positively staining cells were observed as single cells, pairs of cells or small groups of cells (3-4 cells). Following diabetes induction, M-classification was less frequently observed and B-classification for PP positive cells became predominant in all DC and EX groups. Again these cells were present as single cells, pairs of cells or small groups; however, larger groups of PP cells were observed and were dispersed throughout the islet. In some islets it was observed that PP positive cells were taking up a large part of the islet. Over all there were only a few cases in the NC, DC and EX groups where PP positive cells were located exclusively within the core (C-classification) of the islet.

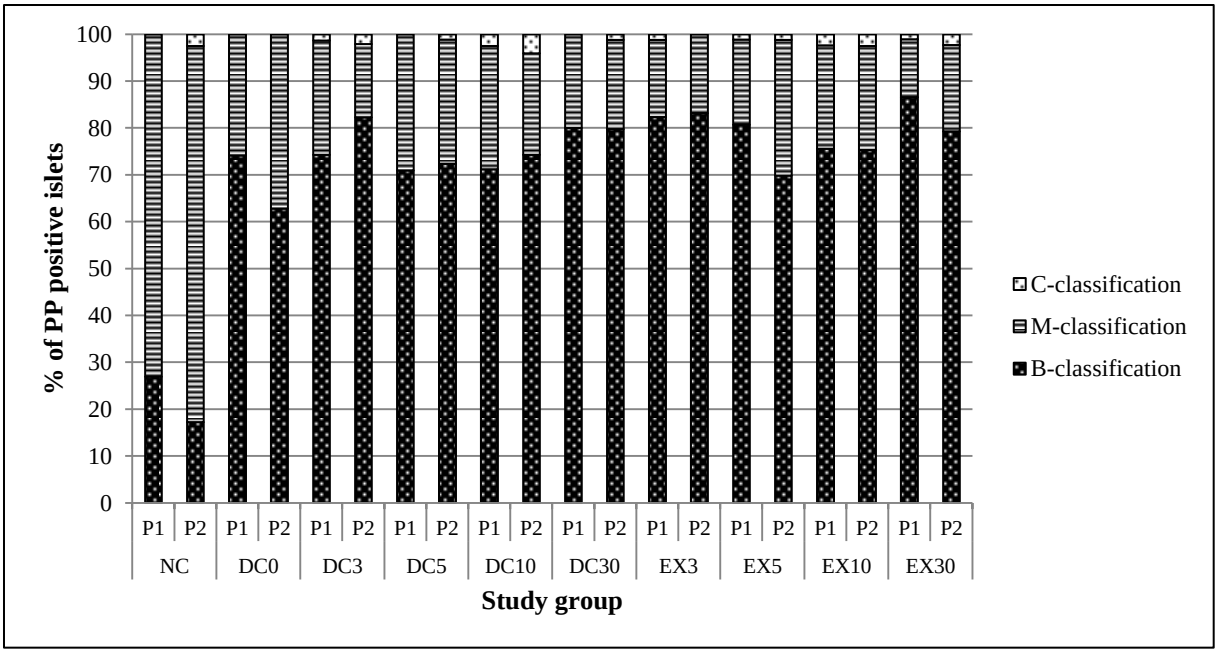

Figure 6.12. Chart showing distribution of pancreatic polypeptide positive cells within the islet of NC, DC and EX groups. (C-classification) core; (M-classification) mantle; (B-classification) both; (NC) normal control; (DC) diabetic control; (EX) experimental; (P1) proximal portion of the pancreas; (P2) distal portion of the pancreas.

6.4.2 Glucagon and Somatostatin protein expression

An immunohistochemical study was done to assess the protein expression of glucagon and somatostatin in the pancreas. The figures that follow demonstrate representative islets from the NC group (Figure 6.13), DC groups (Figure 6.14) and EX Groups (Figure 6.15) stained for glucagon (red) and somatostatin (brown). The IHC slides were used for the sole purpose of determining hormone fractions and to describe hormone staining intensity and distribution within the islet of the P1 and P2 tissue portions in the NC, DC and EX groups.

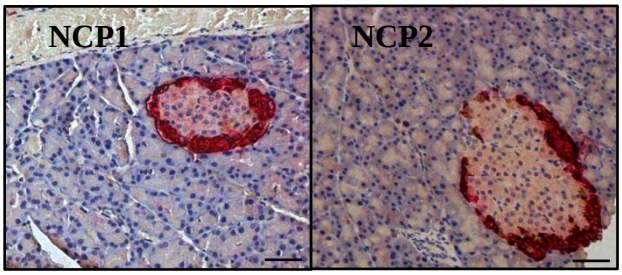

Figure 6.13. Representative immunohistochemical photomicrographs of islets in the P1 and P2 portions of the NC group with glucagon (red) and somatostatin (brown). Scale bar represents 50 µm. (NC) normal control; (P1) proximal portion of the pancreas; (P2) distal portion of the pancreas.

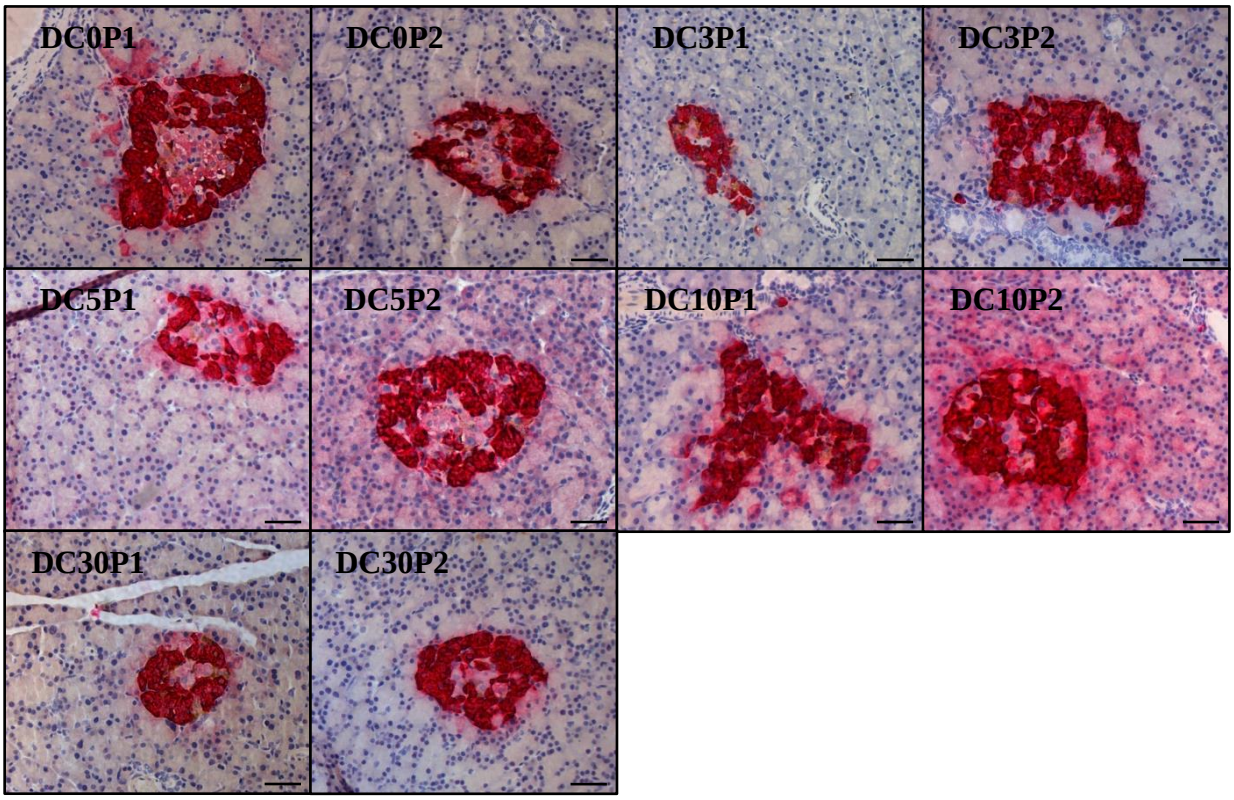

Figure 6.14. Representative immunohistochemical photomicrographs of islets in the P1 and P2 portions of the DC groups with glucagon (red) and somatostatin (brown). Scale bar represents 50 µm. (DC) diabetic control; (P1) proximal portion of the pancreas; (P2) distal portion of the pancreas.

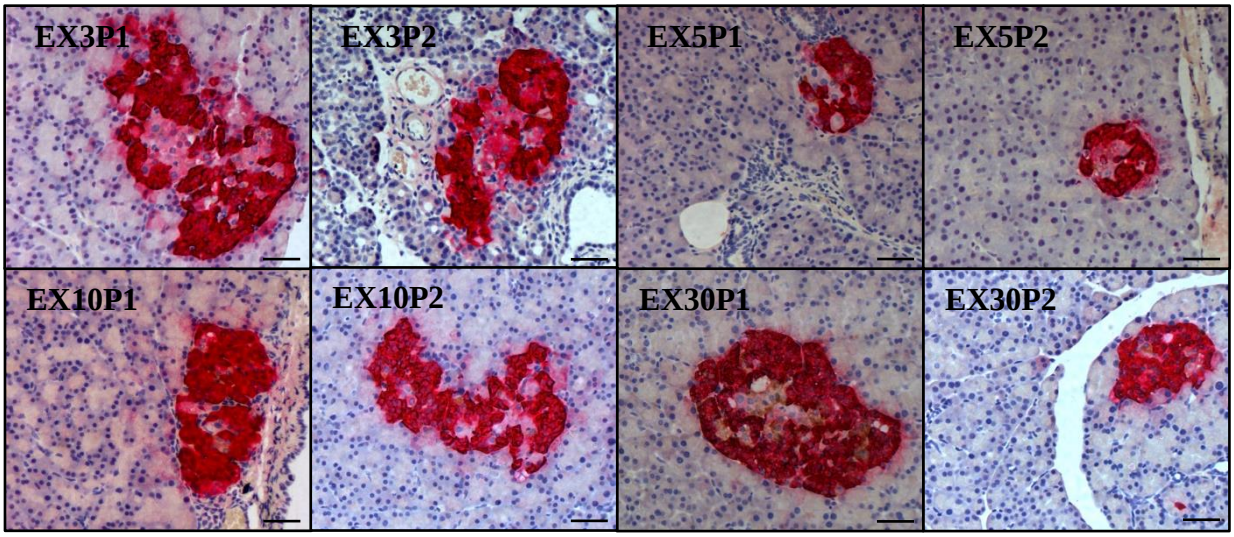

Figure 6.15. Representative IHC photomicrographs of islets in the P1 and P2 portions of the DC groups with glucagon (red) and somatostatin (brown). Scale bar represents 50 µm. (DC) diabetic control; (P1) proximal portion of the pancreas; (P2) distal portion of the pancreas.

6.4.2.1 Glucagon Fraction

Islet glucagon fraction was morphometrically determined to establish the islet composition. This data was normally distributed; therefore coefficients are interpreted as per normal regression (Table 3).

Glucagon fractions in the P1 and P2 portions were compared within each group. Glucagon fraction tended to be 3.98% lower in the P2 portion compared to the P1 portion of the NC group (95%CI -7.98, 0.02; p=0.051). In the DC0 group there was no significant difference between glucagon fraction in the P1 and the P2 portions of the pancreas (p=0.675). Similarly, no significant difference was found between glucagon fraction in the P1 and P2 portions of the DC5 group. Glucagon fraction was, however, significantly higher in the P2 portions of the DC3 group (with 6.50%; 95%CI 1.12, 11.88; p=0.018), DC10 group (with 5.16%, 95%CI 0.34, 9.98; p=0.036) and DC30 group (with 6.71%; 95%CI 1.15, 12.26; p=0.018) when compared to their respective P1 portions. Glucagon fraction did not differ significantly between the P1 and P2 portions of the EX3, EX5, EX10 and EX30 groups (p=0.171, p=0.529, p=0.855 and p=0.071, respectively).

Glucagon fractions were compared between the P1 portion of the NC group and the P1 portions of all DC and EX groups; similarly glucagon fractions were compared between the P2 portion of the NC group and the P2 portions of all DC and EX groups. All P1 portions of the DC and EX groups had significant higher glucagon fractions, compared to the P1 portion of the NC group (p=0.000). Glucagon fraction was on average more than 30% higher in in all

P1 portions of the DC and EX groups. Similarly, all P2 portions of the DC and EX groups had a significantly higher glucagon fraction compared to the P2 portion of the NC group (p=0.000); glucagon fraction was on average more than 35% higher in all P2 portions of the DC and EX groups.

Glucagon fractions were compared between the P1 portion of the DC0 group and the P1 portions of the DC3, DC5, DC10, DC30 and all EX groups; similarly glucagon fractions were compared between the P2 portion of the DC0 groups and the P2 portions of the DC3, DC5, DC10, DC30 and all EX groups. Glucagon fractions did not significantly differ between the DC0 group and the DC3, DC5, DC10, DC30 and all EX groups when comparing the P1 portions (p=0.5375) and the P2 portions (p=0.4391).

Glucagon fractions of corresponding portions (P1 or P2) were compared between DC and EX groups of the same experimental day. Glucagon fractions in both the P1 and P2 portions did not differ when comparing the DC and EX groups of day 3, 5 and 30 (p>0.1). Similarly, the P1 portions of the DC10 group and EX10 group did not differ significantly in terms of glucagon fraction (p=0.591). The P2 portions of the DC10 group and EX10 group did, however, have significantly different glucagon fractions (p=0.036); glucagon fraction was 4.74% (95%CI -9.16, -0.31) lower in the P2 portion of the EX10 group compared to the P2 portion of the DC10 group.

Table 3. Glucagon fraction data summary for 100 islets per portion of the pancreas

Group		25th percentile	50th percentile (median)	75th percentile	Arithmetic mean [95%CI]	Geometric mean (GM) [95%CI]
NC	P1	18.02	24.45	35.25	27.61 [24.92-30.29]	25.26 [22.93-27.82]
	P2	15.28	21.46	28.51	23.83 [20.78-26.89]	21.05 [18.62-23.79]
DC0	P1	53.52	63.76	75.23	63.04 [59.37-66.71]	59.23 [54.72-64.12]
	P2	55.28	65.77	78.94	64.13 [60.50-67.76]	60.54 [56.14-65.29]
DC3	P1	44.26	57.34	71.70	57.56 [53.80-61.32]	53.85 [49.80-58.24]
	P2	49.74	66.28	80.20	64.06 [59.54-68.59]	57.88 [52.08-64.34]
DC5	P1	48.75	63.74	74.78	60.46 [56.46-64.45]	55.70 [50.83-61.04]
	P2	48.83	62.14	75.10	59.37 [55.27-63.46]	55.31 [50.40-60.70]
DC10	P1	58.67	71.68	80.46	67.68 [63.64-71.72]	61.92 [55.45-69.15]
	P2	63.24	74.80	82.04	72.84 [70.03-75.64]	71.35 [68.42-74.40]
DC30	P1	44.26	64.55	78.23	58.14 [53.03-63.25]	52.98 [46.68-60.12]
	P2	52.81	69.22	82.60	65.59 [61.41-69.77]	60.06 [54.10-66.69]
EX3	P1	55.02	70.55	84.02	66.10 [62.07-70.14]	61.67 [56.66-67.12]
	P2	61.42	72.01	80.98	69.26 [65.70-72.82]	64.62 [58.21-71.73]
EX5	P1	52.48	65.30	76.65	61.48 [57.57-65.40]	58.47 [53.17-64.29]
	P2	53.82	63.58	75.39	62.97 [59.63-66.30]	60.18 [56.38-64.24]
EX10	P1	60.29	70.40	80.61	67.43 [63.70-71.16]	61.45 [54.55-69.21]
	P2	55.04	71.12	79.71	66.97 [63.40-70.55]	63.12 [58.14-68.52]
EX30	P1	50.32	65.14	80.73	64.47 [60.32-68.61]	57.18 [48.94-66.82]
	P2	58.33	70.35	81.55	69.14 [66.05-72.23]	66.91 [63.27-70.76]

(NC) normal control; (DC) diabetic control; (EX) experimental; (P1) proximal portion of the pancreas; (P2) distal portion of the pancreas.

6.4.2.2 Glucagon Staining Intensity

Glucagon staining intensity was observed and classified as none, low, moderate or high. Figure 6.16 represents glucagon staining intensity obtained from 100 islets per tissue portion (P1 and P2) in each one of the study groups.

Glucagon staining intensity was predominantly classified as high in all groups. In the normal group, six islets devoid of glucagon were observed, while only seven islets in total were devoid of glucagon in all DC and EX groups.

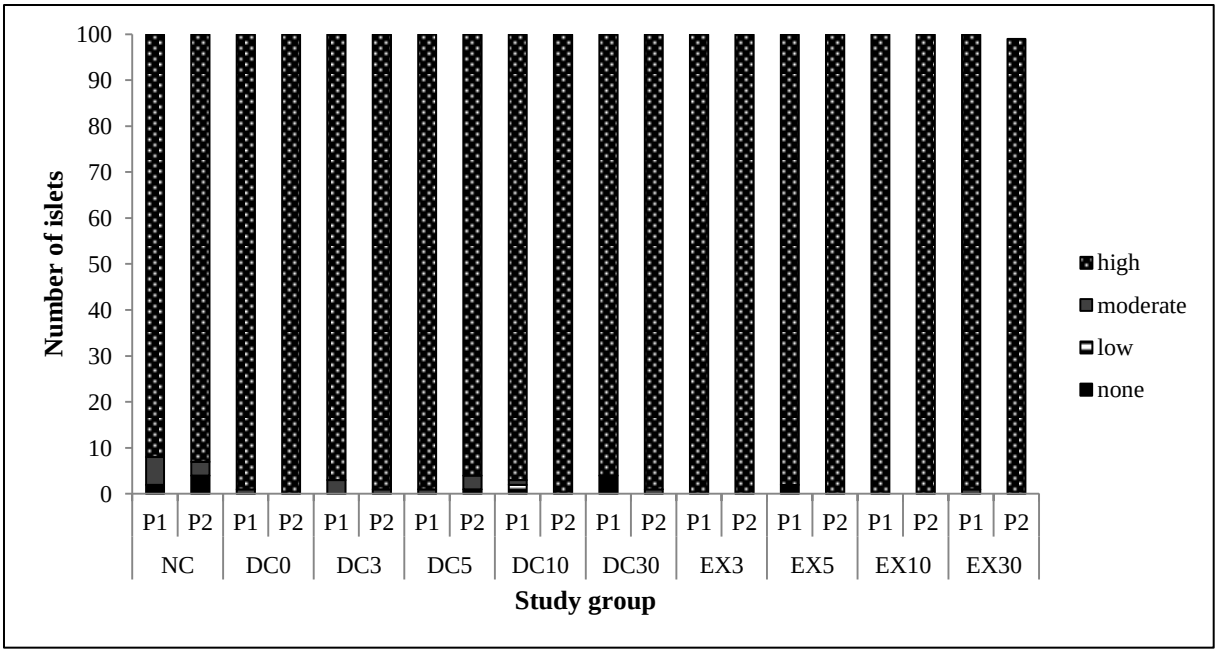

Figure 6.16. Chart showing glucagon staining intensity obtained from 100 islets per tissue portion (P1 and P2) in NC, DC and EX groups. (NC) normal control; (DC) diabetic control; (EX) experimental; (P1) proximal portion of the pancreas; (P2) distal portion of the pancreas.

6.4.2.3 Glucagon Distribution

Glucagon positive cells in NC, DC and EX groups were classified according to their locations within the islet as core (C-classification), mantle (M-classification) or both (B-classification). The distribution of glucagon positive cells in the P1 and P2 portions of the pancreas of each study group is represented in Figure 6.17.

In the NC group, glucagon positive cells were predominantly located in the mantle of the islet (M-classification) where these cells formed a discontinuous layer. Glucagon distribution was disrupted in all treated pancreata (DC and EX groups). The discontinuous glucagon layer appeared expanded, extending from the mantle into the islet core, therefore B-classification became predominant. In some islets glucagon positive cells took up the largest area of the islet. Only one islet was observed where glucagon appeared exclusively in the islet core (C-classification) (EX10P1).

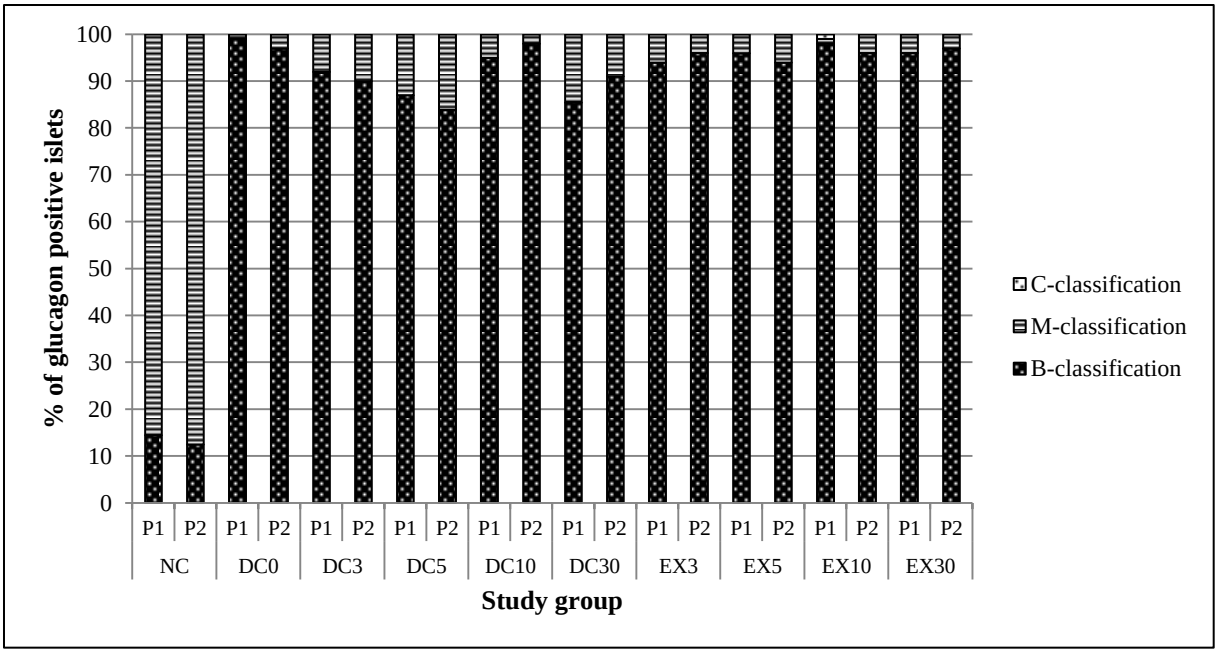

Figure 6.17. Chart showing distribution of glucagon positive cells within the islets of NC, DC and EX groups. (C-classification) core; (M-classification) mantle; (B-classification) both; (NC) normal control; (DC) diabetic control; (EX) experimental; (P1) proximal portion of the pancreas; (P2) distal portion of the pancreas.

6.4.2.4 Somatostatin Fraction

Islet somatostatin fraction was morphometrically determined to establish the islet composition. This data was log transformed and the coefficients were interpreted as a percentage change in the geometric mean (GM) (Table 4).

Somatostatin fractions in the P1 and P2 portions were compared within each group. The P2 portion of the NC group had a significant higher somatostatin fraction compared to the P1 portion of the NC group (p=0.000). On average, somatostatin fraction GM was 62.04% higher in the P2 portion compared to the P1 portion of the NC pancreata. Somatostatin fraction GM was also significantly increased (with an average of 39.97%) in the P2 portion of the DC0 group compared to the P1 portion of the DC0 group (p=0.001). The two portions of the pancreas did not significantly differ in terms of somatostatin fraction in the DC3 and DC10 groups (p=0.162 and p=0.297, respectively). Somatostatin fraction did, however, significantly differ between the respective P1 and P2 portions of the DC5 and DC30 groups (p=0.003 and p=0.000). In these two groups somatostatin fraction GM of the P2 portions was respectively 42.08% and 60.28% lower compared to their P1 portions. No significant difference in somatostatin fraction was observed between the P1 and P2 portions of the EX3, EX5 and EX10 groups, respectively (p=0.322, p=0.843 and p=0.411, respectively). In the EX30 group,

however, somatostatin fraction was significantly lower in the P2 portion compared to the P1 portion (p=0.00); in the P2 portion the somatostatin fraction GM was on average 94.02% lower.

Somatostatin fractions were compared between the P1 portion of the NC group and the P1 portions of all DC and EX groups; similarly, somatostatin fractions were compared between the P2 portion of the NC group and the P2 portions of all DC and EX groups. Somatostatin fraction was significantly increased in the P1 portions of the DC0 and DC3 groups compared to the P1 portion of the NC group (p=0.013 and p=0.005 respectively). On average the somatostatin fraction GM was 42.55% higher in the P1 portions of the DC0 group and 47.46% higher in the P1 portion of the DC3 group when respectively compared to the P1 portion of the NC group. No significant difference in somatostatin fraction was found when comparing the P1 portions of the DC5 and DC10 groups to P1 portion of the NC group (p=0.378 and p=0.741, respectively). The P1 portions of the EX3, EX5 and EX10 groups also did not significantly differ when compared to the P1 portion of the NC group (p=0.443, p=0.308 and p=0.631, respectively). On day 30, however, the P1 portions of both the DC30 and EX30 groups had a significant higher somatostatin fraction compared to the P1 portion of the NC group (p=0.000 in both cases). In the P1 portion of the DC30 group somatostatin fraction GM was on average 72.16% higher compared to normal, while in EX30P1 pancreata somatostatin fraction GM was 129.58% higher compared to the NC group. When comparing P2 portions, the DC0, DC3, DC10 and DC30 groups' somatostatin fraction did not differ significantly from the P2 portion of the NC group (p=0.380, p=0.175, p=0.205 and p=0.061, respectively). The P2 portion of the DC5 group did, however, have a significantly lower somatostatin fraction compared to the P2 portion of the NC group (p=0.001). The somatostatin fraction GM was on average 87.30% lower in the P2 portion of the DC5 group. Somatostatin fraction in the P2 portions of the EX5 and EX30 groups did not differ significantly from the somatostatin fraction in the P2 portion in the NC group (p=0.071 and p=0.314, respectively), while somatostatin fraction GM was significantly lower (with 90.15% and 62.65% on average, respectively) in the P2 portions of the EX3 and EX10 groups compared to the P2 portion of the NC group (p=0.001 and p=0.015, respectively).

Somatostatin fractions were compared between the P1 portion of the DC0 group and the P1 portions of the DC3, DC5, DC10, DC30 and all EX groups; similarly, somatostatin fractions were compared between the P2 portion of the DC0 group and the P2 portions of the DC3, DC5, DC10, DC30 and all EX groups. Somatostatin fraction did not significantly differ when

comparing the P1 portions of the DC3, DC5 and DC30 groups to the P1 portion of the DC0 group ($p=0.764$, $p=0.110$ and $p=0.075$, respectively). A significant difference was found between the P1 portions of the DC10 and DC0 groups ($p=0.043$); somatostatin fraction GM was on average 36.18% lower than in the P1 portion of the DC10 group. P1 portions of the EX5 and EX10 groups did not significantly differ from the P1 portion of the DC0 group in terms of somatostatin fraction ($p=0.145$ and $p=0.092$, respectively). Somatostatin fractions of the P1 portions of the EX3 and EX30 groups did, however, differ significantly from the P1 portion of the DC0 group ($p=0.001$ and $p=0.000$, respectively). The P1 portions of the EX3 and EX30 groups had a somatostatin fraction GM that was on average 56.28% lower and 87.04% higher, respectively, when compared to the P1 portion of the DC0 group. Somatostatin fraction was significantly lower in the P2 portions of the DC3, DC5, DC10, DC30, EX3, EX5 and EX10 groups ($p<0.050$) In all of these groups the somatostatin fraction GM was on average more than 54% lower compared to the P2 portion of the DC0 group. Only the P2 portion of the EX30 group did not significantly differ from the P2 portion of the DC0 group ($p=0.063$).

Somatostatin fractions of corresponding portions (P1 or P2) were compared between DC and EX groups of the same experimental day. A significant difference was observed between the P1 portions of the DC3 and EX3 groups' somatostatin fraction ($p=0.014$). The somatostatin fraction GM was on average 63.41% lower in the EX3 group. The P2 portions did not significantly differ between DC3 and EX3 groups in terms of somatostatin fraction ($p=0.100$). The somatostatin fractions in the DC5 and EX5 groups did not significantly differ when respectively comparing their P1 and P2 portions ($p=0.918$ and $p=0.120$, respectively). The P1 portions of the DC10 and EX10 groups did not significantly differ in terms of somatostatin fractions ($p=0.998$); at this time point, however, P2 portions of the EX10 group had a significantly lower somatostatin fraction GM (31.29% on average) compared to the DC10 group. Conversely, somatostatin fraction GM was on average 57.42% higher in the P1 portion of the EX30 group compared to the P1 portion of the DC30 group ($p=0.001$). No significant difference was found between somatostatin fraction in the P2 portions of the DC30 and EX30 groups ($p=0.428$).

Table 4. Somatostatin fraction data summary for 100 islets per portion of the pancreas

Group		25th percentile	50th percentile (median)	75th percentile	Arithmetic mean [95%CI]	Geometric mean (GM) [95%CI]
NC	P1	0.53	1.42	3.56	2.45 [1.84-3.05]	2.15 [1.75-2.64]
	P2	2.06	3.85	7.39	5.32 [4.32-6.31]	3.93 [3.27-4.73]
DC0	P1	1.60	2.87	5.18	3.85 [3.21-4.49]	3.28 [2.82-3.81]
	P2	2.52	5.13	7.89	6.40 [5.23-7.58]	4.90 [4.08-5.89]
DC3	P1	1.71	2.88	5.91	4.96 [3.72-6.20]	3.45 [2.84-4.19]
	P2	0.71	2.10	5.36	3.78 [2.79-4.78]	2.75 [2.19-3.46]
DC5	P1	0.78	2.41	3.78	2.80 [2.27-3.34]	2.51 [2.11-2.99]
	P2	0.40	1.07	2.65	2.19 [1.58-2.79]	1.63 [1.29-2.06]
DC10	P1	0.00	1.05	2.78	2.89 [1.76-4.01]	2.36 [1.79-3.12]
	P2	0.00	1.45	2.99	2.63 [1.86-3.41]	2.84 [2.28-3.53]
DC30	P1	2.00	4.06	7.79	6.07 [4.71-7.41]	4.41 [3.67-5.31]
	P2	0.34	1.83	4.09	2.93 [2.18-3.67]	2.52 [2.03-3.13]
EX3	P1	0.00	1.02	2.57	1.89 [1.38-2.39]	1.90 [1.50-2.41]
	P2	0.00	0.00	1.38	0.96 [0.64-1.28]	1.59 [1.21-2.10]
EX5	P1	0.45	1.92	4.11	2.78 [2.13-3.44]	2.54 [2.09-3.09]
	P2	0.00	1.29	3.12	2.14 [1.59-2.70]	2.48 [2.03-3.02]
EX10	P1	0.00	0.00	2.14	1.54 [1.00-2.07]	2.36 [1.83-3.04]
	P2	0.00	1.31	2.58	2.14 [1.61-2.66]	2.07 [1.71-2.52]
EX30	P1	3.66	8.53	13.94	10.66 [8.60-12.72]	7.84 [6.24-9.85]
	P2	0.12	2.10	4.87	3.37 [2.62-4.11]	3.06 [2.44-3.83]

(NC) normal control; (DC) diabetic control; (EX) experimental; (P1) proximal portion of the pancreas; (P2) distal portion of the pancreas.

6.4.2.5 Somatostatin Staining Intensity

Somatostatin staining intensity was observed and classified as none, low, moderate or high. Figure 6.18 represents somatostatin staining intensity obtained from 100 islets per tissue portion (P1 and P2) in each one of the study groups.

Somatostatin staining intensity in NC group (P1 and P2 portions) was predominantly classified as moderate. In the DC and EX groups, somatostatin staining intensity was predominantly low, except in the P1 portion of the EX10 group and in the P2 portion of the EX3 group, where islets were predominantly negative for somatostatin. Between day 3 and day 30, EX pancreata collectively had more islets (n=263) where somatostatin was absent from the islet compared to DC pancreata collectively (n=165).

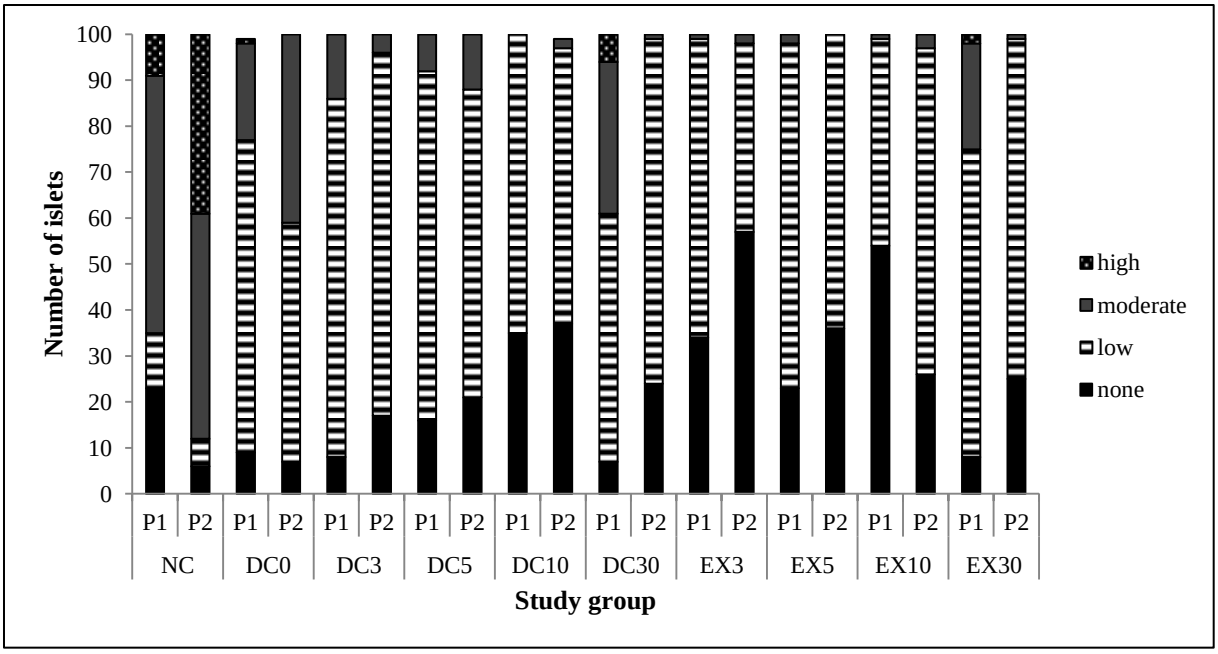

Figure 6.18. Chart showing somatostatin staining intensity obtained from 100 islets per tissue portion (P1 and P2) in NC, DC and EX groups. (NC) normal control; (DC) diabetic control; (EX) experimental; (P1) proximal portion of the pancreas; (P2) distal portion of the pancreas.

6.4.2.6 Somatostatin Distribution

Somatostatin positive cells in NC, DC and EX groups were classified according to their locations within the islet as core (C-classification), mantle (M-classification) or both (B-classification). The distribution of somatostatin positive cells in the P1 and P2 portions of the pancreas of each study group is represented in Figure 6.19.

Somatostatin positive cells were predominantly located in the mantle of islets (M-classification) in the P1 and P2 portions of the NC group; a few somatostatin positive islets, however, had C-classification and B-classification. The somatostatin positive cells were scattered in the mantle as single cells, pairs of cells or in small groups (3-4 cells). Following diabetes induction, somatostatin distribution became disrupted in both the DC and EX groups. In all of these groups somatostatin positive cells were predominantly observed in both the core and mantle of islets (B-classification). Compared to the NC group, the treated groups also show an increased number of islets with C-classification. Similar to the NC islets, somatostatin positive cells were observed as single cells, pairs of cells or small groups of cells (3-4 cells) in the DC and EX islets.

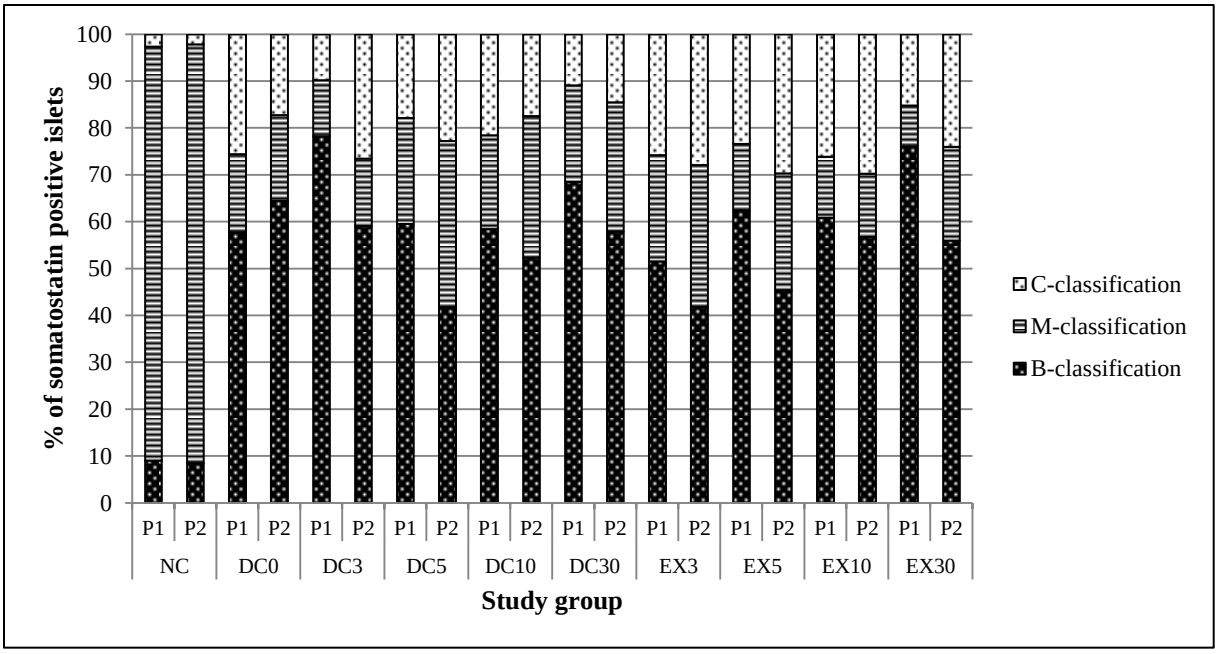

Figure 6.19. Chart showing distribution of somatostatin positive cells within the islets of NC, DC and EX groups. (C-classification) core; (M-classification) mantle; (B-classification) both; (NC) normal control; (DC) diabetic control; (EX) experimental; (P1) proximal portion of the pancreas; (P2) distal portion of the pancreas.

6.4.3 Islet composition in the pancreas

Hormone fractions for insulin, pancreatic polypeptide, glucagon and somatostatin were used to summarise the comparative islet composition of P1 and P2 portions of the pancreas in NC and DC0 groups (Figure 6.20), in DC3 and EX3 group (Figure 6.21), in DC5 and EX5 groups (Figure 6.22), in DC10 and EX10 groups (Figure 6.23) and in DC30 and EX30 groups (Figure 6.24).

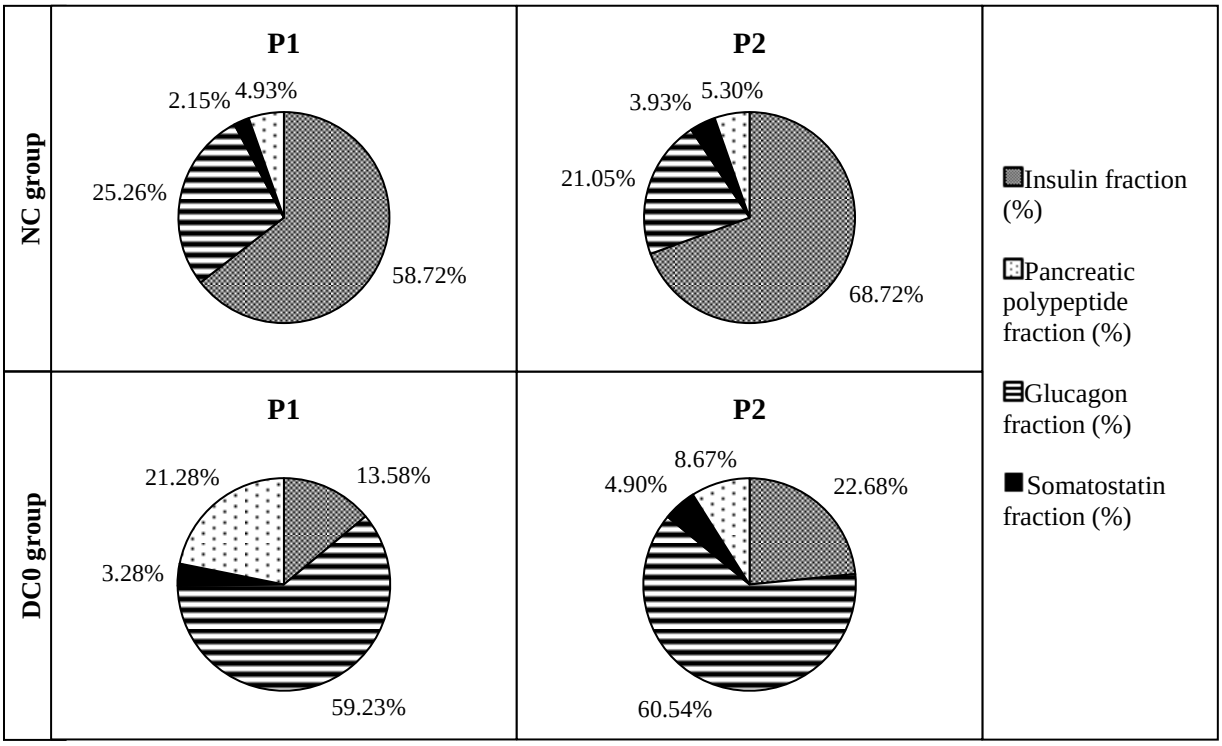

Figure 6.20. Pie charts showing islet composition in the P1 and P2 portions of the pancreas of the NC group and the DC0 group. (NC) normal control; (DC0) diabetic control baseline; (P1) proximal portion of the pancreas; (P2) distal portion of the pancreas.

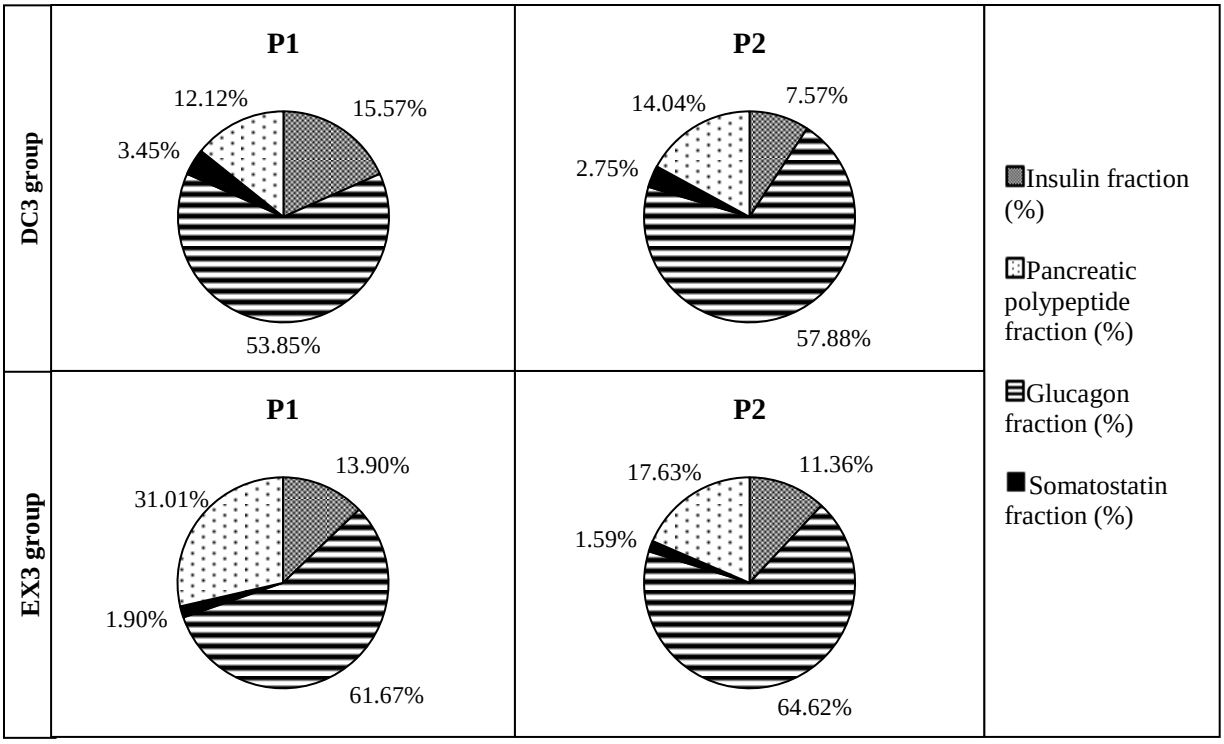

Figure 6.21. Pie charts showing islet composition in the P1 and P2 portions of the pancreas of the DC3 group and the EX3 group. (DC3) diabetic control day 3; (EX3) experimental day 3; (P1) proximal portion of the pancreas; (P2) distal portion of the pancreas.

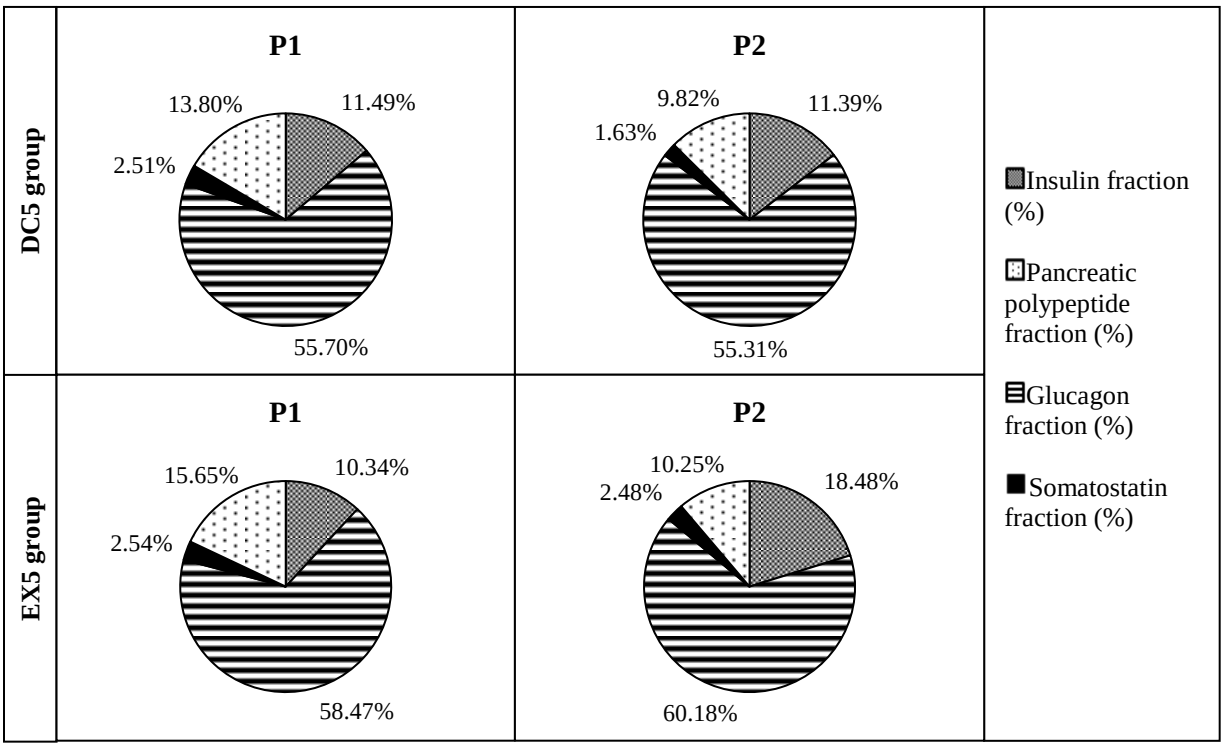

Figure 6.22. Pie charts showing islet composition in the P1 and P2 portions of the pancreas of the DC5 group and the EX5 group. (DC5) diabetic control day 5; (EX5) experimental day 5; (P1) proximal portion of the pancreas; (P2) distal portion of the pancreas.

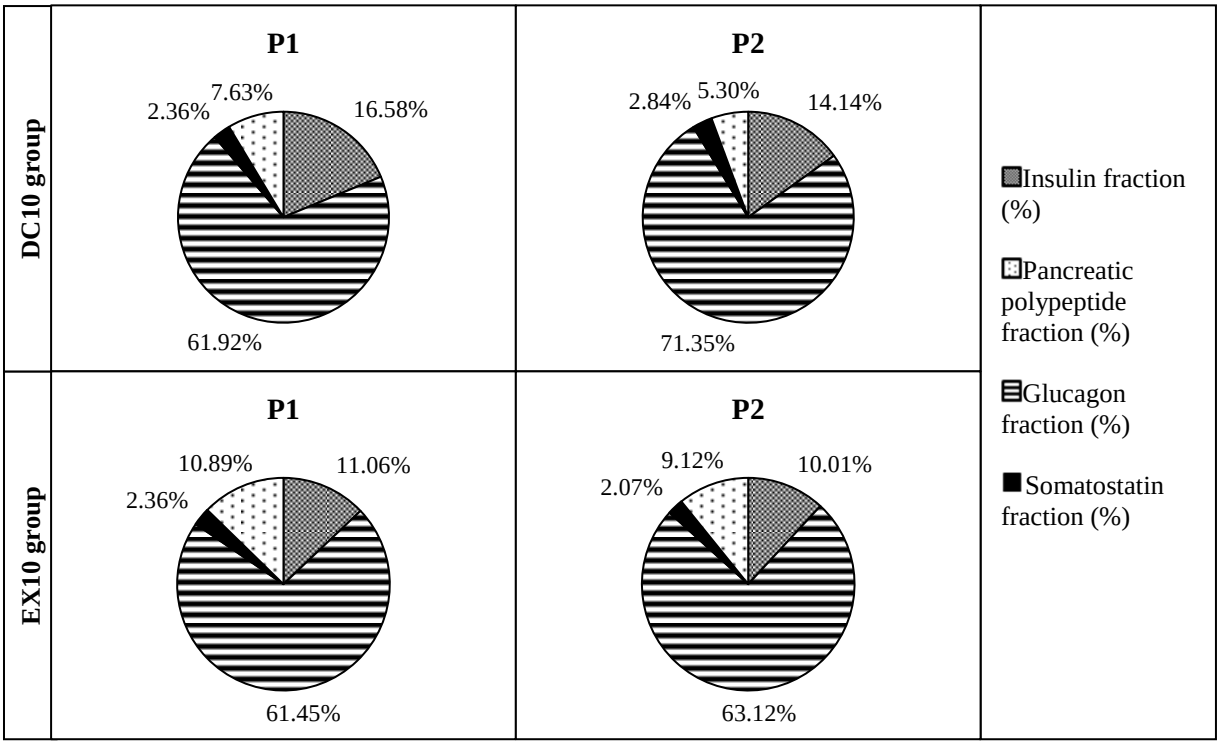

Figure 6.23. Pie charts showing islet composition in the P1 and P2 portions of the pancreas of the DC10 group and the EX10 group. (DC10) diabetic control day 10; (EX10) experimental day 10; (P1) proximal portion of the pancreas; (P2) distal portion of the pancreas.

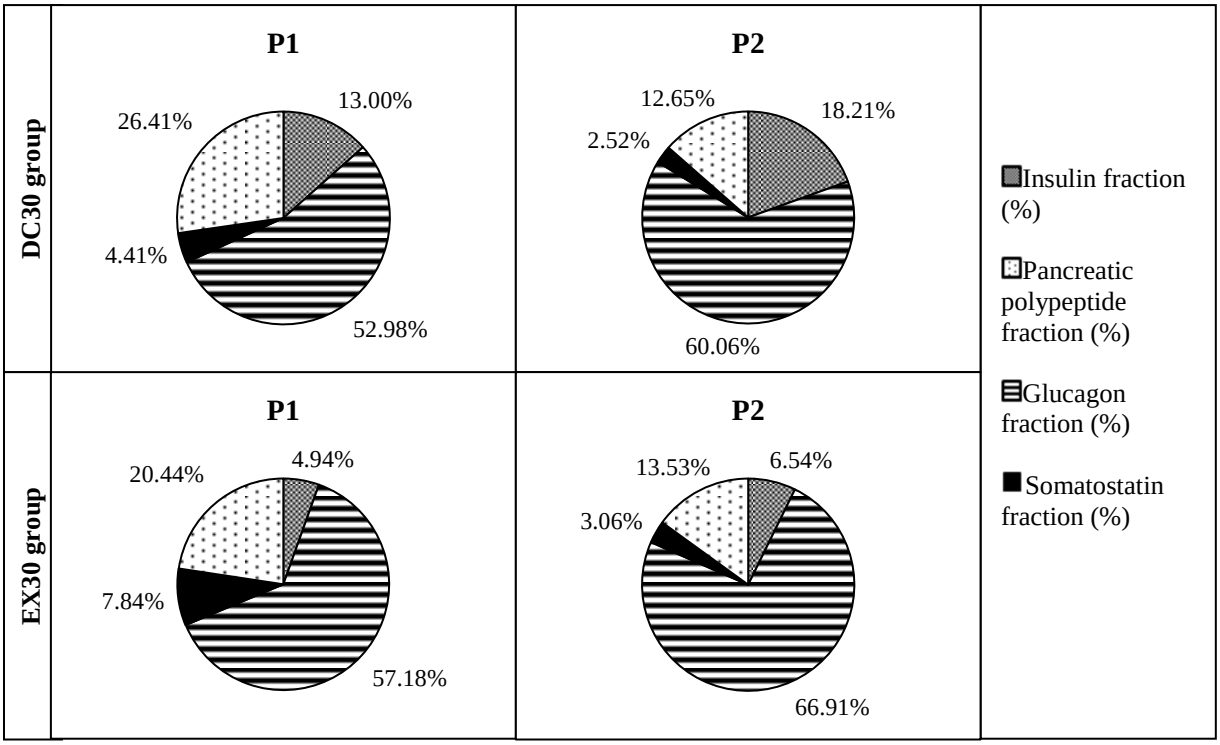

Figure 6.24. Pie chart showing islet composition in the P1 and P2 portions of the pancreas of the DC30 group and the EX30 group. (DC30) diabetic control day 30; (EX30) experimental day 30; (P1) proximal portion of the pancreas; (P2) distal portion of the pancreas.

7. DISCUSSION

7.1 BLOOD GLUCOSE, BODY WEIGHT AND SERUM INSULIN

Diabetes was successfully induced over a period of 10 days by a single intraperitoneal injection of STZ at a dose of 45 mg/kg. The average BGL was above 23 mmol/L throughout the diabetes induction period and peaked on day 10 post-STZ injection (29.39 mmol/L). During the experimental period hyperglycaemia remained stable, with body weight decreasing over time. Other studies have successfully used STZ at similar and higher doses (40-70 mg/kg) to produce diabetic rats within as little as two days (Coskun, Ocakci *et al*. 2004, Coskun, Kanter *et al*. 2005, Adewole, Caxton-Martins *et al*. 2006,Akinola, Caxton-Martins *et al*. 2010, Toma, Makonnen *et al*. 2015). However, there is a risk of acute STZ toxicity and mortality between day 6 and 10 post-administration (Deeds, Anderson *et al*. 2011). Our study subjected animals that survived 10 days diabetes induction with stable hyperglycaemia to PDL treatment. Additionally, to ensure effectiveness of this relatively low dose of STZ, animals were fasted prior to STZ injection. Lowering blood glucose prior to STZ injection results in more severe beta cell destruction compared to the same dose of STZ administered to animals in a fed state (Cavelti-Weder, Shtessel *et al*. 2013). This is due to the fact that less glucose is occupying beta cell GLUT2 receptors, allowing STZ to readily enter the beta cell (Cavelti-Weder, Shtessel *et al*. 2013).

No spontaneous recovery from STZ-induced diabetes was observed in control groups over the total of 40 days (diabetes induction period and experimental period). This is in agreement with the findings of previous studies, specifically in models or groups where no intervention was done to aid glycaemic control (Coskun, Kanter *et al*. 2005, Adewole, Caxton-Martins *et al*. 2006, Yin, Tao *et al*. 2006, Akinola, Caxton-Martins *et al*. 2010). Endogenous beta-cell recovery in STZ-diabetic mice is, however, reported to occur following 120 days of islet transplantation or insulin implant (Grossman, Lee *et al*. 2010, Yin, Tao *et al*. 2006). Since the current study aimed to induce endogenous beta-cell recovery by PDL alone, no insulin was administered to diabetic animals as this could interfere with the results.

The animals' body weights during the diabetes induction period decreased following the overnight fast. Following STZ injection the weights remained decreased and did not return to baseline values even 10 days post-STZ injection. During the subsequent experimental period body weight fluctuated, with no tendency to increase in the DC animals as would be expected

in non-diabetic animals. Body weight of the DC animals also did not show a tendency to decrease over time during the experimental period; these findings are concomitant with the repot of Toma *et al.* (2015). Other researchers, however, reported decreasing body weight in STZ-induced diabetic rats over extended periods of time (28-30 days) (Coskun, Kanter *et al*. 2005, Adewole, Caxton-Martins *et al*. 2006). In the EX groups, body weight decreased with time (EX30) compared to DC groups where body weight remained relatively constant. This observation was not in line with the literature that reports that PDL does not affect body weight of non-diabetic animals (Xu, D'Hoker *et al*. 2008, Rankin, Wilbur *et al*. 2013).

Serum insulin levels were variable, with most of the measurements falling outside the range of the standard curve. It is interesting to note that one animal in the NC group (that was within the range of the standard curve) had similar values to one animal in the EX30 group, although this result cannot be conclusive. Based on this observation, it may be worth further investigating serum insulin levels in our model. It is expected that using fasting serum samples with an ELISA kit with higher specificity for rat samples may yield better results.

7.2 HISTOMORPHOLOGY OF THE PANCREAS

The portions of the pancreata were morphologically assessed in NC, DC and EX groups. In the DC groups, the exocrine compartment of the pancreas was healthy, with similar histomorphology as observed in the NC group. The histomorphology of the exocrine compartment in the P1 portions of the pancreas in the EX groups was similar to normal, while P2 portions presented with deleterious changes in the exocrine compartment, characterised by the initial apoptosis of acinar cells with concomitant proliferation of the duct cells. This phenomenon is consistently reported in the literature for rodent models of PDL (Tchokonte-Nana 2011, Cavelti-Weder, Shtessel *et al*. 2013, Hakonen, Ustinov *et al*. 2011, Chintinne, Stange *et al*. 2012, Rankin, Wilbur *et al*. 2013). Acinar damage is said to be induced by the premature activation of the pancreatic digestive enzymes within the acinar cells due to disruption of calcium-signalling following PDL (Mooren, Hlouschek *et al*. 2003). An early study provided evidence that some acinar cells may also convert to duct cells following PDL (Churg, Richter 1972).

In our diabetic model, the morphological changes observed in the P2 portions on day three and day five post-PDL are comparable to the third and fourth landmarks described by Tchokonte-Nana (2011) in a non-diabetic rat model (Tchokonte-Nana 2011). These changes were widespread acinar deletion, oedema and ductal proliferation on day three and

remodelling of the exocrine pancreas became evident by day five post-PDL, where lobes with intact exocrine morphology were observed. This remodelling persisted on day 10 and 30 post-PDL in all animals in our study.

The assessment of the endocrine compartment in the DC groups revealed progressive necrotic changes, including degranulation, hydropic changes and pyknotic nuclei. These changes correlate with the histopathology previously reported in STZ-induced diabetic rats (Coskun, Ocakci *et al*. 2004, Coskun, Kanter *et al*. 2005, Adewole, Caxton-Martins *et al*. 2006, Akinola, Caxton-Martins *et al*. 2010). Similarly, necrotic changes were found in the islets of the EX groups, except in the P1 and P2 portions of the pancreas in the EX30 group, where recovery in islet cell morphology was noted. This recovery could possibly be attributed to the remodelling effect of PDL. Moreover, previous studies using PDL alone or in combination with STZ reported that the islets are not damaged by PDL (Tchokonte-Nana 2011, Cavelti-Weder, Shtessel *et al*. 2013), this could substantiate the effects of PDL remodelling in our study.

7.3 ISLET COMPOSITION AND ARCHITECTURE IN THE PANCREAS

7.3.1 Islet composition and architecture in the NC group

In the present study normal islet (NC group) composition varied between the P1 (proximal) and P2 (distal) portions of the pancreas. Normal islets in the P1 portion consisted of 58.72% beta cells, 4.93% PP cells, 25.26% alpha cells and 2.15% delta cells, while normal islets in the P2 portion had 68.72% beta-cells, 5.30% PP cells, 21.05% alpha cells and 3.93% delta cells. Beta and delta cell fractions were higher in the normal P2 portion compared to the P1 portion. These results are in line with normal rodent islet composition reported in the literature (Erlandsen, Hegre *et al*. 1976, Weiczoreck, Pospischil *et al*. 1998, Zafar, Mughal 2002, Brissova, Fowler *et al*. 2005, Steiner, Kim *et al*. 2010, Ruipan, Xiangzhi *et al*. 2014). However, PP cell fraction did not differ between the two portions in the normal pancreas, contradicting a previous report that PP cells may be more numerous in the head region of the pancreas (Elayat, El-Naggar *et al*. 1995). Alpha cell fraction is reported to be higher in the P1 portion (Zafar, Mughal 2002) and this tendency was observed in the present study Previous studies have included classifying hormone staining intensity in their evaluation of the diabetic pancreas (Coskun, Ocakci *et al*. 2004, Coskun, Kanter *et al*. 2005). In the present study, the hormone staining intensity in the P1 and P2 portions of the pancreas in the NC group was strong in beta, alpha and PP cells, while delta cells had medium hormone staining intensity.

Rodent islet architecture, where beta cells occupy the central part of the islet while non-beta cells are located at the islet's periphery, is consistently described in the literature (Erlandsen, Hegre *et al*. 1976, Elayat, El-Naggar *et al*. 1995, Weiczoreck, Pospischil *et al*. 1998, Zafar, Mughal 2002, Brissova, Fowler *et al*. 2005, Steiner, Kim *et al*. 2010). This same general architecture was observed in the present study. While most studies using 2D methods to visualise rodent islet architecture report that the non-beta cells form a relatively continuous mantle layer surrounding the beta-cell core (Erlandsen, Hegre *et al*. 1976, Weiczoreck, Pospischil *et al*. 1998, Brissova, Fowler *et al*. 2005), our study reports that non-beta cells form a discontinuous mantle layer and that the central beta cell mass extends from the core to the mantle area of the islet. Our observations are similar to a report using 3D imaging techniques to visualize islet architecture (Kharouta, Miller *et al*. 2009).

7.3.2 Islet composition and architecture in DC and EX groups

7.3.2.1 Beta cells

Islet beta cell fraction was severely decreased in the DC0 group, compared to the NC group, to only 13.58% in the P1 and 22.68% in the P2 portion of the pancreas and remained low or further decreased over time in DC and EX groups. This observation is consistent with the work of Orci *et al*. (1976), reporting that even 16 months following STZ injection at a dose of 45mg/kg beta cells remain decreased. Additionally, the beta cell fraction differences between islets in the P1 and P2 portions were distorted in the DC and EX groups, indicating disproportionate beta cell loss throughout the pancreas. The observed reduction in beta cell fraction is as a result of STZ-induced beta-cell necrosis observed in the DC and EX groups and is in line with the literature (Li, Karlsson *et al*. 2000, Coskun, Ocakci *et al*. 2004, Coskun, Kanter *et al*. 2005, Adewole, Caxton-Martins *et al*. 2006, Akinola, Caxton-Martins *et al*. 2010, Zhang, Zhang *et al*. 2012).

In the DC and EX groups, the few surviving beta cells were scattered throughout the diabetic islet, unlike in the NC group where they formed a single central mass in the islet. These surviving beta cells did not meet physiological insulin demands and the animals remained severely hyperglycaemic. It is reported that even with 25% beta cell survival, there is no functional insulin response to glucose challenge in STZ-induced diabetic mice (Meier, Ueberberg *et al*. 2011). It is proposed that islet architecture (i.e. the clustering of beta cells) is important for synchronized and sufficient insulin release from the islet (Aspinwall, Lakey *et*

al. 1999); in this regard the observed disruption in islet architecture in both the DC and EX groups may explain the impairment of the function of the remaining beta cells.

There were very few differences in insulin expression between DC and EX groups. However, beta cell hormone staining intensity was even more decreased in EX groups compared to DC groups, indicating that PDL did not have a positive effect on restoring beta cell function in EX groups. Furthermore, the beta cell fraction was significantly decreased in the P1 portion of the EX30 group when compared to the P1 portion of the DC30 group. This observation suggests that PDL negatively affects beta cell fraction in the P1 portion of the pancreas. This is a novel observation, as previous reports indicated no effect of PDL on beta cell fraction in the P1 portion of the pancreas (Wang, Kloppel *et al*. 1995, Hakonen, Ustinov *et al*. 2011, Cavelti-Weder, Shtessel *et al*. 2013).

Many studies report beta cell expansion in the post-ligated portion (P2 portion) of the pancreas following PDL in non-diabetic animals (Xu, D'Hoker *et al*. 2008, Solar, Cardalda *et al*. 2009b, Wang, Zhang *et al*. 2011, Hakonen, Ustinov *et al*. 2011, Van de Casteele, Leuckx *et al*. 2013, De Groef, Leuckx *et al*. 2015). Yet, in the present study the P2 portion of DC and EX groups had similar beta cell fractions, indicating that PDL had no effect on beta cell fraction in the P2 portion of the pancreas. Previous studies may have overestimated beta cell formation as their measurements are normalised to total pancreatic area without taking into account the destruction of the exocrine compartment of the pancreas (Cavelti-Weder, Shtessel *et al*. 2013). As demonstrated by Chintinne *et al*. (2012) beta cell mass (calculated per total area of the pancreas) may be seemingly increased without any significant change in beta cell number (Chintinne, Stange *et al*. 2012). Furthermore, a recent study that quantified total beta cell mass and pancreatic insulin content found no changes following PDL (Rankin, Wilbur *et al*. 2013).

Due to the deficiency in methods for beta cell mass measurements in the PDL model, the present study used beta cell fraction as an indication of beta cell loss and formation. Beta cell fraction is calculated per islet area and is, therefore, not biased by the changes in the exocrine compartment of the P2 portion of the pancreas following PDL. Nonetheless, PDL did not induce beta cell formation within pre-existing islets when applied 10 days following STZ injection. This finding supports previous work of Cavelti-Weder *et al*. (2013), who applied PDL six to seven days post-STZ injection (this was in combination with islet transplants to aid glycaemic control). However, beta cell neoformation was achieved by Chung *et al.* (2010)

when applying PDL only 30 minutes following alloxan injection to destroy beta cells (Chung, Hao *et al*. 2010). This difference in results could be explained by the difference in the time allowed between beta cell ablation and PDL treatment, or by the respective use of STZ and alloxan.

7.3.2.2 PP cells

In the DC and EX groups PP cell fractions were increased compared to the NC group and PP cells were displaced (now found in both the islet core and mantle) by the expanded alpha cell layer of DC and EX islets. This increase in PP cell fraction in the diabetic pancreas is consistent with the findings of Zang *et al*. (2012) and Ruipan *et al*. (2014), while Li *et al*. (2000) in contrast reports no change in PP cell numbers in the STZ-induced diabetic pancreas. The results of these authors may look contradictory due to the fact that Li *et al.* (2000) calculated the mean number of PP cells per islet and did not investigate PP cell fraction. Changes in the PP cell fraction observed in the DC and EX groups of the present study could be the result of disproportionate changes in the other islet cell type fractions. However, the fact that larger groups of PP cells were observed within the diabetic islets may indicate the possibility of an increase in PP cell number. PP cell fraction was significantly higher in the P1 portion of the EX3 group and in the P2 portion of the EX10 group when respectively compared to their DC groups. In the non-diabetic pancreas, PP cells are reportedly deleted from the islet mantle following PDL (Page, du Toit *et al*. 2000). To our knowledge this is the first study investigating changes in PP cell fraction in a model combining STZ and PDL.

7.3.2.3 Alpha cells

Changes in alpha cell composition and distribution were similar in the DC and EX groups. The alpha cell fraction increased to 59.23% in the P1 portion and 60.54% in the P2 portion of the DC0 group. The discontinuous alpha cell layer observed in the NC group appeared expanded and stretched from the mantle to the core of the islet in the DC and EX groups. In DC and EX groups there was no change in hormone staining intensity compared to the NC group, but fewer islets devoid of alpha cells were seen in DC and EX groups. Alpha cell fractions in the DC and EX groups were significantly increased compared to normal for the duration of the 30 day experimental period. Previous studies also reported that STZ-induced diabetic islets have increased alpha cell fractions (Orci, Baetens *et al*. 1976, Zhang, Zhang *et al*. 2012, Ruipan, Xiangzhi *et al*. 2014, Plesner, Ten Holder *et al*. 2014), but authors do not agree on whether total alpha cell area or mass is increased in the diabetic pancreas. The report

from Meier *et al.* (2006 & 2011) indicated no change in alpha cell mass in the diabetic pancreas and is supported by recent findings from Haung *et al*. (2013). In the latter study it is reported that pancreatic glucagon content is increased, without alpha cell number being increased; these alpha cells did, however, have larger glucagon granules and increased glucagon exocytosis (Huang, Rupnik *et al*. 2013). In contrast, alpha cell number is reported to be increased in multiple mouse models of STZ-induced diabetes (Li, Karlsson *et al*. 2000, Lee, Wang *et al*. 2011a, Zhang, Zhang *et al*. 2012, Takeda, Fujita *et al*. 2012, Plesner, Ten Holder *et al*. 2014).

Although total pancreatic alpha cell area was not investigated in the current study, the alpha cell fraction within each islet appeared to be increased following STZ injection. It should be considered that alpha cell fraction will naturally increase due to the loss of beta cells from the islet (Li, Karlsson *et al*. 2000), however, this does not explain the increased thickness of the alpha cell layer that was observed in the present study. This expansion of the alpha cell layer from the periphery into the core of the islet may indicate increased alpha cell numbers. Alpha cell expansion may have occurred via cell proliferation (involved in self-duplication and regeneration) and/or via neogenesis from multipotent progenitors, as was previously reported in a mouse model of STZ-induced diabetes (Zhang, Zhang *et al*. 2012). Interestingly, statistical analyses in the current study indicate that alpha cell fraction did not continue to increase in DC and EX groups over time, but remained at the increased level observed on day 10 post-STZ injection.

In the non-diabetic pancreas, alpha cell volume has been reported to increase following PDL (Wang, Zhang *et al*. 2011, Cai, Yuchi *et al*. 2014).Authors did not take into account the decreased total pancreatic area of the PDL pancreas when calculating alpha cell volume (similar to reported beta cell mass calculations). Nevertheless, an increase in absolute alpha cell number following PDL in the non-diabetic pancreas has also been observed (Chintinne, Stange *et al*. 2012). In contrast, Page *et al*. (2000) reported that alpha cells are deleted from the islet mantle, subsequently forming a very thin discontinuous layer at the islet periphery following PDL. In the present study, alpha cells formed a relatively thick layer following PDL with alpha cell fraction significantly lower in the P2 portion of the EX10 group compared to the P2 portion of the DC10 group; this may indicate deleterious effects of PDL on alpha cells in the diabetic pancreas. However, alpha cell fraction in the P2 portion of the EX10 group did not significantly differ from the alpha cell fraction in the P2 portion of the DC0 group.

7.3.2.4 Delta cells

Delta cell fractions varied in the DC and EX groups, fluctuating between higher and lower fractions compared to the NC group. Increased delta cell fraction in the diabetic pancreas is reported in the literature (Orci, Baetens *et al*. 1976, Ruipan, Xiangzhi *et al*. 2014, Plesner, Ten Holder *et al*. 2014, Alan, Olejar *et al*. 2015), but this finding was not consistent in the present study. Orci *et al.* (1976) suggested that increased delta cell numbers may indicate an adaptive, although unsuccessful, effort by the islets to decrease hyperglucagonemia associated with diabetes, with increased local somatostatin release. Although serum glucagon levels were not evaluated in the present study, it stands to reason that hyperglucagonemia may very well have accompanied the increase in alpha cell fractions observed in the present study. The distribution of delta cells within the islet shifted from the mantle to being observed in both the core and mantle of the islet in both the DC and EX groups. The disruption of delta cell distribution was similar in these groups, although the EX groups presented more frequently with islets devoid of delta cells.

In the non-diabetic pancreas, delta cells are deleted from the islet mantle following PDL (Page, du Toit *et al*. 2000). In line with this observation, delta cell fraction was significantly lower in the P1 portion of the EX3 group and in the P2 portion of the EX10 group compared to their respective control groups. However, on day 30 the delta-cell fraction was increased in the P1 portions of both the DC30 and EX30 groups; moreover, delta cell fraction was significantly higher in the P1 portion of the EX30 group compared to the P1 portion of the DC30 group.

It is interesting to note that, while the literature discussed reported changes only in the P2 (post-ligature) portions of the pancreas, the present study shows that hormone fractions in the P1 portions of the pancreas were also affected following PDL. Furthermore, the only time at which PDL altered the diabetic islet composition in the P2 portions was on day 10. In this portion, the PP cell fraction was increased, while alpha and delta cell fractions were decreased in the EX10 group compared to the DC10 group. At all other days, no differences were found between islet composition in the P2 portions of DC and EX groups. It could be speculated that the observed recovery in the exocrine compartment from day 5 is followed by transient remodelling of islet composition on day 10.

8. CONCLUSION

The project set out to establish islet composition and architecture in diabetic rats following pancreatic duct ligation, and to compare the portions of the pancreas proximal and distal to the ligature. This study demonstrated that the effect of pancreatic duct ligation on the morphology of the diabetic pancreas was similar to that reported in the non-diabetic pancreas. Interestingly, the islets in the experimental 30 day group presented with some apparent morphological recovery. Despite this morphological recovery, islet composition and architecture remained disrupted in the present model combining beta cell ablation and pancreatic duct ligation. Furthermore, pancreatic duct ligation did not restore body weight or normoglycemia.

The portion of the pancreas proximal to the ligation had a decreased beta cell fraction and increased delta cell fraction 30 days following pancreatic duct ligation. These observed changes in diabetic islet composition in the part of the pancreas proximal to the ligature are novel findings. There was no change in the diabetic islet composition in the portion of the pancreas distal to the ligature thirty days following pancreatic duct ligation.

Finally, pancreatic duct ligation did not restore normal islet composition, architecture and physiological glucose homeostasis in STZ-induced diabetic rats in this study. It is possible that the effects of pancreatic duct ligation are limited in an STZ model due to severe damage to pre-existing beta cells and expansion of the alpha cell fraction. Further investigation is warranted to explain the morphological remodelling observed thirty days following pancreatic duct ligation with no improvement in beta cell fraction and function.

9. STRENGTHS, LIMITATIONS AND PERSPECTIVES

The strength of this study lies in the fact that the islet composition and architecture of the four main islet cell types have been established in both portions of the pancreas (proximal and distal to the ligature) in a diabetic PDL model. Hormone fractions were evaluated as part of islet composition. These fractions were also used to indicate the destruction or formation of the various cell types analysed. Since the hormone fractions were determined per islet area, it was not affected by the changes in exocrine pancreas observed in the P2 portion of the pancreas following ligation. Therefore, hormone fractions in the P2 portion of the PDL pancreas could be compared to all other control P1 and P2 portions without being influenced by changes in the exocrine compartment.

However, one of the limitations of the study is that other parameters (apart from hormone fractions) to assess the effects of PDL were not included. For example, changes in islet size and compositional differences between small and large islets, induction of endocrine progenitor activity and replication rate of the islet cell types were not investigated.

The inconclusive serum insulin assessment was also a limitation. Future studies combining STZ and PDL should further investigate serum insulin levels from fasted blood samples and with an ELISA kit with higher specificity for rodent samples. Serum glucagon levels can also be included to assess possible hyperglucagonemia, and this could be correlated with the hormone fractions and staining intensity observed in the pancreas to highlight the physiological significance of the micro-anatomical changes observed.

In perspective, we suggest that the effects of PDL should be investigated in a type 2 diabetic model, where there is limited damage to pre-existing beta cells, for comparison with the present study.

REFERENCES

ADEWOLE, S.O., CAXTON-MARTINS, E.A. and OJEWOLE, J.A., 2006. Protective effect of quercetin on the morphology of pancreatic beta-cells of streptozotocin-treated diabetic rats. *African Journal of Traditional, Complementary, and Alternative Medicines*, **4**(1), pp. 64-74.

ADRIAN, T.E., BLOOM, S.R., BESTERMAN, H.S., BARNES, A.J., COOKE, T.J.C., RUSSELL, R.C.G. and FABER, R.G., 1977. Mechanism of pancreatic polypeptide release in man. *The Lancet*, **309**, pp. 161-163.

AKINOLA, O.B., CAXTON-MARTINS, E.A. and DINI, L., 2010. Chronic Treatment with Ethanolic Extract of the Leaves of Azadirachta indica Ameliorates Lesions of Pancreatic Islets in Streptozotocin Diabetes. *International Journal of Morphology*, **28**(1), pp. 291-302.

ALAN, L., OLEJAR, T., CAHOVA, M., ZELENKA, J., BERKOVA, Z., SMETAKOVA, M., SAUDEK, F., MATEJ, R. and JEZEK, P., 2015. Delta Cell Hyperplasia in Adult Goto-Kakizaki (GK/MolTac) Diabetic Rats. *Journal of Diabetes Research*, **2015**, pp. 385395.

APELQVIST, A., LI, H., SOMMER, L., BEATUS, P., ANDERSON, D.J., HONJO, T., HRABE DE ANGELIS, M., LENDAHL, U. and EDLUND, H., 1999. Notch signalling controls pancreatic cell differentiation. *Nature*, **400**(6747), pp. 877-881.

ASAKAWA, A., INUI, A., YUZURIHA, H., UENO, N., KATSUURA, G., FUJIMIYA, M., FUJINO, M.A., NIIJIMA, A., MEGUID, M.M. and KASUGA, M., 2003. Characterization of the effects of pancreatic polypeptide in the regulation of energy balance. *Gastroenterology*, **124**(5), pp. 1325-1336.

ASPINWALL, C.A., LAKEY, J.R. and KENNEDY, R.T., 1999. Insulin-stimulated insulin secretion in single pancreatic beta cells. *The Journal of Biological Chemistry*, **274**(10), pp. 6360-6365.

ATKINSON, M.A., 2000. Chapter 4. Type 1 diabetes. In: C.R. KAHN, ed, *Atlas of Diabetes.* London: Science Press Limited, pp. 45-57.

BAEYENS, L., BONNE, S., BOS, T., ROOMAN, I., PELEMAN, C., LAHOUTTE, T., GERMAN, M., HEIMBERG, H. and BOUWENS, L., 2009. Notch signaling as gatekeeper of rat acinar-to-beta-cell conversion in vitro. *Gastroenterology*, **136**(5), pp. 1750-60.e13.

BAEYENS, L., LEMPER, M., LEUCKX, G., DE GROEF, S., BONFANTI, P., STANGE, G., SHEMER, R., NORD, C., SCHEEL, D.W., PAN, F.C., AHLGREN, U., GU, G., STOFFERS, D.A., DOR, Y., FERRER, J., GRADWOHL, G., WRIGHT, C.V., VAN DE CASTEELE, M., GERMAN, M.S., BOUWENS, L. and HEIMBERG, H., 2014. Transient cytokine treatment induces acinar cell reprogramming and regenerates functional beta cell mass in diabetic mice. *Nature Biotechnology*, **32**(1), pp. 76-83.

BALLIAN, N. and BRUNICARDI, F.C., 2007. Islet vasculature as a regulator of endocrine pancreas function. *World Journal of Srugery*, **31**, pp. 705-714.

BATTERHAM, R.L., LE ROUX, C.W., COHEN, M.A., PARK, A.J., ELLIS, S.M., PATTERSON, M., FROST, G.S., GHATEI, M.A. and BLOOM, S.R., 2003. Pancreatic polypeptide reduces appetite and food intake in humans. *The Journal of Clinical Endocrinology and Metabolism,* **88**(8), pp. 3989-3992.

BENNINGER, R.K., HEAD, W.S., ZHANG, M., SATIN, L.S. and PISTON, D.W., 2011. Gap junctions and other mechanisms of cell-cell communication regulate basal insulin secretion in the pancreatic islet. *The Journal of Physiology,* **589**(Pt 22), pp. 5453-5466.

BONNER-WEIR, S. and ORCI, L., 1982. New perspectives on the microvasculature of the islets of Langerhans in the rat. *Diabetes,* **31**(10), pp. 883-889.

BOSCO, D., ARMANET, M., MOREL, P., NICLAUSS, N., SGROI, A., MULLER, Y.D., GIOVANNONI, L., PARNAUD, G. and BERNEY, T., 2010. Unique arrangement of alpha- and beta-cells in human islets of Langerhans. *Diabetes,* **59**(5), pp. 1202-1210.

BRAMSWIG, N.C., EVERETT, L.J., SCHUG, J., DORRELL, C., LIU, C., LUO, Y., STREETER, P.R., NAJI, A., GROMPE, M. and KAESTNER, K.H., 2013. Epigenomic plasticity enables human pancreatic alpha to beta cell reprogramming. *The Journal of Clinical Investigation,* **123**(3), pp. 1275-1284.

BRISSOVA, M., FOWLER, M.J., NICHOLSON, W.E., CHU, A., HIRSHBERG, B., HARLAN, D.M. and POWERS, A.C., 2005. Assessment of human pancreatic islet architecture and composition by laser scanning confocal microscopy. *The Journal of Histochemistry and Cytochemistry,* **53**(9), pp. 1087-1097.

BRUNICARDI, F.C., STAGNER, J., BONNER-WEIR, S., WAYLAND, H., KLEINMAN, R., LIVINGSTON, E., GUTH, P., MENGER, M., MCCUSKEY, R., INTAGLIETTA, M., CHARLES, A., ASHLEY, S., CHEUNG, A., IPP, E., GILMAN, S., HOWARD, T. and PASSARO, E.,JR, 1996. Microcirculation of the islets of Langerhans. Long Beach Veterans Administration Regional Medical Education Center Symposium. *Diabetes,* **45**(4), pp. 385-392.

BUTLER, A.E., JANSON, J., BONNER-WEIR, S., RITZEL, R., RIZZA, R.A. and BUTLER, P.C., 2003. Beta-cell deficit and increased beta-cell apoptosis in humans with type 2 diabetes. *Diabetes,* **52**(1), pp. 102-110.

CABRERA, O., BERMAN, D.M., KENYON, N.S., RICORDI, C., BERGGREN, P.O. and CAICEDO, A., 2006. The unique cytoarchitecture of human pancreatic islets has implications for islet cell function. *Proceedings of the National Academy of Sciences of the United States of America,* **103**(7), pp. 2334-2339.

CAI, Y., YUCHI, Y., DE GROEF, S., COPPENS, V., LEUCKX, G., BAEYENS, L., VAN DE CASTEELE, M. and HEIMBERG, H., 2014. IL-6-dependent proliferation of alpha cells in mice with partial pancreatic-duct ligation. *Diabetologia,* **57**(7), pp. 1420-1427.

CATALA, J., DAUMAS, M., CHANH, A.P., LASSERRE, B. and HOLLANDE, E., 2001. Insulin and glucagon impairments in relation with islet cells morphological modifications following long term pancreatic duct ligation in the rabbit - a model of non-insulin-dependent diabetes. *International Journal of Experimental Diabetes Research,* **2**(2), pp. 101-112.

CAVELTI-WEDER, C., SHTESSEL, M., REUSS, J.E., JERMENDY, A., YAMADA, T., CABALLERO, F., BONNER-WEIR, S. and WEIR, G.C., 2013. Pancreatic duct ligation after almost complete beta-cell loss: exocrine regeneration but no evidence of beta-cell regeneration. *Endocrinology,* **154**(12), pp. 4493-4502.

CHERRINGTON, A.D., CALDWELL, M.D., DIETZ, M.R., EXTON, J.H. and CROFFORD, O.B., 1977. The effect of somatostatin on glucose uptake and production by rat tissues in vitro. *Diabetes,* **26**(8), pp. 740-748.

CHINTINNE, M., STANGE, G., DENYS, B., LING, Z., IN 'T VELD, P. and PIPELEERS, D., 2012. Beta cell count instead of beta cell mass to assess and localize growth in beta cell population following pancreatic duct ligation in mice. *PLoS ONE,* **7**(8), pp. e43959.

CHOI, S.K., SHIN, J.S., LEE, J.J., KIM, Y.S., KIM, S.B. and KIM, C.W., 2005. In vitro trans-differentiation of rat mesenchymal cells into insulin-producing cells by rat pancreatic extract. *Biochemical and Biophysical Research Communications*, **330**, pp. 1299-1305.

CHUNG, C.H., HAO, E., PIRAN, R., KEINAN, E. and LEVINE, F., 2010. Pancreatic beta-cell neogenesis by direct conversion from mature alpha-cells. *Stem cells,* **28**(9), pp. 1630-1638.

CHUNG, C.H. and LEVINE, F., 2010. Adult pancreatic alpha-cells: a new source of cells for beta-cell regeneration. *The Review of Diabetic Studies,* **7**(2), pp. 124-131.

CHURG, A. and RICHTER, W.R., 1972. Histochemical distribution of carbonic anhydrase after ligation of the pancreatic duct. *The American Journal of Pathology,* **68**(1), pp. 23-30.

COLLOMBAT, P., MANSOURI, A., HECKSHER-SORENSEN, J., SERUP, P., KRULL, J., GRADWOHL, G. and GRUSS, P., 2003. Opposing actions of Arx and Pax4 in endocrine pancreas development. *Genes & Development,* **17**(20), pp. 2591-2603.

COSKUN, O., KANTER, M., KORKMAZ, A. and OTER, S., 2005. Quercetin, a flavonoid antioxidant, prevents and protects streptozotocin-induced oxidative stress and beta-cell damage in rat pancreas. *Pharmacological Research,* **51**(2), pp. 117-123.

COSKUN, O., OCAKCI, A., BAYRAKTAROGLU, T. and KANTER, M., 2004. Exercise training prevents and protects streptozotocin-induced oxidative stress and beta-cell damage in rat pancreas. *The Tohoku Journal of Experimental Medicine,* **203**(3), pp. 145-154.

CRISCIMANNA, A., SPEICHER, J.A., HOUSHMAND, G., SHIOTA, C., PRASADAN, K., JI, B., LOGSDON, C.D., GITTES, G.K. and ESNI, F., 2011. Duct cells contribute to regeneration of endocrine and acinar cells following pancreatic damage in adult mice. *Gastroenterology,* **141**(4), pp. 1451-62, 1462.e1-6.

DE GROEF, S., LEUCKX, G., VAN GASSEN, N., STAELS, W., CAI, Y., YUCHI, Y., COPPENS, V., DE LEU, N., HEREMANS, Y., BAEYENS, L., VAN DE CASTEELE, M. and HEIMBERG, H., 2015. Surgical Injury to the Mouse Pancreas through Ligation of the Pancreatic Duct as a Model for Endocrine and Exocrine Reprogramming and Proliferation. *Journal of Visualized Experiments,* **102**, pp. 10.3791/52765.

DEEDS, M.C., ANDERSON, J.M., ARMSTRONG, A.S., GASTINEAU, D.A., HIDDINGA, H.J., JAHANGIR, A., EBERHARDT, N.L. and KUDVA, Y.C., 2011. Single dose streptozotocin-induced diabetes: considerations for study design in islet transplantation models. *Laboratory Animals,* **45**(3), pp. 131-140.

DESAI, B.M., OLIVER-KRASINSKI, J., DE LEON, D.D., FARZAD, C., HONG, N., LEACH, S.D. and STOFFERS, D.A., 2007. Preexisting pancreatic acinar cells contribute to acinar cell, but not islet beta cell, regeneration. *The Journal of Clinical Investigation,* **117**(4), pp. 971-977.

DOR, Y., BROWN, J., MARTINEZ, O.I. and MELTON, D.A., 2004. Adult pancreatic beta-cells are formed by self-duplication rather than stem-cell differentiation. *Nature,* **429**(6987), pp. 41-46.

DU TOIT, D.F., LONGO-MBENZA, B., PAGE, B.J. and TCHOKONTE-NANA, V., 2011. Efficency of co-expression of transcription factors Pdx1, Ngn3, NeuroD and Pax6 with insulin: A statistical approach. *International Journal of Diabetes Mellitus,* doi:10.1016/j.ijdm.2011.01.007.

EDLUND, H., 1998. Transcribing pancreas. *Diabetes,* **47**(12), pp. 1817-1823.

EDSTROM, C. and FALKMER, S., 1968. Pancreatic morphology and blood glucose level in rats at various intervals after duct ligation. *Virchows Archiv A: Pathology Pathologische Anatomie,* **345**(2), pp. 139-153.

ELAYAT, A.A., EL-NAGGAR, M.M. and TAHIR, M., 1995. An immunocutochemical and morphometric study of the rat pancreatic islets. *Journal of Anatomy,* **186**, pp. 629-637.

ERLANDSEN, S.L., HEGRE, O.D., PARSONS, J.A., MCEVOY, R.C. and ELDE, R.P., 1976. Pancreatic islet cell hormones distribution of cell types in the islet and evidence for the presence of somatostatin and gastrin within the D cell. *The Journal of Histochemistry and Cytochemistry,* **24**(7), pp. 883-897.

ESNI, F., TALJEDAL, I.B., PERL, A.K., CREMER, H., CHRISTOFORI, G. and SEMB, H., 1999. Neural cell adhesion molecule (N-CAM) is required for cell type segregation and normal ultrastructure in pancreatic islets. *The Journal of Cell Biology,* **144**(2), pp. 325-337.

EZRIN, C., SALTER, J.M., OGRYZLO, M.A. and BEST, C.H., 1958. The clinical and metabolic effects of glucagon. *Canadian Medical Association Journal*, **78**(2), pp. 96-98.

FARHAT, B., ALMELKAR, A., RAMACHANDRAN, K., WILLIAMS, S.J., HUANG, H.H., ZAMIEROWKSI, D., NOVIKOVA, L. and STEHNO-BITTEL, L., 2013. Small human islets comprised of more beta-cells with higher insulin content than large islets. *Islets,* **5**(2), pp. 87-94.

FEINLE-BISSET, C., PATTERSON, M., GHATEI, M.A., BLOOM, S.R. and HOROWITZ, M., 2005. Fat digestion is required for suppression of ghrelin and stimulation of peptide YY and pancreatic polypeptide secretion by intraduodenal lipid. *American Journal of Physiology, Endocrinology and Metabolism,* **289**(6), pp. E948-53.

FRANKLIN, I., GROMADA, J., GJINOVCI, A., THEANDER, S. and WOLLHEIM, C.B., 2005. β-cell secretory products activate α-cell ATP-dependant potassium channels to inhibit glucagon release. *Diabetes,* **54**, pp. 1808-1815.

FUJITA, Y., TAKITA, M., SHIMODA, M., ITOH, T., SUGIMOTO, K., NOGUCHI, H., NAZIRUDDIN, B., LEVY, M.F. and MATSUMOTO, S., 2011. Large human islets secrete less insulin per islet equivalent than smaller islets in vitro. *Islets,* **3**(1), pp. 1-5.

GAO, X., SONG, L., SHEN, K., WANG, H., QIAN, M., NIU, W. and QIN, X., 2014. Bone marrow mesenchymal stem cells promote the repair of islets from diabetic mice through paracrine actions. *Molecular and Cellular Endocrinology,* **388**(1-2), pp. 41-50.

GEORGIA, S. and BHUSHAN, A., 2004. Beta cell replication is the primary mechanism for maintaining postnatal beta cell mass. *The Journal of Clinical Investigation,* **114**(7), pp. 963-968.

GERSELL, D.J., GINGERICH, R.L. and GREIDER, M.H., 1979. Reginal distribution and concentration of pancreatic polypeptide in the human and canine pancreas. *Diabetes,* **28**(1), pp. 11-15.

GITTES, G.K., 2009. Developmental biology of the pancreas: a comprehensive review. *Developmental Biology,* **326**(1), pp. 4-35.

GRADWOHL, G., DIERICH, A., LEMEUR, M. and GUILLEMOT, F., 2000. Neurogenin3 is Required for the Development of the Four Endocrine Cell Lineages of the Pancreas. *Proceedings of the National Academy of Sciences of the United States of America,* **97**(4), pp. 1607-1611.

GREENBAUM, C.J., PRIGEON, R.L. and D'ALESSIO, D.A., 2002. Impaired beta-cell function, incretin effect, and glucagon suppression in patients with type 1 diabetes who have normal fasting glucose. *Diabetes,* **51**(4), pp. 951-957.

GROSSMAN, E.J., LEE, D.D., TAO, J., WILSON, R.A., PARK, S.Y., BELL, G.I. and CHONG, A.S., 2010. Glycemic control promotes pancreatic beta-cell regeneration in streptozotocin-induced diabetic mice. *PLoS ONE,* **5**(1), pp. e8749.

GU, C., STEIN, G.H., PAN, N., GOEBBELS, S., HORNBERG, H., NAVE, K.A., HERRERA, P., WHITE, P., KAESTNER, K.H., SUSSEL, L. and LEE, J.E., 2010. Pancreatic beta cells require NeuroD to achieve and maintain functional maturity. *Cell Metabolism,* **11**(4), pp. 298-310.

GU, G., DUBAUSKAITE, J. and MELTON, D.A., 2002a. Direct evidence for the pancreatic lineage: NGN3+ cells are islet progenitors and are distinct from duct progenitors. *Development,* **129**(10), pp. 2447-2457.

GU, G., DUBAUSKAITE, J. and MELTON, D.A., 2002b. Direct evidence for the pancreatic lineage: NGN3+ cells are islet progenitors and are distinct from duct progenitors. *Development,* **129**(10), pp. 2447-2457.

HAKONEN, E., USTINOV, J., MATHIJS, I., PALGI, J., BOUWENS, L., MIETTINEN, P.J. and OTONKOSKI, T., 2011. Epidermal growth factor (EGF)-receptor signalling is needed for murine beta cell mass expansion in response to high-fat diet and pregnancy but not after pancreatic duct ligation. *Diabetologia,* **54**(7), pp. 1735-1743.

HALD, J., HJORTH, J.P., GERMAN, M.S., MADSEN, O.D., SERUP, P. and JENSEN, J., 2003. Activated Notch1 prevents differentiation of pancreatic acinar cells and attenuate endocrine development. *Developmental Biology,* **260**(2), pp. 426-437.

HAMAMOTO, N., ASHIZAWA, N., NIIGAKI, M., KAJI, T., KATSUBE, T., ENDOH, H., WATANABE, M., SUMI, S. and KINOSHITA, Y., 2002. Morphological changes in the rat exocrine pancreas after pancreatic duct ligation. *Histology and Histopathology,* **17**(4), pp. 1033-1041.

HANLEY, S.C., AUSTIN, E., ASSOULINE-THOMAS, B., KAPELUTO, J., BLAICHMAN, J., MOOSAVI, M., PETROPAVLOVSKAIA, M. and ROSENBERG, L., 2010. {beta}-Cell mass dynamics and islet cell plasticity in human type 2 diabetes. *Endocrinology,* **151**(4), pp. 1462-1472.

HAO, E., LEE, S.H. and LEVINE, F., 2013. Efficient beta-cell regeneration by a combination of neogenesis and replication following beta-cell ablation and reversal of pancreatic duct ligation. *Stem Cells,* **31**(11), pp. 2388-2395.

HAUGE-EVANS, A.C., KING, A.J., CARMIGNAC, D., RICHARDSON, C.C., ROBINSON, I.C., LOW, M.J., CHRISTIE, M.R., PERSAUD, S.J. and JONES, P.M., 2009. Somatostatin secreted by islet delta-cells fulfills multiple roles as a paracrine regulator of islet function. *Diabetes,* **58**(2), pp. 403-411.

HENQUIN, J.C. and RAHIER, J., 2011. Pancreatic alpha cell mass in European subjects with type 2 diabetes. *Diabetologia,* **54**(7), pp. 1720-1725.

HEPTULLA, R.A., RODRIGUEZ, L.M., BOMGAARS, L. and HAYMOND, M.W., 2005. The role of amylin and glucagon in the dampening od glycemic excursions in children with type 1 diabetes. *Diabetes,* **54**, pp. 1100-1107.

HUANG, H.H., NOVIKOVA, L., WILLIAMS, S.J., SMIRNOVA, I.V. and STEHNO-BITTEL, L., 2011. Low insulin content of large islet population is present in situ and in isolated islets. *Islets,* **3**(1), pp. 6-13.

HUANG, Y.C., RUPNIK, M.S., KARIMIAN, N., HERRERA, P.L., GILON, P., FENG, Z.P. and GAISANO, H.Y., 2013. In situ electrophysiological examination of pancreatic alpha cells in the streptozotocin-induced diabetes model, revealing the cellular basis of glucagon hypersecretion. *Diabetes,* **62**(2), pp. 519-530.

ISHIHARA, H., MAECHLER, P., GJINOVCI, A., HERRERA, P.L. and WOLLHEIM, C.B., 2003. Islet β-cell secretion determines glucagon release from neighboring α-cells. *Nature Cell Biology,* **5**, pp. 330-335.

JACOVETTI, C., ABDERRAHMANI, A., PARNAUD, G., JONAS, J.C., PEYOT, M.L., CORNU, M., LAYBUTT, R., MEUGNIER, E., ROME, S., THORENS, B., PRENTKI, M.,

BOSCO, D. and REGAZZI, R., 2012. MicroRNAs contribute to compensatory beta cell expansion during pregnancy and obesity. *The Journal of Clinical Investigation,* **122**(10), pp. 3541-3551.

JESUDASON, D.R., MONTEIRO, M.P., MCGOWAN, B.M., NEARY, N.M., PARK, A.J., PHILIPPOU, E., SMALL, C.J., FROST, G.S., GHATEI, M.A. and BLOOM, S.R., 2007. Low-dose pancreatic polypeptide inhibits food intake in man. *The British Journal of Nutrition,* **97**(3), pp. 426-429.

JIANG, G. and ZHANG, B.B., 2003. Glucagon and regulation of glucose metabolism. *American journal of physiology.Endocrinology and Metabolism,* **284**(4), pp. E671-8.

JUHL, K., BONNER-WEIR, S. and SHARMA, A., 2010. Regenerating pancreatic beta-cells: plasticity of adult pancreatic cells and the feasibility of in-vivo neogenesis. *Current Opinion in Organ Transplantation,* **15**(1), pp. 79-85.

JURGENS, C.A., TOUKATLY, M.N., FLIGNER, C.L., UDAYASANKAR, J., SUBRAMANIAN, S.L., ZRAIKA, S., ASTON-MOURNEY, K., CARR, D.B., WESTERMARK, P., WESTERMARK, G.T., KAHN, S.E. and HULL, R.L., 2011. Beta-Cell Loss and Beta-Cell Apoptosis in Human Type 2 Diabetes are Related to Islet Amyloid Deposition. *The American Journal of Pathology,* **178**(6), pp. 2632-2640.

KAILEY, B., VAN DE BUNT, M., CHELEY, S., JOHNSON, P.P., MACDONALD, P.E., GLOYN, A.L., RORSMAN, P. and BRAUN, M., 2012. SSTR2 is the functionally dominant somatostatin receptor in human pancreatic β- and α-cells. *American Journal of Physiology, Endocrinology and Metabolism,* **303**, pp. E1107-E1116.

KHAROUTA, M., MILLER, K., KIM, A., WOJCIK, P., KILIMNIK, G., DEY, A., STEINER, D.F. and HARA, M., 2009. No mantle formation in rodent islets -- the prototype of islet revisited. *Diabetes Research and Clinical Practice,* **85**(3), pp. 252-257.

KILIMNIK, G., ZHAO, B., JO, J., PERIWAL, V., WITKOWSKI, P., MISAWA, R. and HARA, M., 2011. Altered islet composition and disproportionate loss of large islets in patients with type 2 diabetes. *PLoS ONE,* **6**(11), pp. e27445.

KIM, A., MILLER, K., JO, J., KILIMNIK, G., WOJCIK, P. and HARA, M., 2009. Islet architechture A comparative study. *Islets,* **1**(2), pp. 129-136.

KJEMS, L.L., KIRBY, B.M., WELSH, E.M., VELDHUIS, J.D., STRAUME, M., MCINTYRE, S.S., YANG, D., LEFEBVRE, P. and BUTLER, P.C., 2001. Decrease in beta-cell mass leads to impaired pulsatile insulin secretion, reduced postprandial hepatic insulin clearance, and relative hyperglucagonemia in the minipig. *Diabetes,* **50**(9), pp. 2001-2012.

KOJIMA, S., UENO, N., ASAKAWA, A., SAGIYAMA, K., NARUO, T., MIZUNO, S. and INUI, A., 2007. A role for pancreatic polypeptide in feeding and body weight regulation. *Peptides,* **28**, pp. 459-463.

KOPINKE, D. and MURTAUGH, L.C., 2010. Exocrine-to-endocrine differentiation is detectable only prior to birth in the uninjured mouse pancreas. *Developmental Biology,* **10**, doi:10.1186/1471-213X-10-38.

KOPP, J.L., DUBOIS, C.L., SCHAFFER, A.E., HAO, E., SHIH, H.P., SEYMOUR, P.A., MA, J. and SANDER, M., 2011a. Sox9+ ductal cells are multipotent progenitors throughout development but do not produce new endocrine cells in the normal or injured adult pancreas. *Development,* **138**(4), pp. 653-665.

KOPP, J.L., DUBOIS, C.L., SCHAFFER, A.E., HAO, E., SHIH, H.P., SEYMOUR, P.A., MA, J. and SANDER, M., 2011b. Sox9+ ductal cells are multipotent progenitors throughout development but do not produce new endocrine cells in the normal or injured adult pancreas. *Development,* **138**(4), pp. 653-665.

LEE, Y., WANG, M.Y., DU, X.Q., CHARRON, M.J. and UNGER, R.H., 2011a. Glucagon receptor knockout prevents insulin-deficient type 1 diabetes in mice. *Diabetes,* **60**(2), pp. 391-397.

LEE, Y., WANG, M.Y., DU, X.Q., CHARRON, M.J. and UNGER, R.H., 2011b. Glucagon receptor knockout prevents insulin-deficient type 1 diabetes in mice. *Diabetes,* **60**(2), pp. 391-397.

LEHMANN, R., ZUELLIG, R.A., KUGELMEIER, P., BAENNINGER, P.B., MORITZ, W., PERREN, A., CLAVIEN, P.A., WEBER, M. and SPINAS, G.A., 2007. Superiority of small islets in human islet transplantation. *Diabetes,* **56**(3), pp. 594-603.

LI, W., NAKANISHI, M., ZUMSTEG, A., SHEAR, M., WRIGHT, C., MELTON, D.A. and ZHOU, Q., 2014. In vivo reprogramming of pancreatic acinar cells to three islet endocrine subtypes. *eLife,* **3**, pp. e01846.

LI, W.C., RUKSTALIS, J.M., NISHIMURA, W., TCHIPASHVILI, V., HABENER, J.F., SHARMA, A. and BONNER-WEIR, S., 2010. Activation of pancreatic-duct-derived progenitor cells during pancreas regeneration in adult rats. *Journal of Cell Science,* **123**(16), pp. 2792-2802.

LI, Z., KARLSSON, F.A. and SANDLER, S., 2000. Islet loss and alpha cell expansion in type 1 diabetes induced by multiple low-dose streptozotocin administration in mice. *The Journal of Endocrinology,* **165**(1), pp. 93-99.

LIU, Y., GUTH, P.H., KANEKO, K., LIVINGSTON, E.H. and BRUNICARDI, F.C., 1993. Dynamic in vivo observation of rat islet microcirculation. *Pancreas,* **8**(1), pp. 15-21.

LUDVIGSEN, E., OLSSON, R., STRIDSBERG, M., JANSON, E.T. and SANDLER, S., 2004. Expression and distribution of somatostatin receptor subtypes in the pancreatic islets of mice and rats. *The Journal of Histochemistry and Cytochemistry,* **52**(3), pp. 391-400.

MACGREGOR, R.R., WILLIAMS, S.J., TONG, P.Y., KOVER, K., MOORE, W.V. and STEHNO-BITTEL, L., 2006. Small rat islets are superior to large islets in in vitro function and in transplantation outcomes. *American Journal of Physiology, Endocrinology and Metabolism,* **290**(5), pp. E771-9.

MARQUEZ-AGUIRRE, A.L., CANALES-AGUIRRE, A.A., PADILLA-CAMBEROS, E., ESQUIVEL-SOLIS, H. and DIAZ-MARTINEZ, N.E., 2015. Development of the endocrine

pancreas and novel strategies for beta-cell mass restoration and diabetes therapy. *Brazilian Journal of Medical and Biological Research,* **48**(9), pp. 765-776.

MATSCHINSKY, F.M. and ELLERMAN, J.E., 1967. Metabolism of glucose in the islets of Langerhans. *The Journal of Biological Chemistry,* **243**(10), pp. 2730-2736.

MATVEYENKO, A. and VELLA, A., 2015. Regenerative Medicine in Diabetes. *Myo Clinic Proceedings,* **90**(4), pp. 546-554.

MEDA, P., KOHEN, E., KOHEN, C., RABINOVITCH, A. and ORCI, L., 1982. Direct communication of homologous and heterologous endocrine islet cells in culture. *The Journal of Cell Biology,* **92**(1), pp. 221-226.

MEIER, J.J., BUTLER, A.E., SAISHO, Y., MONCHAMP, T., GALASSO, R., BHUSHAN, A., RIZZA, R.A. and BUTLER, P.C., 2008. Beta-cell replication is the primary mechanism subserving the postnatal expansion of beta-cell mass in humans. *Diabetes,* **57**(6), pp. 1584-1594.

MEIER, J.J., KJEMS, L.L., VELDHUIS, J.D., LEFEBVRE, P. and BUTLER, P.C., 2006. Postprandial suppression of glucagon secretion depends on intact pulsatile insulin secretion: further evidence for the intraislet insulin hypothesis. *Diabetes,* **55**(4), pp. 1051-1056.

MEIER, J.J., UEBERBERG, S., KORBAS, S. and SCHNEIDER, S., 2011. Diminished glucagon suppression after beta-cell reduction is die to impaired alpha-cell function rather than an expansion of alpha-cell mass. *American Journal of Physiology, Endocrinology and Metabolism,* **300**, pp. 717-723.

MENGE, B.A., GRUBER, L., JORGENSEN, S.M., DEACON, C.F., SCHMIDT, W.E., VELDHUIS, J.D., HOLST, J.J. and MEIER, J.J., 2011. Loss of inverse relationship between pulsatile insulin and glucagon secretion in patients with type 2 diabetes. *Diabetes,* **60**(8), pp. 2160-2168.

MEYERHOLZ, D.K. and SAMUEL, I., 2007. Morphologic characterization of early ligation-induced acute pancreatitis in rats. *American Journal of Surgery,* **194**(5), pp. 652-658.

MIRALLES, F., CZERNICHOW, P. and SCHARFMANN, R., 1998. Follistatin regulates the relative proportions of endocrine versus exocrine tissue during pancreatic development. *Development,* **125**(6), pp. 1017-1024.

MIYASHITA, K., MIYATSUKA, T., MATSUOKA, T.A., SASAKI, S., TAKEBE, S., YASUDA, T., WATADA, H., KANETO, H. and SHIMOMURA, I., 2014. Sequential introduction and dosage balance of defined transcription factors affect reprogramming efficiency from pancreatic duct cells into insulin-producing cells. *Biochemical and Biophysical Research Communications,* **444**(4), pp. 514-519.

MOOREN, F.C., HLOUSCHEK, V., FINKES, T., TURI, S., WEBER, I.A., SINGH, J., DOMSCHKE, W., SCHNEKENBURGER, J., KRUGER, B. and LERCH, M.M., 2003. Early changes in pancreatic acinar cell calcium signaling after pancreatic duct obstruction. *The Journal of Biological Chemistry,* **278**(11), pp. 9361-9369.

MORISCOT, C., DE FRAIPONT, F., RICHARD, M.J., MARCHAND, M., SAVATIER, P., BOSCO, D., FAVROT, M. and BENHAMOU, P.Y., 2005. Human bone marrow mesenchymal stem cells can express insulin and key transcription factors of the endocrine pancreas developmental pathway upon genetic and/or microenvironmental manipulation in vitro. *Stem cells,* **23**(4), pp. 594-603.

MURAKAMI, M., FUJITA, T., MIYAKE, T., OHTSUKA, A., TAGUCHI, T. and KIKUTA, A., 1993. The insulo-acinar portal and insulo-venous drainage systems in the pancreas of the mouse, dog, monkey and certain other animals: A scanning electron microscopic study of corrosion casts. *Archives of Histology and Cytology,* **56**(2), pp. 127-147.

MURAKAMI, T., MIYAKE, T., TSUBOUCHI, M., OTHSUKA, A. and FUJITA, T., 1997. Blood flow patterns in the rat pancreas: A simulative demonstration by injection replication and scanning electron microscopy. *Microscopy Research and Technique*, **37**, pp. 497-508.

MYTHILI, M.D., VYAS, R., AKILA, G. and GUNASEKARAN, S., 2004. Effect of streptozotocin on the ultrastructure of rat pancreatic islets. *Microscopy Research and Technique,* **63**(5), pp. 274-281.

NAGASAO, J., YOSHIOKA, K., AMASAKI, H. and MUTOH, K., 2003. Centroacinar and intercalated duct cells as potential precursors of pancreatic endocrine cells in rats treated with streptozotocin. *Annals of Anatomy,* **185**(3), pp. 211-216.

NIR, T., MELTON, D.A. and DOR, Y., 2007. Recovery from diabetes in mice by beta cell regeneration. *The Journal of Clinical Investigation,* **117**(9), pp. 2553-2561.

NISHIMURA, W., KONDO, T., SALAMEH, T., EL KHATTABI, I., DODGE, R., BONNER-WEIR, S. and SHARMA, A., 2006. A switch from MafB to MafA expression accompanies differentiation to pancreatic beta-cells. *Developmental Biology,* **293**, pp. 526-539.

NOLLEVAUX, M.C., RAHIER, J., MARCHANDISE, J., THURION, P., GODECHARLES, S., VAN DEN STEEN, G., JAMART, J., SEMPOUX, C., JACQUEMIN, P. and GUIOT, Y., 2013. Characterization of beta-cell plasticity mechanisms induced in mice by a transient source of exogenous insulin. *American Journal of Physiology, Endocrinology and Metabolism,* **304**(7), pp. E711-23.

NYMAN, L.R., WELLS, K.S., HEAD, W.S., MCCAUGHEY, M., FORD, E., BRISSOVA, M., PISTON, D.W. and POWERS, A.C., 2008. Real-time, multidimensional in vivo imaging used to investigate blood flow in mouse pancreatic islets. *The Journal of Clinical Investigation,* **118**(11), pp. 3790-3797.

OHTANI, O. and WANG, Q.X., 1997. Comparative analysis of insulo-acinar portal system in rats, guinea pigs, and dogs. *Microscopy Research and Technique*, **37**(5-6), pp. 489-496.

ORCI, L., BAETENS, D., RUFENER, C., AMHERDT, M., RAVAZZOLA, M., STUDER, P., MALAISSE-LAGAE, F. and UNGER, R.H., 1976. Hypertrophy and hyperplasia of somatostatin-containing D-cells in diabetes. *Proceedings of the National Academy of Sciences of the United States of America,* **73**(4), pp. 1338-1342.

ORCI, L., MALAISSE-LAGAE, F., RAVAZZOLA, M., ROUILLER, D., RENOLD, A.E., PERRELET, A. and UNGER, R., 1975. A morphological basis for intercellular communication between alpha- and beta-cells in the endocrine pancreas. *The Journal of Clinical Investigation,* **56**(4), pp. 1066-1070.

PAGE, B.J., DU TOIT, D.F., MULLER, C.J., MATTYSEN, J. and LYNERS, R., 2000. An immunocytochemical profile of the endocrine pancreas using an occlusive duct ligation model. *JOP : Journal of the Pancreas,* **1**(4), pp. 191-203.

PAGE, B.J., 2000. *A histological and morphometric assessment of endocrine and ductular proliferation in the adult rat pancreas using an occlusive pancreatic duct ligation model,* Stellenbosch University.

PLESNER, A., TEN HOLDER, J.T. and VERCHERE, C.B., 2014. Islet remodeling in female mice with spontaneous autoimmune and streptozotocin-induced diabetes. *PLoS ONE,* **9**(8), pp. e102843.

PONTIROLI, A.E., PERFETTI, M.G., ANDREOTTI, A.C., FATTOR, B., MONTI, L.D. and POZZA, G., 1993. Metabolic effects of graded glucagon infusions in man: inhibition of glucagon, insulin, and somatostatin response to arginine. *Metabolism: Clinical and Experimental,* **42**(10), pp. 1242-1248.

PRALONG, W.F., BARTLEY, C. and WOLLHEIM, C.B., 1990. Single islet beta-cell stimulation by nutrients: relationship between pyridine nucleotides, cytosolic Ca2+ and secretion. *The EMBO Journal,* **9**(1), pp. 53-60.

RACKHAM, C.L., JONES, P.M. and KING, A.J., 2013. Maintenance of islet morphology is beneficial for transplantation outcome in diabetic mice. *PLoS ONE,* **8**(2), pp. e57844.

RANKIN, M.M., WILBUR, C.J., RAK, K., SHIELDS, E.J., GRANGER, A. and KUSHNER, J.A., 2013. β-cells are not generated in pancreatic duct ligation-induced injury in adult mice. *Diabetes,* **62**, pp. 1634-1645.

REUBI, J.C., KAPPELER, A., WASER, B., SCHONBRUNN, A. and LAISSUE, J., 1998. Immunohistochemical localization of somatostatin receptro sst2A in human pancreatic islets. *Journal of Clinical Endocrinology and Metabolism,* **83**(10), pp. 3746-3749.

ROMER, A.I. and SUSSEL, L., 2015. Pancreatic islet cell development and regeneration. *Current Opinion in Endocrinology, Diabetes and Obesity,* **22**(4), pp. 255-264.

RORSMAN, P., ELIASSON, L., RENSTROM, E., GROMADA, J., BARG, S. and GOPEL, S., 2000. The Cell Physiology of Biphasic Insulin Secretion. *News in Physiological Sciences,* **15**, pp. 72-77.

ROVIRA, M., SCOTT, S.G., LISS, A.S., JENSEN, J., THAYER, S.P. and LEACH, S.D., 2010. Isolation and characterization of centroacinar/terminal ductal progenitor cells in adult mouse pancreas. *Proceedings of the National Academy of Sciences of the United States of America,* **107**(1), pp. 75-80.

RUIPAN, Z., XIANGZHI, M., LI, L., YING, Z., MINGLIANG, Q., PENG, J., JINGWEI, L., ZIJUN, Z. and YAN, G., 2014. Differential expression and localization of neuropeptide Y peptide in pancreatic islet of diabetic and high fat fed rats. *Peptides*, **54**, pp. 33-38.

SADLER, T.W. and LANGMAN, J., 2012. *Langman's Medical Embryology*. 12th edn. Philadelphia: Wolters Kluwer Health/Lippincott Williams & Wilkins.

SAISHO, Y., BUTLER, A.E., MANESSO, E., ELASHOFF, D., RIZZA, R.A. and BUTLER, P.C., 2013. Beta-Cell Mass and Turnover in Humans: Effects of Obesity and Aging. *Diabetes Care*, **36**(1), pp. 111-117.

SAMOLS, E., STAGNER, J.I., EWART, R.B.L. and MARKS, V., 1988. The order of islet microvascular cellular perfusion is B A D in the perfused rat pancreas. *Journal of Clinical Investigation*, **82**, pp. 350-353.

SANDER, M., NEUBUSER, A., KALAMARAS, J., EE, H.C., MARTIN, G.R. and GERMAN, M.S., 1997. Genetic analysis reveals that PAX6 is required for normal transcription of pancreatic hormone genes and islet development. *Genes & Development*, **11**(13), pp. 1662-1673.

SANDER, M., SUSSEL, L., CONNERS, J., SCHEEL, D., KALAMARAS, J., DELA CRUZ, F., SCHWITZGEBEL, V., HAYES-JORDAN, A. and GERMAN, M., 2000. Homeobox gene Nkx6.1 lies downstream of Nkx2.2 in the major pathway of beta-cell formation in the pancreas. *Development*, **127**(24), pp. 5533-5540.

SCHMIDT, P.T., NASLUND, E., GRYBACK, P., JACOBSSON, H., HOLST, J.J., HILSTED, L. and HELLSTROM, P.M., 2005. A role for pancreatic polypeptide in the regulation of gastric emtying and short-term metabolic control. *The Journal of Clinical Endocrinology & Metabolism*, **90**(9), pp. 5241-5246.

SHERWOOD, L., 2010. The peripheral endocrine glands. In: M. ARBOGAST and L. OLIVEIRA, eds, *Human Physiology: From Cells to Systems, 7th Ed.* Canada: Brooks/Cole Cengage Learning, pp. 710-726.

SINGH, V., BRENDEL, M.D., ZACHARIAS, S., MERGLER, S., JAHR, H., WIEDENMAN, B., BRETZEL, R.G., PLOCKINGER, U. and STROWSKI, M.Z., 2007. Characterization of somatostatin receptor subtype-specific regulation of insulin and glucagon secretion: An in vitro study on isolated human pancreatic islets. *Journal of Clinical Endocrinology & Metabolism*, **92**(2), pp. 673-680.

SOLAR, M., CARDALDA, C., HOUBRACKEN, I., MARTI´N, M., MAESTRO, M., DE MEDTS, N., XU, X., GRAU, V., HEIMBERG, H., BOUWENS, L. and FERRER, J., 2009a. Pancreatic Exocrine Duct Cells Give Rise to Insulin-Producing β Cells during Embryogenesis but Not after Birth. *Developmental Cell*, **17**, pp. 849-860.

SOLAR, M., CARDALDA, C., HOUBRACKEN, I., MARTIN, M., MAESTRO, M.A., DE MEDTS, N., XU, X., GRAU, V., HEIMBERG, H., BOUWENS, L. and FERRER, J., 2009b. Pancreatic exocrine duct cells give rise to insulin-producing beta cells during embryogenesis but not after birth. *Developmental Cell*, **17**(6), pp. 849-860.

SONG, K.H., KO, S.H., AHN, Y.B., YOO, S.J., CHIN, H.M., KANETO, H., YOON, K.H., CHA, B.Y., LEE, K.W. and SON, H.Y., 2004. In vitro transdifferentiation of adult pancreatic acinar cells into insulin-expressing cells. *Biochemical and Biophysical Research Communications,* **316**(4), pp. 1094-1100.

SORDI, V., MALOSIO, M.L., MARCHESI, F., MERCALLI, A., MELZI, R., GIORDANO, T., BELMONTE, N., FERRARI, G., LEONE, B.E., BERTUZZI, F., ZERBINI, G., ALLAVENA, P., BONIFACIO, E. and PIEMONTI, L., 2005. Bone marrow mesenchymal stem cells express a restricted set of functionally active chemokine receptors capable of promoting migration to pancreatic islets. *Blood,* **106**(2), pp. 419-427.

STAGNER, J.I., SAMOLS, E. and BONNER-WEIR, S., 1988. β→ α → δ pancreatic islet cellular perfusion in dogs. *Diabetes,* **37**, pp. 1715-1721.

STAGNER, J.I. and SAMOLS, E., 1992. The vascular order of islet cellular perfusion in the human pancreas. *Diabetes,* **41**(1), pp. 93-97.

STAGNER, J.I. and SAMOLS, E., 1986. Retrograde perfusion as a model for testing the relative effects of glucose versus insulin on the A cell. *The Journal of Clinical Investigation,* **77**(3), pp. 1034-1037.

STEINER, D.J., KIM, A., MILLER, K. and HARA, M., 2010. Pancreatic islet plasticity: Interspecies comparison of islet architecture and composition. *Islets,* **2**(3), pp. 135-145.

STOZER, A., GOSAK, M., DOLENSEK, J., PERC, M., MARHL, M., RUPNIK, M.S. and KOROSAK, D., 2013. Functional connectivity in islets of Langerhans from mouse pancreas tissue slices. *PLoS Computational Biology,* **9**(2), pp. e1002923.

SUGIYAMA, T., BENITEZ, C.M., GHODASARA, A., LIU, L., MCLEAN, G.W., LEE, J., BLAUWKAMP, T.A., NUSSE, R., WRIGHT, C.V., GU, G. and KIM, S.K., 2013. Reconstituting pancreas development from purified progenitor cells reveals genes essential for islet differentiation. *Proceedings of the National Academy of Sciences of the United States of America,* **110**(31), pp. 12691-12696.

SWALES, N., MARTENS, G.A., BONNE, S., HEREMANS, Y., BORUP, R., VAN DE CASTEELE, M., LING, Z., PIPELEERS, D., RAVASSARD, P., NIELSEN, F., FERRER, J. and HEIMBERG, H., 2012. Plasticity of adult human pancreatic duct cells by neurogenin3-mediated reprogramming. *PLoS ONE,* **7**(5), pp. e37055.

TAKEDA, Y., FUJITA, Y., HONJO, J., YANAGIMACHI, T., SAKAGAMI, H., TAKIYAMA, Y., MAKINO, Y., ABIKO, A., KIEFFER, T.J. and HANEDA, M., 2012. Reduction of both beta cell death and alpha cell proliferation by dipeptidyl peptidase-4 inhibition in a streptozotocin-induced model of diabetes in mice. *Diabetologia,* **55**(2), pp. 404-412.

TCHOKONTE-NANA, V., 2011. *Cellular mechanisms involved in the recapitulation of endocrine development in the duct ligated pancreas,* Stellenbosch University.

TETA, M., RANKIN, M.M., LONG, S.Y., STEIN, G.M. and KUSHNER, J.A., 2007. Growth and regeneration of adult beta cells does not involve specialized progenitors. *Developmental Cell*, **12**(5), pp. 817-826.

THOREL, F., NEPOTE, V., AVRIL, I., KOHNO, K., DESGRAZ, R., CHERA, S. and HERRERA, P.L., 2010. Conversion of adult pancreatic alpha-cells to beta-cells after extreme beta-cell loss. *Nature*, **464**(7292), pp. 1149-1154.

TIMPER, K., SEBOEK, D., EBERHARDT, M., LINSCHEID, P., CHRIST-CRAIN, M., KELLER, U., MULLER, B. and ZULEWSKI, H., 2006. Human adipose tissue-derived mesenchymal stem cells differentiate into insulin, somatostatin, and glucagon expressing cells. *Biochemical and Biophysical Research Communications*, **341**(4), pp. 1135-1140.

TOMA, A., MAKONNEN, E., MEKONNEN, Y., DEBELLA, A. and ADISAKWATTANA, S., 2015. Antidiabetic activities of aqueous ethanol and n-butanol fraction of Moringa stenopetala leaves in streptozotocin-induced diabetic rats. *Complementary and Alternative Medicine*, **15**, pp. 242-015-0779-0.

UENO, N., INUI, A., IWAMOTO, M., KAGA, T., ASAKAWA, A., OKITA, M., FUJIMIYA, M., NAKAJIMA, Y., OHMOTO, Y., OHNAKA, M., NAKAYA, Y., MIYAZAKI, J.I. and KASUGA, M., 1999. Decreased food intake and body weight in pancreatic polypeptide-overexpressing mice. *Gastroenterology*, **117**(6), pp. 1427-1432.

VAN DE CASTEELE, M., LEUCKX, G., BAEYENS, L., CAI, Y., YUCHI, Y., COPPENS, V., DE GROEF, S., ERIKSSON, M., SVENSSON, C., AHLGREN, U., AHNFELT-RONNE, J., MADSEN, O.D., WAISMAN, A., DOR, Y., JENSEN, J.N. and HEIMBERG, H., 2013. Neurogenin 3+ cells contribute to beta-cell neogenesis and proliferation in injured adult mouse pancreas. *Cell Death & Disease*, **4**, pp. e523.

WANG, H., ZHANG, W., CAI, H., XU, S., SUI, W., JIANG, Y., DENG, S. and LOU, J., 2011. alpha-Cell loss from islet impairs its insulin secretion in vitro and in vivo. *Islets*, **3**(2), pp. 58-65.

WANG, R.N., KLOPPEL, G. and BOUWENS, L., 1995. Duct- to islet-cell differentiation and islet growth in the pancreas of duct-ligated adult rats. *Diabetologia*, **38**(12), pp. 1405-1411.

WEICZORECK, G., POSPISCHIL, A. and PERENTES, E., 1998. A comparative immunohistochemical study of pancreatic islets in laboratory animals (rats, dogs, minipigs, nonhuman primates). *Experimental and Toxicologic Pathology*, **50**, pp. 151-172.

WEIR, G.C., SAMOLS, E., LOO, S., PATEL, Y.C. and GABBAY, K.H., 1979. Somatostatin and pancreatic polypeptide secretion: effects of glucagon, insulin, and arginine. *Diabetes*, **28**(1), pp. 35-40.

XU, X., D'HOKER, J., STANGE, G., BONNE, S., DE LEU, N., XIAO, X., VAN DE CASTEELE, M., MELLITZER, G., LING, Z., PIPELEERS, D., BOUWENS, L., SCHARFMANN, R., GRADWOHL, G. and HEIMBERG, H., 2008. Beta cells can be generated from endogenous progenitors in injured adult mouse pancreas. *Cell*, **132**(2), pp. 197-207.

YIN, D., TAO, J., LEE, D.D., SHEN, J., HARA, M., LOPEZ, J., KUZNETSOV, A., PHILIPSON, L.H. and CHONG, A.S., 2006. Recovery of islet beta-cell function in streptozotocin- induced diabetic mice: an indirect role for the spleen. *Diabetes*, **55**(12), pp. 3256-3263.

YU, X., PARK, B.H., WANG, M.Y., WANG, Z.V. and UNGER, R.H., 2008. Making insulin-deficient type 1 diabetic rodents thrive without insulin. *Proceedings of the National Academy of Sciences of the United States of America*, **105**(37), pp. 14070-14075.

ZAFAR, M. and MUGHAL, A., 2002. Distribution of cell types of the islets of Langerhans in the pancreas of the albino rats. *The Professional*, **9**(1), pp. 71-76.

ZHANG, Y., ZHANG, Y., BONE, R.N., CUI, W., PENG, J.B., SIEGAL, G.P., WANG, H. and WU, H., 2012. Regeneration of pancreatic non-beta endocrine cells in adult mice following a single diabetes-inducing dose of streptozotocin. *PLoS ONE*, **7**(5), pp. e36675.

ZHOU, Q., BROWN, J., KANAREK, A., RAJAGOPAL, J. and MELTON, D.A., 2008. In vivo reprogramming of adult pancreatic exocrine cells to beta-cells. *Nature*, **455**(7213), pp. 627-632.

APPENDICES

APPENDIX A: Standard rat pellets

- Aquanutro Laboratory Animal Food, Rodent Breeder (Nutrocience (Pty) Ltd, Malmesbury, South Africa)

APPENDIX B: Materials and methods - Blood glucose and body weight measurments

Materials:

- GlucoPlus Meter (GlucoPlus, Montreal, Canada)
- GlucoPlus Blood Glucose Test Strip (GlucoPlus, Montreal, Canada)
- Electronic scale (TE1502S, Sartorius, Germany)

Methods: Blood glucose measurements

- A small blood sample was collected from the tip of the animal's tail by gently pricking the tail with a sterile lancet
- The blood drop was collected using a glucose test strip inserted into the glucometer
- The reading appeared on the glucometer's screen

APPENDIX C: Materials - Diabetes induction

- Streptozocin (Sigma-Aldrich, South Africa)
- Sodium citrate buffer, pH 4.5, 10mM (Kimix Chemicals, Cape Town, South Africa)
- Syringes
- Needles, 27G, BD Microlance 3 (Beckton Dickinson SA, Gauteng, South Africa)

APPENDIX D: Study groups

Table D: Study groups

	Study group	Sub-group
Non-diabetic	Normal control (n=6)	-
Diabetic	Diabetic control (n=27)	DC day 0 (n=6) DC day 3 (n=6) DC day 5 (n=5) DC day 10 (n=5) DC day 30 (n=5)
	Experimental (n=22)	EX day 3 (n=6) EX day 5 (n=6) EX day 10 (n=5) EX day 30 (n=5)
	Total:	**n=55**

APPENDIX E: Materials - Pancreatic duct ligation

- Isofor (Safeline Pharmaceuticals (Pty) Ltd, Roodepoot, South Africa)
- Electric shaver
- Alcohol 70%
- Surgical instruments: scalpel, clamps, scissors, forceps, cotton buds
- Zeiss OPMi-1 operating microscope (Carl Zeiss, AG, Oberkochen, Germany)
- DISMED Povidine Iodine solution (10%) (Dismed Pharma (Pty) Ltd, Randjes Park, South Africa)
- Resorbable suture material: Safil green 3/0 synthetic absorbable surgical suture, polyglycolic acid coated braided (Phodiso Home & Hospital Services (Pty) Ltd, Newlands, South Africa)
- Non-resorbable suture material: CliniSilk 5/0 black braided silk suture (CliniSut (Pty) Ltd, Port Elizabeth, South Africa)
- Baytril 5% Injectable Solution (Bayer (Pty) Ltd, Gauteng, South Africa)
- Temgesic 1ml (Schering-Plough (Pty) Ltd, Woodmead, South Africa)
- 1 mL BD InsulinSyringe with Permanently Attached Needle (Beckton Dickinson SA, Gauteng, South Africa)

APPENDIX F: Materials and methods – Blood sample collection and ELISA

Materials:

- Syringes (10ml slip tip, Beckton Dickinson SA, Gauteng, South Africa)
- Needles, 27G, BD Microlance 3 (Beckton Dickinson SA, Gauteng, South Africa)
- BD Vaccutainer SST II Advance blood collection tubes(Beckton Dickinson SA, Gauteng, South Africa)
- Insulin human ELISA kit (AB100578, Abcam, BIOCOMbiotech, Centurion, South Africa)
- Microplate reader (FLUOstar Omega, BMG Labtech GmbH, Ortenberg, Germany)
- Precision pipettes (2µl to 1ml)
- Adjustable 1-12ml pipettes
- 100ml and 1L graduated cylinder
- Absorbent paper
- Distilled water
- Tubes (50ml)
- Software for ELISA data analysis (MyAssays, BIOCOMbiotech, Centurion, South Africa)

Methods

- Reagents and standards were prepared according to the ab100578 Insulin Human ELISA Kit protocol
- Plasma samples were not diluted for this protocol
- All standards and samples were run in duplicate, 4 samples from each study group were used
- Standards and samples were loaded into the wells of the microplate as shown in the table below:

Table F: Microplate (96-well)

	1	2	3	4	5	6	7	8	9	10	11	12
A	Std 1	Std 1	NCA	NCA	DC3A	DC3A	DC10A	DC10A	EX3C	EX3C	EX10A	EX10A
B	Std 2	Std 2	NCB	NCB	DC3C	DC3C	DC10B	DC10B	EX3D	EX3D	EX10B	EX10B
C	Std 3	Std 3	NCC	NCC	DC3D	DC3D	DC10C	DC10C	EX3E	EX3E	EX10D	EX10D
D	Std 4	Std 4	NCD	NCD	DC3F	DC3F	DC10D	DC10D	EX3F	EX3F	EX10F	EX10F
E	Std 5	Std 5	DC0A	DC0A	DC5A	DC5A	DC30A	DC30A	EX5A	EX5A	EX30C	EX30C
F	Std 6	Std 6	DC0D	DC0D	DC5B	DC5B	DC30B	DC30B	EX5B	EX5B	EX30D	EX30D
G	Std 7	Std 7	DC0E	DC0E	DC5C	DC5C	DC30C	DC30C	EX5D	EX5D	EX30E	EX30E
H	Blank	Blank	DC0F	DC0F	DC5D	DC5D	DC30F	DC30F	EX5F	EX5F	EX30F	EX30F

- The assay procedure was followed according to the ab100578 Insulin Human ELISA Kit protocol
- Immediately after the assay procedure was complete, the microplate was inserted into a microplate reader to determine absorbance at 450nm
- Data was imported into Excel and transferred to the online MyAssays software for analysis

APPENDIX G: Materials and methods - Standard histological processing

Materials:

- Tissue processor
- 70%, 80%, 95%, 99% ethanol
- Parrafin wax (Paraplast; melting point 58ºC)
- Xylene (Kimix Chemicals, Cape Town, South Africa)
- Embedding moulds

Method:

- Fix tissue in formalin for 48 hours
- Process tissue using the tissue processor (Table F)

- Embed processed tissue in paraffin and block

Table G: Tissue processing protocol

Step	Solution	Time (min)	Temperature (ºC)
1	70% Ethanol	30	40
2	80% Ethanol	30	40
3	95% Ethanol	45	40
4	95% Ethanol	45	40
5	100% Ethanol	45	40
6	100% Ethanol	45	40
7	100% Xylene	45	40
8	100% Xylene	45	40
9	Paraffin	30	58
10	Paraffin	30	58
11	Paraffin	30	58
12	Paraffin	30	58

APPENDIX H: Materials – Histology

- Formalin 10%
- Surgical blade, forceps
- 50ml sample bottels
- Embedding Cassette (SPL Life Sciences, Pocheon, Korea)
- paraffin wax (Paraplast; melting point 58ºC)
- Leica EG 1160 Embedder
- Leica Auto Stainer XL (Leica ST5010, Serial number 1732/07.2007)
- Leica RM 2125 RT microtome
- Leica Bond Autostainer (SMM Instruments (Pty) Ltd, Midrand, South Africa)
- Bond Polymer Refine Detection Kit (SMM Instruments (Pty) Ltd, Midrand, South Africa)
- Bond Polymer Refine Red Detection Kit (SMM Instruments (Pty) Ltd, Midrand, South Africa)
- Bond™ Software ©2009, Version 4.0 (Leica Biosystems, Melbourne, Australia)
- Xylene (Kimix Chemicals, Cape Town, South Africa)
- Ethanol (99% & 96%)
- Acid alcohol (1%)
- Mayer's Haematoxylin (Kimix Chemicals, Cape Town, South Africa)
- Eosin Yellowish (Kimix Chemicals, Cape Town, South Africa)
- Plastic rack
- Ammonia (0.2%)
- Bio-Scan Microscope Slides Frosted (Trifal Imaging, Chatsworth, USA)

- Bio-Scan Microscope Slides Positive Charge (Trifal Imaging, Chatsworth, USA)
- Cover slips
- PDX Mountant (Kimix Chemicals, Cape Town, South Africa)
- Pariodic acid
- Distilled water
- Schiff's solution
- Tap water
- Harris's Haematoxylin
- Staining rack
- Glass container
- Coplin staining jar

APPENDIX I: H&E staining protocol

- Place slides into the plastic rack and into the autostainer, then following the pre-programmed procedure as tabulated below

Table E: H&E staining protocol

Step	Solution	Time	Repetitions
1	Xylene	10 min	2
2	Ethanol (99%)	5 min	2
3	Ethanol (96%)	2 min	1
4	Ethanol (70%)	2 min	1
5	Distilled water	5 sec	1
6	Haematoxylin	8 min	1
7	Running water	5 min	1
8	Ethanol (1% acid alcohol)	30 sec	1
9	Running water	1 min	1
10	Ammonia (0.2%)	45 sec	1
11	Running water	5 min	2
12	Ethanol (96%)	10 dips	1
13	Eosin	45 sec	1
14	Ethanol (96%)	5 min	2
15	Xylene	5 min	2

- When staining procedures are complete, mount a cover slip on the glass slides with PDX

APPENDIX J: IHC staining protocol and manual rehydration

Table J1: Automated IHC double staining protocol

Step	Solution	Incubation Time	Temperature
1	Bond Wash Solution	0 min	72˚C
2	Bond Wash Solution	0 min	72˚C
3	Bond Wash Solution	0 min	Ambient
4	Alcohol	0 min	Ambient
5	Alcohol	0 min	Ambient
6	Alcohol	0 min	Ambient
7	Bond Wash Solution	0 min	Ambient
8	Bond Wash Solution	0 min	Ambient
9	Bond Wash Solution	0 min	Ambient
10	Bond ER Solution 1	0 min	Ambient
11	Bond ER Solution 1	0 min	Ambient
12	Bond ER Solution 1	20 min	100˚C
13	Bond ER Solution 1	12 min	Ambient
14	Bond Wash Solution	0 min	35˚C
15	Bond Wash Solution	0 min	35˚C
16	Bond Wash Solution	0 min	35˚C
17	Bond Wash Solution	3 min	Ambient
18	Peroxide Block	5 min	Ambient
19	Bond Wash Solution	0 min	Ambient
20	Bond Wash Solution	0 min	Ambient
21	Bond Wash Solution	0 min	Ambient
22	Primary Antibody 1	30 min	Ambient
23	Bond Wash Solution	0 min	Ambient
24	Bond Wash Solution	0 min	Ambient
25	Bond Wash Solution	0 min	Ambient
26	Post Primary	8 min	Ambient
27	Bond Wash Solution	2 min	Ambient
28	Bond Wash Solution	2 min	Ambient
29	Bond Wash Solution	2 min	Ambient
30	Polymer	8 min	Ambient
31	Bond Wash Solution	2 min	Ambient
32	Bond Wash Solution	2 min	Ambient
33	Deionized Water	0 min	Ambient
34	Mixed DAB Refine	0 min	Ambient
35	Mixed DAB Refine	10 min	Ambient
36	Deionized Water	0 min	Ambient
37	Deionized Water	0 min	Ambient
38	Deionized Water	0 min	Ambient
39	Haematoxylin	5 min	Ambient
40	Deionized Water	0 min	Ambient
41	Bond Wash Solution	0 min	Ambient
42	Deionized Water	0 min	Ambient
43	Primary Antibody 2	15 min	Ambient
44	Bond Wash Solution	0 min	Ambient
45	Bond Wash Solution	0 min	Ambient
46	Bond Wash Solution	0 min	Ambient
47	Post Primary AP	20 min	Ambient
48	Bond Wash Solution	2 min	Ambient
49	Bond Wash Solution	2 min	Ambient
50	Bond Wash Solution	2 min	Ambient

51	Polymer AP	30 min	Ambient
52	Bond Wash Solution	2 min	Ambient
53	Bond Wash Solution	2 min	Ambient
54	Bond Wash Solution	5 min	Ambient
55	Bond Wash Solution	2 min	Ambient
56	Bond Wash Solution	0 min	Ambient
57	Deionized Water	0 min	Ambient
58	Mixed Red Refine	10 min	Ambient
59	Mixed Red Refine	5 min	Ambient
60	Deionized Water	0 min	Ambient
61	Deionized Water	0 min	Ambient
62	Deionized Water	0 min	Ambient
63	Haematoxylin	5 min	Ambient
64	Deionized Water	0 min	Ambient
65	Bond Wash Solution	0 min	Ambient
66	Deionized Water	0 min	Ambient

Table J2: Manual rehydration protocol

Step	Solution	Time	Repetitions
1	Ethanol (70%)	5 dips	1
2	Ethanol (96%)	5 dips	1
3	Ethanol (99%)	5 dips	1
4	Xylene	1 min	2

APPENDIX K: IHC – Antibodies

Table K: Summary of antibodies

Antibody	Source	Antibody ID	Clonality	Raised in	Dilution
Anti-insulin	BioGenex	MU029-UC	Monoclonal	Mouse	1:1000
Anti-pancreatic polypeptide	Abcam	Ab113694	Polyclonal	Rabbit	1:1500
Anti-glucagon	Abcam	Ab10988	Monoclonal	Mouse	1:5000
Anti-somatostatin	Abcam	Ab22682	Polyclonal	Rabbit	1:2000

APPENDIX L: Raw data – Blood glucose measurements

Grp	ID	BL	F	STZ1	STZ3	STZ5	STZ7	STZ9	d0	d1	d3	d5	d7	d9	d10	d12	d14	d16	d18	d20	d22	d24	d26	d28	d30
NC	A	3.4																							
	B	7.7																							
	C	6.7																							
	D	3.3																							
	E	6.9																							
	F	7.1																							
DC0	A	6.8	4.7	33.3	27.6	15.1	22.4	20.1	25.2																
	B	6.4	3.7	27.7	20.2	10.7	20.2	20.2	32.1																
	C	6.1	3.7	33.3	23.9	20.7	22.2	33.3	31.6																
	D	6.6	3.9	33.3	23.7	20.8	26.1	26.6	26.7																
	E	6.6	3.6	22.9	23.6	15.6	19.6	28.3	33.3																
	F	6.8	3.6	27.6	20.1	11.2	19.2	19.8	19.8																
DC3	A	3.9	2.7	16.9	26.7	21.1	13.7	33.3	33.3	29.9	29.1														
	B	6	5.4	33.3	22.9	16.8	33.3	33.3	26.7	33.3	33.3														
	C	4.9	4.7	16.9	22.2	12.1	22.9	26.4	17	26.4	25.7														
	D	7.7	5.1	20.8	24.7	13.6	16.4	33.3	23.4	33.3	33.3														
	E	6.3	4.8	23.3	24.8	17.2	33.3	28.1	33.3	33.3	30.3														
	F	5.7	4.1	19.9	26.9	14.7	22.9	23.5	33.3	15.1	33.3														
EX3	A	7.4	4.2	23	23.2	33.3	26.7	31.4	33.3	33.3	27.1														
	B	7.1	4.2	33.3	26	33.3	26.8	30.4	33.3	23.1	31.1														
	C	6.7	4.5	19.3	25.9	33.3	17.6	33.3	27.6	16.3	25.6														
	D	7.3	3.7	27.9	25.7	33.3	24	31.1	33.3	33	33.3														
	E	5.9	3.2	33.3	26	30	27.1	24.3	28.1	13.1	20.7														
	F	6.8	3.9	20.7	29.2	30.3	26.4	31.3	31.3	19.4	33.3														
DC5	A	7.8	4.9	26.1	33.3	33.3	23.8	26.3	27.3	18.8	29.5	25.7													
	B	7.9	4.9	33.3	29.6	33.3	32.9	33.3	33.3	33.3	33.3	33.3													
	C	8	4.9	25.9	24.3	25.4	31	18.4	25.3	26.4	33.3	30.4													

Grp	ID	BL	F	STZ1	STZ3	STZ5	STZ7	STZ9	d0	d1	d3	d5	d7	d9	d10	d12	d14	d16	d18	d20	d22	d24	d26	d28	d30
	D	8.1	4.8	17.6	9.2	8.3	5.2	9.2	14.4	11.8	9.1	16													
	F	7.9	5.3	22.7	22.4	31.9	15.7	21.2	21.6	31.1	33.3	27.6													
EX5	A	8	3.6	28.1	27.8	17.8	24.8	18.4	29.1	27.8	33.3	25.2													
	B	6.9	4.6	24.9	33.3	18.8	19.7	16.9	30.4	27.1	15.4	29.7													
	C	7.3	4.3	32.7	29.7	24.6	27.7	33.3	33.3	33.3	31.6	33.3													
	D	7.3	3.9	31.1	31.1	12.4	18.3	33.3	22.1	9	12.4	8.2													
	E	5.9	3.7	20.1	32.6	23.3	25.7	19.3	33.3	33.3	21.3	30.9													
	F	6.8	3.9	28.6	28.7	18.7	20.1	23.1	33.3	22.4	33.3	12.9													
DC10	A	7.5	4.6	32.1	33.3	20.6	33.3	33.3	33.3	25	33.3	33.3	30.1	25.6	33.3										
	B	7.1	4.3	23.9	28.7	18.8	26.3	33.3	28.6	33.3	33.3	16.7	30.5	28.6	33.3										
	C	6.6	3.7	12.4	25.7	22	25.3	19	24.4	33.3	33.3	33.3	33.3	21.9	33.3										
	D	6.7	4.2	18.3	28.6	16.7	24.3	22.9	33.1	33.3	33.3	20.4	29.8	22.6	33.3										
	E	6.5	3.9	33.3	28.7	28.7	24.6	33.3	28.9	33.3	33.3	33.3	30.3	33.3	33.3										
EX10	A	7.7	3.1	24.7	27.1	33.3	20.1	33.3	32.3	33.3	13.9	27.8	19.7	25.9	19										
	B	6.6	4.6	15.7	26	33.3	19.6	32.3	33.3	31.3	15.7	33.3	16.9	33.3	33.3										
	C	6.7	4.6	32.3	32.1	32.9	23.6	19.6	33.3	19.8	33.3	33.3	33.3	33.3	33.3										
	D	6.5	3.5	19.7	33.3	27.4	21.9	33.3	29.6	13.6	25.7	23.6	31.5	24.6	25										
	F	6.7	3.6	18.9	33.2	27.6	21.8	33.3	32.7	19.4	33.3	23.2	26.7	17.7	28.5										
DC30	A	5.8	6.7	27.3	22.1	27.6	28.4	23.4	25.1	26.1	16.9	25.4	21.7	19.2	19.7	25.9	22.1	33.3	19.3	23.8	23.2	24.1	17.3	22.7	19.4
	B	7.3	8.8	24.4	19.4	19.1	11	14.2	18	11.9	7.7	9.8	11.1	7.4	7.7	10.9	12.4	24.2	9.3	9.3	12.2	7.3	6.8	9.4	8.8
	C	7.1	4.3	25.6	21.4	20.1	26.8	31.7	33.3	23.7	25.4	25.9	20.9	21.9	26.1	25.6	25	24.2	28.5	28.6	22.6	24.6	26.1	20.5	28.5
	E	3.6	4.1	33.3	28.1	26.8	18.6	28.2	33.3	23.8	17	33.3	30.7	26.1	21.2	20.7	26.1	24.4	33.3	30.3	33.3	33.3	33.3	33.3	33.3
	F	8.9	5	31.4	24.8	30.3	31.8	28.1	33.3	25.2	30.3	26.1	30.3	32.3	33.3	33.3	31.1	31.3	33.3	33.3	30.8	26.7	33.3	33.3	33.3
EX30	A	8	4.8	33.3	19.6	28.6	17.5	33.3	33.3	32.3	25.9	33.3	33.3	32.3	33.3	33.3	29.6	33.3	33.3	33.3	25.7	33.3	33.3	33.3	33.3
	C	9.1	4.7	24.7	14.3	26.9	16.3	22.7	28.8	18.8	27.8	33.3	21.7	33.3	32.2	26.6	29.4	33.3	33.3	33.3	25.6	33.3	33.3	33.3	33.3
	D	7.3	4.1	33.3	19.4	22.7	30.1	33.3	33.3	21.8	33.3	33.3	28.3	29.1	33.3	33.3	33.3	33.3	33.3	33.3	33.3	33.3	33.3	33.3	33.3
	E	8.3	4.1	18.3	16.6	28.2	25.3	24.7	33.3	22.7	18	21.3	17.9	20.8	32.5	27.8	27.9	33.3	33.3	33.3	33.3	33.3	33.3	33.3	33.3
	F	8.4	5.1	17.6	28.6	26.4	16.8	33.3	32.9	32.1	26.2	24	28.4	25.4	33.3	33.3	22.5	33.3	33.3	33.3	33.3	33.3	33.3	33.3	32.3

APPENDIX M: Raw data – Body weight measurements

Grp	ID	BL	F	STZ1	STZ3	STZ5	STZ7	STZ9	d0	d1	d3	d5	d7	d9	d10	d12	d14	d16	d18	d20	d22	d24	d26	d28	d30
NC	A	223																							
	B	226																							
	C	226																							
	D	222																							
	E	219																							
	F	233																							
DC0	A	215	201	202	200	197	187	184	204																
	B	235	221	220	220	213	203	191	217																
	C	263	250	250	238	230	211	199	222																
	D	233	222	211	215	226	206	197	220																
	E	243	228	227	228	226	214	207	229																
	F	247	232	224	229	226	215	215	240																
DC3	A	217	213	218	218	218	220	227	222	222	224														
	B	216	210	207	199	192	207	206	200	203	213														
	C	208	202	203	206	206	213	215	214	209	222														
	D	234	226	224	219	215	222	218	219	219	221														
	E	294	289	281	275	264	268	266	261	255	258														
	F	207	202	197	201	200	210	220	210	201	216														
EX3	A	185	173	171	167	173	155	156	169	172	169														
	B	210	195	195	192	203	178	170	197	190	193														
	C	255	244	242	239	246	220	223	240	239	238														
	D	257	246	24	234	250	224	220	246	242	252														
	E	252	235	235	232	238	218	210	232	221	229														
	F	235	226	222	221	224	202	201	223	220	220														
DC5	A	207	194	195	202	209	213	220	229	225	236	242													
	B	217	202	201	204	210	216	215	221	211	224	219													
	C	217	204	205	200	207	215	217	216	210	222	219													

Grp	ID	BL	F	STZ1	STZ3	STZ5	STZ7	STZ9	d0	d1	d3	d5	d7	d9	d10	d12	d14	d16	d18	d20	d22	d24	d26	d28	d30
	D	204	194	206	211	221	228	234	239	204	248	257													
	F	234	225	218	205	200	203	203	207	207	206	205													
EX5	A	204	192	189	190	200	185	183	202	197	196	204													
	B	228	214	211	218	221	200	190	225	218	215	227													
	C	235	221	216	212	207	188	188	204	204	203	203													
	D	246	236	242	246	251	243	246	272	260	258	266													
	E	239	227	224	228	231	211	207	236	233	242	245													
	F	236	223	219	214	209	200	190	210	203	199	212													
DC10	A	198	186	183	184	183	185	175	188	186	190	189	192	182	193										
	B	193	181	191	188	194	200	190	209	207	204	212	218	211	217										
	C	258	248	239	234	233	236	225	236	237	236	234	233	227	240										
	D	232	220	219	217	219	255	206	227	223	222	221	221	216	228										
	E	253	227	225	224	222	222	213	228	223	216	218	226	215	216										
EX10	A	212	195	199	208	213	200	202	226	223	219	231	230	220	235										
	B	226	213	206	208	205	191	190	212	209	207	208	211	214	214										
	C	251	237	231	224	220	199	192	216	207	210	213	207	207	210										
	D	237	226	225	220	217	200	200	219	212	215	210	221	218	230										
	F	230	215	212	216	217	199	200	220	220	219	222	225	225	234										
DC30	A	216	211	210	209	213	207	212	212	212	214	221	211	222	222	225	222	228	228	226	226	227	228	223	231
	B	214	208	216	206	211	211	216	220	225	227	233	235	236	238	239	239	245	242	245	247	250	250	248	253
	C	228	221	212	208	194	201	209	208	208	207	211	209	217	210	209	207	217	217	219	213	218	222	218	220
	E	224	214	207	199	204	207	203	201	200	202	200	200	195	191	187	187	186	185	185	186	185	189	189	179
	F	234	228	218	213	216	218	216	226	216	222	215	219	214	216	211	219	220	213	211	212	218	215	217	204
EX30	A	211	198	197	196	208	207	212	215	204	207	205	200	206	206	202	180	194	205	196	207	208	211	213	208
	C	208	198	210	212	218	204	193	210	196	200	201	202	200	198	192	157	177	183	184	188	195	184	195	183
	D	221	214	222	223	230	183	181	190	185	179	191	178	184	176	180	157	165	172	170	174	177	185	177	164
	E	211	201	197	183	190	191	185	197	186	283	174	180	184	180	184	169	171	185	174	183	180	184	189	183
	F	216	206	201	190	197	200	192	196	201	189	180	190	182	180	177	139	170	172	165	180	181	178	183	175

APPENDIX N: Raw data – Insulin ELISA

Table O1: Absorbance values at 450nm (displayed as optical density)

	1	2	3	4	5	6	7	8	9	10	11	12
A	1.78	1.698	0.152	0.184	0.084	0.091	0.081	0.075	0.12	0.138	0.087	0.131
B	1.428	1.351	0.113	0.078	0.081	0.107	0.08	0.083	0.098	0.149	0.122	0.187
C	1.243	1.098	0.105	0.08	0.084	0.107	0.107	0.12	0.129	0.095	0.125	0.21
D	0.77	0.694	0.102	0.092	0.07	0.101	0.115	0.101	0.128	0.181	0.128	0.108
E	0.473	0.461	0.085	0.079	0.072	0.1	0.082	0.1	0.097	0.126	0.036	0.346
F	0.281	0.255	0.082	0.084	0.095	0.1	0.092	0.105	0.102	0.11	0.155	0.116
G	0.119	0.125	0.077	0.087	0.084	0.079	0.086	0.118	0.11	0.11	0.13	0.128
H	0.068	0.067	0.082	0.077	0.086	0.092	0.09	0.098	0.127	0.128	0.181	0.124

Results obtained from MyAssays online analysis tool:

Insulin 1

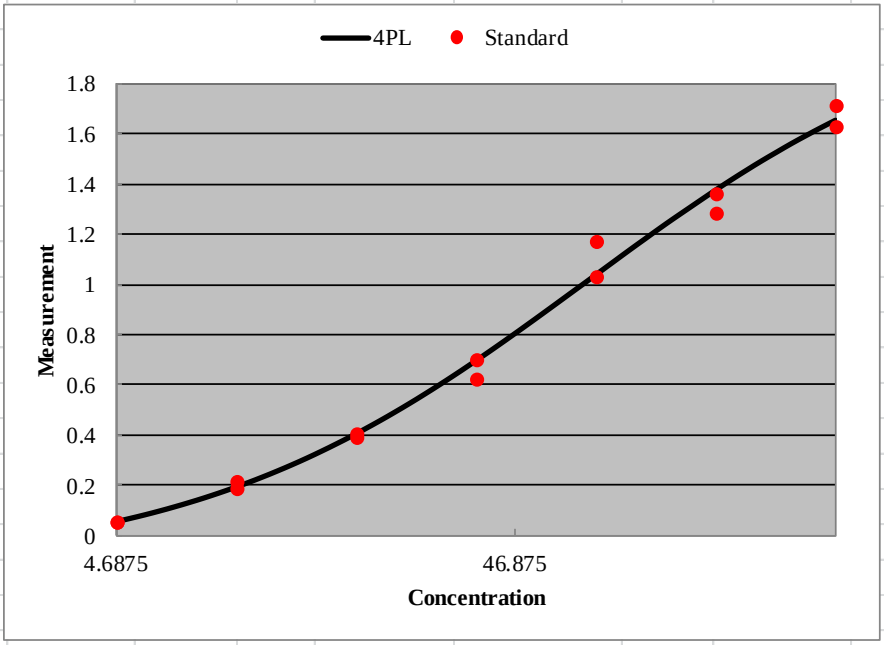

a	-0.1345
b	0.8855
c	70.79
d	2.152
MSE	0.002643
R^2	0.9917
SS	0.03701
SYX	0.06083

Calibrator	Conc.	Wells	Raw (Corrected)	SEM	Backfit	Recovery %
Standard1	300	A1	1.71	0.041	357.9	119.3
		A2	1.63		280.3	93.44
Standard2	150	B1	1.36	0.0385	145.1	96.74
		B2	1.28		123.1	82.06
Standard3	75	C1	1.18	0.0725	98.61	131.5
		C2	1.03		73.88	98.51
Standard4	37.5	D1	0.703	0.038	38.07	101.5
		D2	0.627		32.27	86.06
Standard5	18.75	E1	0.406	0.006	18.8	100.3
		E2	0.394		18.19	97.02
Standard6	9.375	F1	0.214	0.013	10.18	108.6
		F2	0.188		9.184	97.96
Standard7	4.688	G1	0.0515	0.003	4.582	97.75
		G2	0.0575		4.765	101.6

Sample	Dilution	Wells	Raw	Background Corrected	Conc.	Conc. (Average)	%CV	SD	SEM
NCA	1	A3	0.152	0.1	5.61	6.135	12.1	0.743	0.525
		A4	0.184		6.66				
NCB	1	B3	0.113	0.028	4.401	3.893	18.5	0.719	0.508
		B4	0.078		3.385				
NCC	1	C3	0.105	0.025	4.163	3.802	13.4	0.511	0.361
		C4	0.08		3.441				
NCD	1	D3	0.102	0.0295	4.075	3.929	5.24	0.206	0.146
		D4	0.092		3.784				
DC0A	1	E3	0.085	0.0145	3.583	3.498	3.44	0.12	0.085
		E4	0.079		3.413				
DC0D	1	F3	0.082	0.0155	3.497	3.526	1.14	0.0402	0.0284
		F4	0.084		3.554				
DC0E	1	G3	0.077	0.0145	3.356	3.498	5.73	0.2	0.142
		G4	0.087		3.64				
DC0F	1	H3	0.082	0.012	3.497	3.427	2.91	0.0998	0.0705
		H4	0.077		3.356				
DC3A	1	A5	0.084	0.02	3.554	3.655	3.88	0.142	0.1
		A6	0.091		3.755				
DC3C	1	B5	0.081	0.0265	3.469	3.846	13.9	0.533	0.377
		B6	0.107		4.223				
DC3D	1	C5	0.084	0.028	3.554	3.888	12.2	0.473	0.334
		C6	0.107		4.223				
DC3F	1	D5	0.07	0.018	3.161	3.603	17.4	0.625	0.442
		D6	0.101		4.046				
DC5A	1	E5	0.072	0.0185	3.217	3.616	15.6	0.565	0.4
		E6	0.1		4.016				
DC5B	1	F5	0.095	0.03	3.87	3.943	2.61	0.103	0.0729
		F6	0.1		4.016				
DC5C	1	G5	0.084	0.014	3.554	3.483	2.87	0.1	0.0708
		G6	0.079		3.413				
DC5D	1	H5	0.086	0.0215	3.611	3.697	3.3	0.122	0.0862
		H6	0.092		3.784				
DC10A	1	A7	0.081	0.0105	3.469	3.385	3.53	0.119	0.0844
		A8	0.075		3.3				
DC10B	1	B7	0.08	0.014	3.441	3.483	1.72	0.0601	0.0425
		B8	0.083		3.526				
DC10C	1	C7	0.107	0.046	4.223	4.418	6.24	0.276	0.195
		C8	0.12		4.613				
DC10D	1	D7	0.115	0.0405	4.462	4.254	6.91	0.294	0.208
		D8	0.101		4.046				
DC30A	1	E7	0.082	0.0235	3.497	3.757	9.76	0.367	0.259
		E8	0.1		4.016				
DC30B	1	F7	0.092	0.031	3.784	3.974	6.76	0.269	0.19
		F8	0.105		4.163				
DC30C	1	G7	0.086	0.0345	3.611	4.082	16.3	0.665	0.47
		G8	0.118		4.552				
DC30F	1	H7	0.09	0.0265	3.726	3.842	4.27	0.164	0.116
		H8	0.098		3.958				

EX3C	1	A9	0.12	0.0615	4.613	4.89	8.02	0.392	0.277
		A10	0.138		5.167				
EX3D	1	B9	0.098	0.056	3.958	4.736	23.2	1.1	0.778
		B10	0.149		5.514				
EX3E	1	C9	0.129	0.0445	4.888	4.379	16.4	0.719	0.509
		C10	0.095		3.87				
EX3F	1	D9	0.128	0.087	4.857	5.708	21.1	1.2	0.851
		D10	0.181		6.559				
EX5A	1	E9	0.097	0.044	3.929	4.362	14.1	0.613	0.433
		E10	0.126		4.795				
EX5B	1	F9	0.102	0.0385	4.075	4.193	3.99	0.167	0.118
		F10	0.11		4.312				
EX5D	1	G9	0.11	0.0425	4.312	4.312	0	0	0
		G10	0.11		4.312				
EX5F	1	H9	0.127	0.06	4.826	4.841	0.449	0.0217	0.0154
		H10	0.128		4.857				
EX10A	1	A11	0.087	0.0415	3.64	4.295	21.6	0.926	0.655
		A12	0.131		4.949				
EX10B	1	B11	0.122	0.087	4.673	5.717	25.8	1.48	1.04
		B12	0.187		6.761				
EX10D	1	C11	0.125	0.1	4.765	6.159	32	1.97	1.39
		C12	0.21		7.553				
EX10F	1	D11	0.128	0.0505	4.857	4.555	9.39	0.427	0.302
		D12	0.108		4.252				
EX30C	1	E11	0.036	0.123	2.251	7.542	99.2	7.48	5.29
		E12	0.346		12.83				
EX30D	1	F11	0.155	0.068	5.706	5.099	16.8	0.859	0.607
		F12	0.116		4.492				
EX30E	1	G11	0.13	0.0615	4.918	4.888	0.891	0.0436	0.0308
		G12	0.128		4.857				
EX30F	1	H11	0.181	0.085	6.559	5.647	22.9	1.29	0.912
		H12	0.124		4.734				
Blank		H1	0.068	0	3.106	3.092	0.631	0.0195	0.0138
		H2	0.067		3.078				

The highlighted samples are outside the range of the standard measurements.